

**FABRICATION AND USE OF NEW SOLID STATE  
PHOSPHATE ION SELECTIVE ELECTRODES FOR  
MONITORING PHOSPHORYLATION AND  
DEPHOSPHORYLATION REACTIONS**

by

**EMEKA MARTIN ENEMCHUKWU**

submitted in accordance with the requirements for  
the degree of

**Doctor of Philosophy**

in the subject

**Chemistry**

at the

**University of South Africa**

**Supervisor: Professor Fikru Tafesse**

**June 2012**

STUDENT NUMBER: 41537025

I declare that **FABRICATION AND USE OF NEW SOLID STATE PHOSPHATE ION SELECTIVE ELECTRODES FOR MONITORING PHOSPHORYLATION AND DEPHOSPHORYLATION REACTIONS** is my own work and that all the sources that I have used or quoted have been indicated and acknowledged by means of complete references.

---

SIGNATURE

EMEKA MARTIN ENEMCHUKWU

---

DATE

## DEDICATION

This is dedicated to my loving wife Adaoma Nwamaka Enemchukwu (Baby Chichi), Ada, I count myself lucky everyday for your presence in my life.

To my parents Mr. and Mrs. Ambrose Grace Enemchukwu, Dad, Mum I think I made it. Thanks to you guys.

To my in-laws, Mr and Mrs Bennett Helen Okoye, You are my source of inspiration.

And above all, to the will of the Almighty God.

## ACKNOWLEDGEMENTS

My sincere gratitude goes to my supervisor Professor Fikru Tafesse. Sir, I want you to know that you are and will always remain my mentor.

To Professor Jack Malose Mphahlele, Sir, words can never express how obliged I am towards your unending support to me and my colleagues.

To Professor Mamokgethi Setati, You are a mum to many and I count myself lucky to be one of your kids. The constant quote under each mail gets me up every morning.

To Elochukwu Enemchukwu, How I wish we were born twins.

To Vincent DD Enemchukwu, I love you till death, I just want you to know that.

To Uche Florence Uwagwu and Nkeiru Celestina Uzoechi, my lovely sisters, I love you guys a lot.

To Raymond Anyasi, it's up to you bro to make Dr. a permanent prefix to your name.

To Esotu Izuchukwu Ben, in you I find a brother, Thanks for keeping me close to your heart.

To Ubani Onyedikachi, You will always remain my brother and my companion.

To Ikpe Dennis, how I wish I can get it together like you, you inspire me.

To Tlou Makwakwa, Kennedy Eguzozie, Ifeanyi KC Nwaiwu, Doc. Ogbonnaya I owe you guys a lot.

My sincere gratitude also goes to the Department of Chemistry, College of Science, Engineering and Technology and the University of South Africa for the financial assistance extended to me in the form of post graduate academic assistantship. Above all I give glory to God.

## ABSTRACT

Highly selective and sensitive phosphate sensors have been fabricated by constructing a solid membrane disk consisting of variable mixtures of aluminium powder (Al), aluminium phosphate ( $\text{AlPO}_4$ ) and powdered copper (Cu). Both binary and ternary electrode systems are produced depending on their composition. The ternary membranes exhibit greater selectivity over a wide range of concentrations. The ternary electrode with the composition 25%  $\text{AlPO}_4$ , 25% Cu and 50% Al was selected as our preferred electrode. The newly fabricated ternary membrane phosphate selective electrodes exhibited linear potential response in the concentration range of  $1.0 \times 10^{-6}$  to  $1.0 \times 10^{-1} \text{ mol L}^{-1}$ . The electrodes also exhibit a fast response time of  $<60 \text{ s}$ . Their detection limit is  $1.0 \times 10^{-6} \text{ mol L}^{-1}$ . The unique feature of the described electrodes is their ability to maintain a steady and reproducible response in the absence of an ionic strength control. The electrodes have a long lifetime and can be stored in air when not in use. The selectivity of the new phosphate selective electrodes with respect to other common ions is excellent. The results obtained provide further insight into the working principles of the newly fabricated phosphate selective electrodes.

Dephosphorylation and phosphorylation reactions were monitored using the preferred phosphate selective electrode. The following reactions were studied and inferences drawn; (a) the reactions between  $*[\{\text{CoN}_4(\text{OH})(\text{OH}_2)\}]^{2+}$  and  $*[\text{OH}(\text{PO}_2\text{O})]^{2-}$  for 1:1, 2:1 and 3:1  $*[\{\text{CoN}_4(\text{OH})(\text{OH}_2)\}]^{2+}$  to  $*[\text{OH}(\text{PO}_2\text{O})]^{2-}$  ratios.

(b) the reactions between  $*[\{\text{CoN}_4(\text{OH})(\text{OH}_2)\}]^{2+}$  and  $*[\text{O}_2\text{NC}_6\text{H}_4\text{PO}_2(\text{O})(\text{OH})]^-$  for 1:1, 2:1 and 3:1  $*[\{\text{CoN}_4(\text{OH})(\text{OH}_2)\}]^{2+}$  to  $*[\text{O}_2\text{NC}_6\text{H}_4\text{PO}_2(\text{O})(\text{OH})]^-$  ratios. (c) the reactions between  $*[\{\text{CoN}_4(\text{OH})(\text{OH}_2)\}]^{2+}$  and  $*[(\text{OH})_2(\text{PO}_2)_2\text{O}]^{2-}$  for 1:1, 2:1 and 3:1  $*[\{\text{CoN}_4(\text{OH})(\text{OH}_2)\}]^{2+}$  to  $*[(\text{OH})_2(\text{PO}_2)_2\text{O}]^{2-}$  ratios, and (d) the reactions between  $*[\{\text{CoN}_4(\text{OH})(\text{OH}_2)\}]^{2+}$  and  $*[(\text{OH})_2(\text{PO}_2)_3\text{O}_2]^{3-}$  for the 1:1, 2:1 and 3:1  $*[\{\text{CoN}_4(\text{OH})(\text{OH}_2)\}]^{2+}$  to  $*[(\text{OH})_2(\text{PO}_2)_3\text{O}_2]^{3-}$  ratios. Further insight into dephosphorylation and phosphorylation reactions is unravelled by the novel phosphate selective electrode monitoring.

*\*For clarity of the complexes utilized, see chapter 4, table 4.1.*

KEY WORDS; Dephosphorylation, phosphorylation, ion selective electrodes, phosphate ion selective electrode, decontamination, electromotive force, potential difference, activity, concentration, selectivity coefficient, calibration, ionic strength, hydrolysis, inorganic phosphates, nitrophenylphosphate, pyrophosphate, tripolyphosphate, organophosphate esters.

## TABLE OF CONTENTS

DECLARATION.....	II
DEDICATION.....	III
ACKNOWLEDGEMENTS.....	IV
ABSTRACT.....	V
TABLE OF CONTENTS.....	VII
LIST OF ABBREVIATIONS.....	XIII
LIST OF TABLES.....	XIV
LIST OF FIGURES.....	XVII
LIST OF REACTION SCHEMES.....	XX

### CHAPTER ONE

#### PROJECT BACKGROUND

1.0 PHOSPHATES IN THE ENVIRONMENT.....	1
1.1 PHOSPHATES IN LIFE PROCESSES.....	4
1.2 MONITORING PHOSPHATES.....	6
1.2.1 PHOSPHATE SELECTIVE ELECTRODES.....	9
1.3 PROJECT AIMS.....	11
1.4 PROJECT APPROACH.....	12
1.5 THESIS ORGANISATION.....	13

## CHAPTER TWO

### ANALYTICAL TECHNIQUES FOR THE DETERMINATION OF PHOSPHATES IN THE ENVIRONMENT: LITERATURE SURVEY

2.0 INTRODUCTION.....	15
2.1 COLORIMETRIC DETERMINATION OF PHOSPHATE.....	18
2.1.1 METHODS FOR MEASURING ORTHOPHOSPHATE: THE PHOSPHOMOLYBDATE COMPLEX ROUTE.....	19
2.1.2 UV-VISIBLE ABSORPTION SPECTROSCOPY.....	23
2.1.2.1 PRINCIPLES OF UV-VISIBLE ABSORPTION SPECTROSCOPY..	25
2.1.2.2 FACTORS THAT AFFECT ACCURACY IN UV-VISIBLE ABSORPTION SPECTROPHOTOMETRY.....	27
2.1.2.2.1 EFFECT OF SOLVENT, SAMPLE PREPARATION, CONCENTRATION, pH, AND TEMPERATURE .....	28
2.1.2.2.2 EFFECT OF SPECTRAL BANDWIDTH AND BAND SLIT WIDTH.....	30
2.1.2.2.3 OTHER METHODS FOR THE ANALYSIS OF ORTHOPHOSPHATE AND COMBINED PHOSPHATE.....	31
2.2 <sup>31</sup> P NMR SPECTROSCOPY.....	32
2.2.1 <sup>31</sup> P NMR CHEMICAL SHIFTS.....	32
2.2.2 <sup>31</sup> P NMR SPIN-SPIN COUPLING.....	36



2.2.3 TYPICAL <sup>31</sup> P NMR INSTRUMENTATION AND SAMPLE REQUIREMENTS.....	39
2.3 ION SELECTIVE ELECTRODES.....	41
2.3.1 TYPICAL CONFIGURATION OF AN ION SELECTIVE ELECTRODE.....	43
2.3.2 ELECTRON TRANSFER AT THE SOLUTION-ELECTRODE INTERFACE.....	44
2.3.3 THE NERNST EQUATION.....	47
2.3.4 CLASSIFICATION OF ION SELECTIVE ELECTRODES.....	49
2.3.4.1 METALLIC ELECTRODES.....	50
2.3.4.1.1 ELECTRODES OF THE FIRST KIND.....	50
2.3.4.1.2 ELECTRODES OF THE SECOND KIND.....	51
2.3.4.1.3 ELECTRODES OF THE THIRD KIND.....	52
2.3.4.1.4 REDOX ELECTRODES.....	52
2.3.4.2 MEMBRANE ELECTRODES.....	53
2.3.4.2.1 CRYSTALLINE ELECTRODES.....	53
2.3.4.2.2 NON-CRYSTALLINE ELECTRODES.....	55
2.3.4.2.3 MULTIPLE MEMBRANES (MULTILAYER) ION SELECTIVE ELECTRODES (COMPOUND ELECTRODES).....	61
2.3.4.2.4 METAL CONTACT OR ALL-SOLID-STATE ION SELECTIVE ELECTRODES.....	63
2.3.5 CHARACTERIZATION OF AN ION SELECTIVE ELECTRODE.....	64
2.3.5.1 ACTIVITY VS CONCENTRATION.....	65
2.3.5.2 SELECTIVITY OF ION SELECTIVE ELECTRODES.....	68

2.3.5.3 NERNSTIAN RESPONSE.....	73
2.3.5.4 CALIBRATION THEORY.....	73
2.3.5.5 IONIC STRENGTH AND TOTAL IONIC STRENGTH ADJUSTMENT BUFFERS (TISAB).....	76
2.3.6 METHOD OF ANALYSIS USING ION SELECTIVE ELECTRODES.....	79

## **CHAPTER THREE**

### **DESIGN AND FABRICATION OF THE NEW SOLID STATE**

#### **PHOSPHATE SELECTIVE ELECTRODES**

3.0 INTRODUCTION.....	82
3.1 EXPERIMENTAL SECTION.....	84
3.1.1 INSTRUMENTS AND REAGENTS.....	84
3.1.2 CHOICE OF MEMBRANE MATERIALS.....	87
3.2 FABRICATION OF SOLID STATE MEMBRANE.....	89
3.3 ELECTRODE CONSTRUCTION.....	91
3.4 CONDITIONING OF THE ELECTRODES.....	92
3.5 PROTOCOL OF THE STUDY.....	94
3.5.1 CALIBRATION CURVE STUDIES.....	94
3.6 RESULT AND DISCUSSION.....	95
3.6.1 THE EFFECT OF pH ON THE DIFFERENT ELECTRODES.....	107
3.6.2 THE RESPONSE TIME OF THE ELECTRODES.....	108
3.6.3 INTERFERENCE STUDIES.....	110

**CHAPTER FOUR**

**MONITORING DEPHOSPHORYLATION AND PHOSPHORYLATION**

**REACTIONS USING A NOVEL PHOSPHATE SOLID STATE ION**

**SELECTIVE ELECTRODE**

4.0 PHOSPHORYLATION AND DEPHOSPHORYLATION REACTIONS.....	119
4.1 EXPERIMENTAL SECTION.....	126
4.1.1 INSTRUMENTS AND REAGENTS.....	126
4.1.2 CHOICE OF MODEL SYSTEMS.....	126
4.1.2.1 SODIUM PYROPHOSPHATE ( $\text{Na}_4\text{P}_2\text{O}_7 \cdot 10\text{H}_2\text{O}$ ) AND SODIUM	
TRIPOLYPHOSPHATE ( $\text{Na}_5\text{P}_3\text{O}_{10}$ ): SUBSTRATE MODELS FOR	
UNACTIVATED PHOSPHATE ESTER.....	127
4.1.2.2 4-NITROPHENYLPHOSPHATE (4-NPP): SUBSTRATE MODEL	
FOR ACTIVATED PHOSPHATE ESTER.....	128
4.1.2.3 PREPARATION OF THE ENZYME MODEL.....	129
4.1.2.4 PREPARATION OF THE SUBSTRATE MODELS.....	130
4.2 PROTOCOL OF THE STUDIES.....	130
4.3 RESULTS AND DISCUSSION.....	136
4.3.1 RESULTS FOR COBALT(III) BIS-TRIMETHYLENEDIAMINE	
HYDROLYSIS OF PHOSPHATE COMPLEXES.....	137
4.3.2 RESULTS FOR COBALT(III) BIS-TRIMETHYLENEDIAMINE	
HYDROLYSIS OF 4-NITROPHENYLPHOSPHATE.....	140

4.3.3 RESULTS FOR COBALT(III) BIS-TRIMETHYLENEDIAMINE	
HYDROLYSIS OF PYROPHOSPHATE.....	144
4.3.4 RESULTS FOR COBALT(III) BIS-TRIMETHYLENEDIAMINE	
HYDROLYSIS OF SODIUM TRIPOLYPHOSPHATE.....	148

## CHAPTER FIVE

5.0 GENERAL CONCLUSION.....	154
5.1 FUTURE WORK.....	159
REFERENCES.....	161

## LIST OF ABBREVIATIONS

ATP	Adenosine Triphosphate
CWE	Coated Wire Electrode
DNA	Deoxyribonucleic Acid
EMF	Electromotive Force
ISE	Ion Selective Electrode
IUPAC	International Union Of Pure and Applied Chemistry
4-NPP	4-Nitrophenyl Phosphate
$^{31}\text{P}$ NMR	Phosphorus 31 Nuclear Magnetic Resonance Spectroscopy
RNA	Ribonucleic Acid
TISAB	Total Ionic Strength Adjustment Buffer

## LIST OF TABLES

TABLE 2.1	CHEMICAL SHIFTS ( $\delta$ ) RANGES OF SELECTED PHOSPHORUS COMPOUNDS, REFERENCED TO 85% H <sub>3</sub> PO <sub>4</sub> .....	34
TABLE 2.2	TYPICAL <sup>31</sup> P PHOSPHORUS COUPLING CONSTANTS.....	37
TABLE 3.1	PREPARATION OF 0.1 M SODIUM PHOSPHATE BUFFER AT 25 <sup>o</sup> C.....	85
TABLE 3.2	PROPERTIES OF THE FABRICATED MEMBRANE PELLETS.....	90
TABLE 3.3	AVERAGE NERNSTIAN SLOPES FOR DIFFERENT PHOSPHATE SENSITIVE ELECTRODES.....	103
TABLE 3.4	THE EFFECT OF INTERFERING IONS ON THE ELECTRODE RESPONSE.....	111
TABLE 3.5	SELECTIVITY COEFFICIENTS ( $K_{A,B}^{pot}$ ) FOR THE PHOSPHATE ELECTRODE (25% AlPO <sub>4</sub> + 25% CU + 50% Al MEMBRANE ELECTRODE) IN MIXED SOLUTIONS.....	115
TABLE 4.1	COMPLEXES ENCOUNTERED IN THIS STUDY.....	132
TABLE 4.2	EMF (mV) READINGS OF ALL REAGENTS USED IN THE STUDY.....	136
TABLE 4.3	EMF (mV) VALUES RECORDED FOR THE REACTION BETWEEN [CON <sub>4</sub> (OH)(OH <sub>2</sub> )] <sup>2+</sup> AND [HPO <sub>4</sub> ] <sup>2-</sup> FOR 1:1 [CON <sub>4</sub> (OH)(OH <sub>2</sub> )] <sup>2+</sup> TO [HPO <sub>4</sub> ] <sup>2-</sup> RATIOS.....	137
TABLE 4.4	EMF (mV) VALUES RECORDED FOR THE REACTION BETWEEN [CON <sub>4</sub> (OH)(OH <sub>2</sub> )] <sup>2+</sup> AND [HPO <sub>4</sub> ] <sup>2-</sup> FOR 2:1 [CON <sub>4</sub> (OH)(OH <sub>2</sub> )] <sup>2+</sup> TO [HPO <sub>4</sub> ] <sup>2-</sup> RATIOS.....	138

TABLE 4.5	EMF (mV) VALUES RECORDED FOR THE REACTION BETWEEN [ $\{\text{CON}_4(\text{OH})(\text{OH}_2)\}^{2+}$ ] AND $[\text{HPO}_4]^{2-}$ FOR 3:1 [ $\{\text{CON}_4(\text{OH})(\text{OH}_2)\}^{2+}$ ] TO $[\text{HPO}_4]^{2-}$ RATIOS.....	138
TABLE 4.6	EMF (mV) VALUES RECORDED FOR THE REACTION BETWEEN [ $\{\text{CON}_4(\text{OH})(\text{OH}_2)\}^{2+}$ ] AND 4-NPP FOR 1:1 [ $\{\text{CON}_4(\text{OH})(\text{OH}_2)\}^{2+}$ ] TO 4-NPP RATIOS.....	141
TABLE 4.7	EMF (mV) VALUES RECORDED FOR THE REACTION BETWEEN [ $\{\text{CON}_4(\text{OH})(\text{OH}_2)\}^{2+}$ ] AND 4-NPP FOR 2:1 [ $\{\text{CON}_4(\text{OH})(\text{OH}_2)\}^{2+}$ ] TO 4-NPP RATIOS.....	141
TABLE 4.8	EMF (mV) VALUES RECORDED FOR THE REACTION BETWEEN [ $\{\text{CON}_4(\text{OH})(\text{OH}_2)\}^{2+}$ ] AND 4-NPP FOR 3:1 [ $\{\text{CON}_4(\text{OH})(\text{OH}_2)\}^{2+}$ ] TO 4-NPP RATIOS.....	142
TABLE 4.9	EMF (mV) VALUES RECORDED FOR THE REACTION BETWEEN [ $\{\text{CON}_4(\text{OH})(\text{OH}_2)\}^{2+}$ ] AND $[\text{H}_2\text{P}_2\text{O}_{10}]^{2-}$ FOR 1:1 [ $\{\text{CON}_4(\text{OH})(\text{OH}_2)\}^{2+}$ ] TO $[\text{H}_2\text{P}_2\text{O}_7]^{2-}$ RATIOS.....	145
TABLE 4.10	EMF (mV) VALUES RECORDED FOR THE REACTION BETWEEN [ $\{\text{CON}_4(\text{OH})(\text{OH}_2)\}^{2+}$ ] AND $[\text{H}_2\text{P}_2\text{O}_{10}]^{2-}$ FOR 2:1 [ $\{\text{CON}_4(\text{OH})(\text{OH}_2)\}^{2+}$ ] TO $[\text{H}_2\text{P}_2\text{O}_7]^{2-}$ RATIOS.....	146
TABLE 4.11	EMF (mV) VALUES RECORDED FOR THE REACTION BETWEEN [ $\{\text{CON}_4(\text{OH})(\text{OH}_2)\}^{2+}$ ] AND $[\text{H}_2\text{P}_2\text{O}_{10}]^{2-}$ FOR 3:1 [ $\{\text{CON}_4(\text{OH})(\text{OH}_2)\}^{2+}$ ] TO $[\text{H}_2\text{P}_2\text{O}_7]^{2-}$ RATIOS.....	146
TABLE 4.12	EMF (mV) VALUES RECORDED FOR THE REACTION BETWEEN [ $\{\text{CON}_4(\text{OH})(\text{OH}_2)\}^{2+}$ ] AND $[\text{H}_2\text{P}_2\text{O}_{10}]^{2-}$ FOR 1:1 [ $\{\text{CON}_4(\text{OH})(\text{OH}_2)\}^{2+}$ ] TO $[\text{H}_2\text{P}_3\text{O}_{10}]^{3-}$ RATIOS.....	149

TABLE 4.13	EMF (mV) VALUES RECORDED FOR THE REACTION BETWEEN $[\{\text{CON}_4(\text{OH})(\text{OH}_2)\}]^{2+}$ AND $[\text{H}_2\text{P}_2\text{O}_{10}]^{2-}$ FOR 2:1 $[\{\text{CON}_4(\text{OH})(\text{OH}_2)\}]^{2+}$ TO $[\text{H}_2\text{P}_3\text{O}_{10}]^{3-}$ RATIOS.....	149
------------	--	-----

TABLE 4.14	EMF (mV) VALUES RECORDED FOR THE REACTION BETWEEN $[\{\text{CON}_4(\text{OH})(\text{OH}_2)\}]^{2+}$ AND $[\text{H}_2\text{P}_2\text{O}_{10}]^{2-}$ FOR 3:1 $[\{\text{CON}_4(\text{OH})(\text{OH}_2)\}]^{2+}$ TO $[\text{H}_2\text{P}_3\text{O}_{10}]^{3-}$ RATIOS.....	150
------------	--	-----



## LIST OF FIGURES

FIGURE 2.1	AQUATIC PHOSPHORUS FRACTIONS.....	16
FIGURE 2.2	ELECTRONIC ENERGY LEVELS AND TRANSITIONS.....	26
FIGURE 2.3	A CROSS SECTION OF A TYPICAL ION SELECTIVE ELECTRODE.....	43
FIGURE 2.4	THE ENERGY OF ELECTRONS IN THE IONS IN SOLUTION AND IN THE METAL WIRE.....	45
FIGURE 2.5	A TYPICAL CRYSTALLINE ELECTRODE.....	54
FIGURE 2.6	THE pH METER (A GLASS ELECTRODE).....	56
FIGURE 2.7	THE CALCIUM ELECTRODE (A LIQUID BASED ISE).....	60
FIGURE 2.8	THE CO <sub>2</sub> ELECTRODE.....	62
FIGURE 2.9	CALIBRATION CURVE FOR ELECTRODE RESPONSE TO THE LOGARITHM OF ACTIVITY AND STOICHIOMETRIC CONCENTRATION.....	66
FIGURE 2.10	TYPICAL CALIBRATION CURVE OF AN ION-SELECTIVE ELECTRODE.....	74
FIGURE 3.1	PHOSPHATE ION SPECIATION DIAGRAM.....	86
FIGURE 3.2	OVERALL ARRANGEMENT OF THE PHOSPHATE SOLID STATE ION SELECTIVE ELECTRODE.....	92
FIGURE 3.3	THE EFFECT OF MEDIA ON THE PERFORMANCE OF THE ELECTRODES.....	93

FIGURE 3.4	CALIBRATION CURVE FOR THE PHOSPHATE SENSITIVE ELECTRODE COMBINATION 10% $\text{AlPO}_4$ + 90% Al.....	96
FIGURE 3.5	CALIBRATION CURVE FOR THE PHOSPHATE SENSITIVE ELECTRODE COMBINATION 20% $\text{AlPO}_4$ + 80% Al.....	96
FIGURE 3.6	CALIBRATION CURVE FOR THE PHOSPHATE SENSITIVE ELECTRODE COMBINATION 30% $\text{AlPO}_4$ + 70% Al.....	97
FIGURE 3.7	CALIBRATION CURVE FOR THE PHOSPHATE SENSITIVE ELECTRODE COMBINATION 40% $\text{AlPO}_4$ + 60% Al.....	97
FIGURE 3.8	CALIBRATION CURVE FOR THE PHOSPHATE SENSITIVE ELECTRODE COMBINATION 50% $\text{AlPO}_4$ + 50% Al.....	98
FIGURE 3.9	CALIBRATION CURVE FOR THE PHOSPHATE SENSITIVE ELECTRODE COMBINATION 60% $\text{AlPO}_4$ + 40% Al.....	98
FIGURE 3.10	CALIBRATION CURVE FOR THE PHOSPHATE SENSITIVE ELECTRODE COMBINATION 10% $\text{AlPO}_4$ + 90% Cu.....	99
FIGURE 3.11	CALIBRATION CURVE FOR THE PHOSPHATE SENSITIVE ELECTRODE COMBINATION 20% $\text{AlPO}_4$ + 80% Cu.....	99
FIGURE 3.12	CALIBRATION CURVE FOR THE PHOSPHATE SENSITIVE ELECTRODE COMBINATION 30% $\text{AlPO}_4$ + 70% Cu.....	100
FIGURE 3.13	CALIBRATION CURVE FOR THE PHOSPHATE SENSITIVE ELECTRODE COMBINATION 10% $\text{AlPO}_4$ + 10% Cu + 80% Al.....	100
FIGURE 3.14	CALIBRATION CURVE FOR THE PHOSPHATE SENSITIVE ELECTRODE COMBINATION 15% $\text{AlPO}_4$ + 15% Cu + 70% Al.....	101
FIGURE 3.15	CALIBRATION CURVE FOR THE PHOSPHATE SENSITIVE ELECTRODE COMBINATION 20% $\text{AlPO}_4$ + 20% Cu + 60% Al.....	101

FIGURE 3.16	CALIBRATION CURVE FOR THE PHOSPHATE SENSITIVE ELECTRODE COMBINATION 25% $\text{AlPO}_4$ + 25% Cu + 50% Al.....	102
FIGURE 3.17	CALIBRATION CURVE FOR THE PHOSPHATE SENSITIVE ELECTRODE COMBINATION 30% $\text{AlPO}_4$ + 30% Cu +40% Al.....	102
FIGURE 3.18	CALIBRATION CURVE FOR THE PHOSPHATE SENSITIVE ELECTRODE COMBINATION 35% $\text{AlPO}_4$ + 35% Cu +30% Al.....	103
FIGURE 3.19	THE pH DEPENDENCE OF THE ELECTRODE WITH MEMBRANE COMPOSITION OF 25% $\text{AlPO}_4$ + 25% Cu + 50% Al....	108
FIGURE 3.20	THE DEPENDENCE OF RESPONSE TIME WITH CONCENTRATION (25% $\text{AlPO}_4$ + 25% Cu + 50% Al MEMBRANE ELECTRODE).....	109
FIGURE 3.21	THE RESPONSE OF THE ELECTRODE AGAINST SOME ANIONS IN THE PRESENCE OF $1 \times 10^{-2}$ M PHOSPHATE (25% $\text{AlPO}_4$ + 25% Cu + 50% Al MEMBRANE ELECTRODE).....	113
FIGURE 3.22	THE RESPONSE OF THE ELECTRODE AGAINST SOME CATIONS IN THE PRESENCE OF $1 \times 10^{-2}$ M PHOSPHATE (25% $\text{AlPO}_4$ + 25% Cu + 50% Al MEMBRANE ELECTRODE).....	113
FIGURE 3.23	A PLOT SHOWING SELECTIVITY COEFFICIENT FOR FLOURIDE ION OVER THE PRIMARY ION FOR THE PHOSPHATE ELECTRODE (25% $\text{AlPO}_4$ + 25% Cu + 50% Al).....	116

## LIST OF REACTION SCHEMES

SCHEME 4.1	PLAUSIBLE SCHEME FOR THE REACTION OF [CON <sub>4</sub> (OH)(H <sub>2</sub> O)] <sup>2+</sup> WITH TRIPOLYPHOSPHATE [H <sub>2</sub> P <sub>3</sub> O <sub>10</sub> ] <sup>2-</sup> FOR 1:1 [CON <sub>4</sub> (OH)(H <sub>2</sub> O)] <sup>2+</sup> TO [H <sub>2</sub> P <sub>3</sub> O <sub>10</sub> ] <sup>2-</sup> RATIO.....	150
SCHEME 4.2	PLAUSIBLE SCHEME FOR THE REACTION OF [CON <sub>4</sub> (OH)(H <sub>2</sub> O)] <sup>2+</sup> WITH TRIPOLYPHOSPHATE [H <sub>2</sub> P <sub>3</sub> O <sub>10</sub> ] <sup>2-</sup> FOR 2:1 AND 3:1 [CON <sub>4</sub> (OH)(H <sub>2</sub> O)] <sup>2+</sup> TO [H <sub>2</sub> P <sub>3</sub> O <sub>10</sub> ] <sup>2-</sup> RATIO.....	151

# *CHAPTER ONE*

## **PROJECT BACKGROUND**

### **1.0 PHOSPHATES IN THE ENVIRONMENT**

Phosphate rock is a non-renewable natural resource, mainly found in sedimentary and igneous deposits. Weathering and erosion of rocks gradually releases phosphorus as phosphate ions which are soluble in water. Most of the phosphate is washed into the natural waters from leaching processes. Plants and algae utilize phosphates as a nutrient for growth. Stunted and excess growth of plants and algae has been attributed to deficiency and surplus of phosphate ion respectively. When plant materials and waste products decay through bacterial action, the phosphate is released and returned to the environment for reuse.

A large percentage of the phosphate in water is precipitated as iron phosphate which is insoluble. If the phosphate is in shallow sediments, it may be readily recycled back into the water for further reuse. In deeper sediments in water, it is available for use only as part of a general uplifting of rock formations, for the cycle to repeat itself. The phosphorus cycle differs from the other major biogeochemical cycles in that it does not include a gas phase; although small amounts of phosphoric acid ( $\text{H}_3\text{PO}_4$ ) may make their way into the atmosphere, contributing in some cases to acid rain. Human use of

phosphate based products is steadily on the rise as they are easy and cheap to acquire. There still exist very few substitutes for their ecological and biological functions.

Humans have drastically altered the phosphorus cycle in many ways which includes the cutting of tropical rain forests, the radical use of phosphate containing food additives and the use of phosphate containing products like fertilizers and detergents. Rainforest ecosystems are supported primarily through the recycling of nutrients, with little or no nutrient reserves in their soils. As the forest is cut and/or burned, nutrients originally stored in plants and rocks are quickly washed away by heavy rains, causing the land to become unproductive. Agricultural runoff provides much of the phosphate found in waterways. Crops often cannot absorb all of the fertilizer in the soils, causing excess fertilizer runoff and increasing phosphate levels in rivers and other bodies of water.

The use of laundry detergents contributes to significant concentrations of phosphates in rivers, lakes, and streams. Phosphates are present in detergents as a builder in the form of pentasodium tri-polyphosphate (STPP). This acts as hard water softener by complexing calcium, ferric and magnesium ions. It also assists in the cleaning process by buffering the pH of the washing solution, preventing rust and corrosion, and keeping dirt particles in suspension. STPP is easily hydrolyzed in the presence of water to bio-available orthophosphate ( $\text{PO}_4^{3-}$ ).<sup>1</sup> It is important to note that the element phosphorus (P) is contained in other components of detergents, such as the fluorescers and optical brighteners.

Studies<sup>2,3</sup> have shown that leaching of phosphate ions as small as  $0.01 \text{ mgL}^{-1}$  from agricultural land can contribute to eutrophication. This process results from the increase of phosphate nutrients within the body of water which in turn create algal growth. The algae die more quickly than they can be decomposed. This dead plant matter builds up and together with sediment entering the water, fills in the bed of the bay or lake making it shallower. Hyperphosphatemia leads to rapid growth of sea algae and weeds and these may choke the waterway. Algae and weeds use up large amounts of precious oxygen. In the absence of photosynthesis, the algae and plants die and are consumed by aerobic bacteria, these eventually result to the death of many fishes and aquatic organisms.<sup>4,5</sup>

Due to problems associated with non regulated phosphate presence in the ecosystem, environmentalists have been trying to ban phosphate containing laundry products for years.<sup>6</sup> Though, there are many non-phosphate containing substitutes in the advanced countries, many third world countries still support the use phosphate containing compounds. Over the years, many green soap makers are coming up with phosphate-free detergents. Irrespective of these advancements, it should be understood that most local and some modern manufacturers are still stuck with their original phosphate formulation recipes. This can be attributed to comfort of already established process, ease of manufacture, cost efficiency and in some cases lack of technical know-how of the new inventions.<sup>7</sup> It is very important to mention that phosphates and its derivatives

also find wide applications in pharmaceutical industries, food industries, lasers and sensor technologies<sup>8-11</sup> to mention but a few .

The need to regulate phosphate use cannot be overstated. Regular assessment of phosphates is important in a wide variety of situations which is based on the importance of phosphates in environmental, biochemical and physiological processes.

### **1.1 PHOSPHATES IN LIFE PROCESSES**

Phosphates are important in life processes. They are an integral component of the nucleic acids that comprise DNA (deoxyribonucleic acid) and RNA (ribonucleic acid). Approximately 85% of the human body's phosphate is present in the mineral phase of bone. The remainder of body phosphate is present in a variety of inorganic and organic compounds distributed within both intracellular and extracellular compartments. About 0.1% of phosphorus is present in extracellular fluids, and it is this fraction that is measured with a serum phosphorus test. In the human body, phosphates are involved in processes like cell signaling,<sup>12</sup> energy metabolism,<sup>13,14</sup> nucleic acid synthesis<sup>15,16</sup> and the maintenance of acid-base balance by urinary buffering.<sup>17,18</sup> The recommended dietary phosphate intake is 800 mg/day, although a normal diet provides between 1000 and 2000 mg/day depending on the extent to which phosphate rich foods are consumed.<sup>19</sup>

Mammals with a high-phosphate diet intake exhibit severe hyperphosphatemia that causes phosphate toxicity leading to accelerated mammalian aging,<sup>20</sup> kidney damage



and osteoporosis. Digestive problems could also occur from extremely high levels of phosphate. Low mammalian phosphate level causes hypophosphataemia;<sup>21</sup> an electrolyte disturbance in which there is an abnormally low level of phosphate in the blood. The condition has many causes, but is most commonly seen when malnourished patients (especially chronic alcoholics) are given large amounts of carbohydrates. This creates a high phosphorus demand by cells, removing phosphate from the blood.<sup>22</sup>

It should be noted that a decrease in the level of serum phosphate (hypophosphatemia) should be distinguished from a decrease in total body storage of phosphate (phosphate deficiency). Phosphates in mammals are critical for an incredible array of cellular processes. Phosphate bonds of ATP (Adenosine triphosphate) carry the energy required for all cellular functions. The transfer (phosphorylation and dephosphorylation) of phosphate groups in enzymes and proteins are common mechanisms for the regulation of their activity. In view of the sheer breadth of influence of this mineral, the fact that phosphate homeostasis is a highly regulated process is not surprising.<sup>23,24</sup>

Phosphates in the form of organophosphate esters also find wide application in the environment as a component of pesticides and insecticides formulations. Some common organophosphate insecticides include; diazinon, malathion, parathion, chlorothion, dichlorovos and so many others.<sup>25</sup> Organophosphates pesticides poison insects and mammals primarily by phosphorylation of the acetylcholinesterase enzyme (AChE) at nerve endings. The result is a loss of available AChE so that the effector organ becomes over stimulated by the excess acetylcholine. Acetylcholinesterase enzyme is critical to

normal control of nerve impulse transmission from nerve fibers to smooth and skeletal muscle cells, glandular cells, and autonomic ganglia, as well as within the central nervous system (CNS).<sup>26</sup>

More harmful chemical formulations in the same group include the so called chemical warfare nerve agents. They are termed nerve agents (neurotoxins) because they cause cumulative damage to the nervous system and the liver and eventually lead to death. Cumulative mammalian exposure to organophosphates can cause inhibition of brain-cells development and complete annihilation of the neuro-transmitter system.<sup>27,28</sup> In the 1930's, organophosphates were used as insecticides, but the German military developed these substances as neurotoxins in World War II. They are easily absorbed by the victim through inhalation, skin contact, or mucosal absorption. Some known nerve agents include; Tabun(O-ethyl N,N-dimethylphosphoroamidocyanidate), Sarin (O-isopropyl methylphosphonofluoridate), Soman (O-pinacolylmethylphosphonofluoridate), VX (O-ethyl-S-2-diisopropylamino-ethylmethylphosphonothiolate), and VR (O-isobutyl-S-[2-diethylaminoethyl] methyl-thiophosphonate).<sup>26</sup> The presence of phosphates in fertilizers, minerals, industrial water effluents and most life processes obviously calls for improved and suitable techniques for its monitoring.<sup>29</sup>

## 1.2 MONITORING PHOSPHATES

The analysis of all forms of phosphates in waters rests essentially on the measurement of free orthophosphate ( $\text{PO}_4^{3-}$ ). Previous known methods for the determination of

phosphate ions in real samples involve ion chromatography and spectrophotometric methods such as molybdenum blue and indirect lanthanum chloranilate methods.<sup>30-35</sup> Under favorable circumstances, it is possible to measure accurately the free orthophosphate and organically combined phosphates (which can be photo-oxidized to yield orthophosphate directly and total condensed phosphates).

The need for accurate measurement of the true concentrations of inorganic phosphate in solutions is obvious. As reported by Burton,<sup>36</sup> there are inherent disadvantages to the classical colorimetric methods. For example, most water samples are preserved by acidification. Acidification of samples may lead to changes in phosphate content due to hydrolysis of other phosphorus-containing compounds and desorption of phosphate from suspended particles. While some of these methods are often surpassed for accuracy, they are generally too tedious to be conducted with great irregularities. They are usually not very portable or suitable for real time measurements. Most of them can only be measured when treated with catalysts or derivatized. Monitoring of the phosphate concentration in real time is of paramount importance without the rigors of sample storing, transportation and eventual measurement. Some of these problems can be addressed if a suitable phosphate selective electrode is readily available.

The need for a simple phosphate sensitive electrode that will be an alternative probe to the traditional colorimetric phosphate analysis has long been recognized. Ion selective electrodes are generally based on highly selective ionophores embedded in hydrophobic membranes. They are usually contacted with aqueous electrolytes or

conductive wire and an internal or external reference. Analyte recognition process takes place followed by the conversion of chemical information into an electrical or optical signal. The ionophore is primarily responsible for the ion selectivity of the sensor by selectively and reversibly binding the analyte of interest. With optimized membrane formulations, the measured zero-current membrane potential can be directly related to the free ion activity of the analyte in the sample.<sup>37</sup>

Ion selective electrodes measure the concentration of ions in equilibrium at the membrane surface. In dilute solutions, this is directly related to the total number of ions in the solution but at higher concentrations, inter ionic interactions between all ions in the solution (both positive and negative) tend to reduce the mobility and thus there are relatively fewer of the measured ions in the vicinity of the membrane than in the bulk solution. Thus, the measured voltage is less than it would be if it reflected the total number of measured ions in the solution. This causes erroneously low estimates of the ion concentration in samples with a high concentration or a complex matrix. The activity coefficient is always less than one and becomes smaller as the ionic strength increases; thus the difference between the measured activity and the actual concentration differs at higher concentrations. This effect causes problems with ion selective electrode measurement. It has been observed that when plotting a calibration graph using concentration units, the line is seen to deviate from linearity as the concentration increases (it remains straight, up to the highest concentrations if activity units are used). Again, it is most likely that sample solutions will contain other ions in

addition to the one being measured and the ionic strength of the samples may be significantly higher than that of the standards. This creates incompatibility between the calibration curve and the measured samples leading to errors in the interpolated results.<sup>38</sup>

To circumvent the above difficulties, previous investigators<sup>39,40</sup> have employed the use of Total Ionic Strength Adjustment Buffers (TISAB) to keep the ionic strength and pH of both standards and test solutions constant. This is welcomed by researchers, but it does not always create room for versatility. For a technology that is envisaged to provide quick, accurate and real-time results, it is time consuming as samples and standards must be treated with TISAB every time. This research looks at the fabrication of a suitable ion selective electrode that will circumvent most of the difficulties encountered in the analysis of phosphates in environmental samples.

### **1.2.1 PHOSPHATE SELECTIVE ELECTRODES**

The design and formulation of phosphate selective electrodes and membranes have been on-going for decades.<sup>41-54</sup> In most cases, the later designs try to augment for the deficiencies of the previous designs. None of the experimental recorded designs have attained commercial production. The work done so far does little to suggest that good selectivity for phosphate ions in solution has been achieved.

A big point of concern in the construction of phosphate ion selective electrodes is the choice of sensing material. The design of a sensing material (i.e. ionophore) for the

selective recognition of phosphate is especially challenging. Due to the very high hydration energy of phosphates, ion selective membranes have a very poor selectivity for phosphates.<sup>55-57</sup> The Hofmeister series order of the common anions are;  $\text{ClO}_4^- > \text{SCN}^- > \text{I}^- > \text{NO}_3^- > \text{Br}^- > \text{Cl}^- > \text{HCO}_3^- > \text{SO}_4^{2-} > \text{HPO}_4^{2-}$ . The Hofmeister series ranks ions in order of decreasing hydrophobicity.<sup>58-60</sup> Phosphate, being at the end of the series, shows the lowest selectivity response towards the anions.<sup>61,62</sup> This is because the free energy of the phosphate species is very small and the large size of the orthophosphate ions prohibits the use of size-exclusion principles for increased selectivity.<sup>63</sup> Hence, selectivity for conventional anion electrodes is quite good for perchlorate and thiocyanate, but it is extremely poor for phosphates. In view of the selectivity problems with regard to the Hofmeister characterization, some research interests are now focused on membranes that exhibit anti-Hofmeister behavior.<sup>64-66</sup>

Ion selective electrodes come in various shapes and sizes. Each manufacturer has its own distinctive features, but very few give details of the internal construction of the electrode or composition of the ion-selective membranes. These are the most important factors which control the performance of the electrode, and are often kept as closely guarded trade secrets. Nevertheless, there are certain features that are common to all. All consist of a cylindrical tube, generally made of a plastic material, between 5 and 15 mm in diameter and 5 to 10 cm long. An ion-selective membrane is fixed at one end so that the external solution can only come into contact with the outer surface, and the other end is fitted with a low noise cable or gold plated pin for connection to the

potential measuring device. In some cases the internal connections are completed by a liquid or gel electrolyte, in others by metal wires.

The traditional barrel configuration of conventional electrodes (with internal filling solution) can prove cumbersome for some applications, so attempts at miniaturization brought about some new sensing systems, namely solid contact (SC) electrodes; such as solid crystal membranes, conducting filled polymer electrodes, and coated wire electrodes (CWE).<sup>67</sup> This move to the total elimination of the internal filling solution of the conventional electrodes to the all-solid-state electrodes provides new advantages such as; (a) simplicity of design, (b) lower costs, (c) mechanical flexibility, i.e. the electrode can be used horizontally, vertically, or inverted, and (d) the possibilities of miniaturization and micro fabrication. These have widened the applications for solid crystal membrane electrodes, especially in the fields of medicine and biotechnology.<sup>68</sup>

### **1.3 PROJECT AIMS**

The two main thrusts of the research are;

- (1) To fabricate novel and robust solid state electrodes for the monitoring of phosphates in solution. The effective recognition of the ion of interest in test solutions is entirely dependent on the membrane of the ion selective electrode. Ion selective electrodes are not ion specific. They can to some extent detect other ions in solution. Membrane selectivity to the ion of interest should be paramount when choosing the membrane compositions for the fabrication of the electrode.

- (2) To utilize the fabricated electrodes in mimicking phosphorylation and dephosphorylation reactions by utilizing model compounds.

#### 1.4 PROJECT APPROACH

This study is designed to follow three important steps;

- (1) Production of the different solid state ion selective electrodes (Details to be given in chapter three).
- (2) Conditioning of the phosphate selective electrodes, calibration studies, response time measurement, pH effect and interference studies.
- (3) Monitoring phosphorylation and dephosphorylation reactions: Model compounds\* were used to mimic phosphorylation and dephosphorylation reaction. The reactions monitored are; (a) the reactions between  $[\{\text{CoN}_4(\text{OH})(\text{OH}_2)\}]^{2+}$  and  $[\text{HPO}_4]^{2-}$  for 1:1, 2:1 and 3:1  $[\{\text{CoN}_4(\text{OH})(\text{OH}_2)\}]^{2+}$  to  $[\text{HPO}_4]^{2-}$  ratios. (b) the reactions between  $[\{\text{CoN}_4(\text{OH})(\text{OH}_2)\}]^{2+}$  and  $[\text{O}_2\text{NC}_6\text{H}_4\text{PO}_2(\text{O})(\text{OH})]^-$  (abbreviated as 4-NPP) for 1:1, 2:1 and 3:1  $[\{\text{CoN}_4(\text{OH})(\text{OH}_2)\}]^{2+}$  to 4-NPP ratios. (c) the reactions between  $[\{\text{CoN}_4(\text{OH})(\text{OH}_2)\}]^{2+}$  and  $[(\text{OH})_2(\text{PO}_2)_2\text{O}]^{2-}$  (abbreviated as  $[\text{H}_2\text{P}_2\text{O}_7]^{2-}$ ) for 1:1, 2:1 and 3:1  $[\{\text{CoN}_4(\text{OH})(\text{OH}_2)\}]^{2+}$  to  $[\text{H}_2\text{P}_2\text{O}_7]^{2-}$  ratios, and (d) the reactions between  $[\{\text{CoN}_4(\text{OH})(\text{OH}_2)\}]^{2+}$  and  $[(\text{OH})_2(\text{PO}_2)_3\text{O}_2]^{3-}$  (abbreviated as  $[\text{H}_2\text{P}_3\text{O}_{10}]^{3-}$ ) for the 1:1, 2:1 and 3:1  $[\{\text{CoN}_4(\text{OH})(\text{OH}_2)\}]^{2+}$  to  $[\text{H}_2\text{P}_3\text{O}_{10}]^{3-}$  ratios.

\* The model compounds utilized in this study are further explained in the experimental section.



## **1.5 THESIS ORGANIZATION**

### **Chapter One**

PROJECT BACKGROUND: This is the introduction to the thesis. It provides a summary of the background of the work, the aims, the approach and the thesis organization.

### **Chapter Two**

ANALYTICAL TECHNIQUES FOR THE DETERMINATION OF PHOSPHATES IN THE ENVIRONMENT: Current literatures on the subject matter are examined. Selected analytical techniques are discussed.

### **Chapter Three**

FABRICATION OF THE NEW PHOSPHATE SOLID STATE ION SELECTIVE ELECTRODES: Detailed description of the design and fabrication of the new solid state phosphate selective electrodes is given here. Results obtained for the conditioning of the electrodes, calibration curves, response time of the electrodes, and interference studies done for various cations and anions are also elaborately discussed.

### **Chapter Four**

MONITORING DEPHOSPHORYLATION AND PHOSPHORYLATION REACTIONS USING A NOVEL PHOSPHATE SOLID STATE ION SELECTIVE ELECTRODE: This chapter describe in detail the application of the selected solid state phosphate electrode

in monitoring dephosphorylation and phosphorylation reactions using model compounds.

## **Chapter Five**

GENERAL CONCLUSION AND RECOMMENDATION: This last chapter states the conclusions drawn from our work and suggests possible directions for future research.

# *CHAPTER TWO*

## **ANALYTICAL TECHNIQUES FOR THE DETERMINATION OF PHOSPHATES IN THE ENVIRONMENT: LITERATURE SURVEY**

### **2.0 INTRODUCTION**

The determination of phosphate species in environmental matrices provides essential data for assessing the health of ecosystems, investigating biogeochemical processes and monitoring compliance with legislation. In the environment, much emphasis has been laid on eutrophication and development of toxic algal blooms, which can have a major impact on global water quality.<sup>69</sup> For accurate measurements, knowledge of phosphate speciation is required as environmental behaviour is often critically dependent on its physico-chemical form. In the natural systems, phosphates are tightly cycled through the plant-soil continuum. Soil phosphates are removed in the crops or animal products and must be replaced if phosphate deficiency is to be avoided.<sup>70</sup> Therefore, mineral phosphate fertilizers and animal manures are applied to agricultural lands to increase the soil's phosphate levels and maintain crop yields. Phosphate fertilizers have been applied to agricultural lands with no concern over losses to water. The route taken by water as it carries phosphates off the land describes the pathway of phosphorus transfer.<sup>71</sup>

In aquatic systems, phosphates are found in dissolved, colloidal and particulate fractions as inorganic or organic compounds which may be biotic or abiotic particles.<sup>72</sup> Their concentrations in natural waters fluctuate with changes in physico-chemical conditions and biological activities. Seasonal changes in pH, dissolved carbon dioxide and total dissolved calcium concentration do affect its availability.<sup>73</sup> The common defined aquatic forms of phosphates and various terms used to describe them are shown schematically in the Figure 2.1 below.<sup>74</sup>

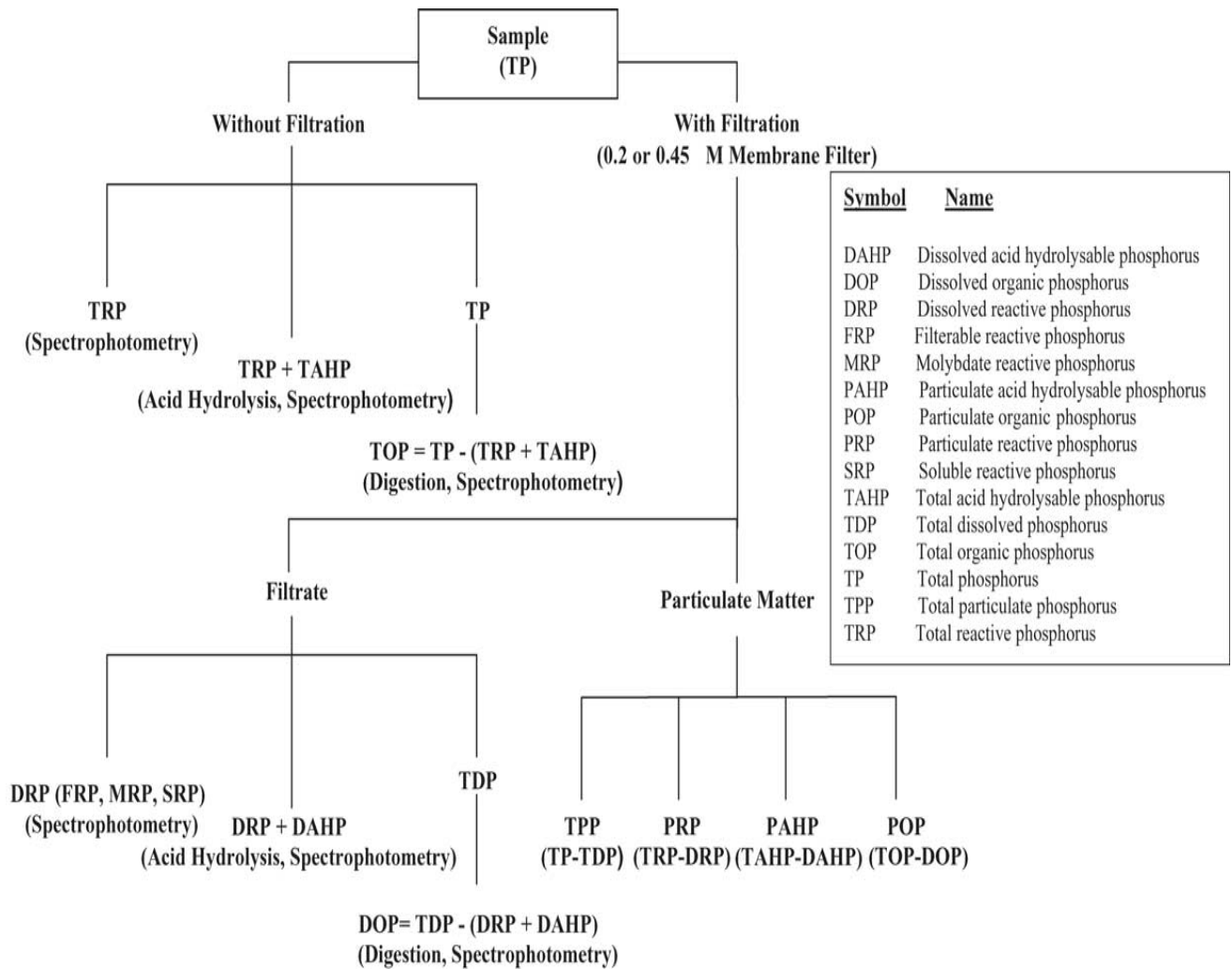


Figure 2.1 Aquatic phosphorus fractions (The reliability and comparability of data for any of these fractions will depend on the operational protocols used and the accuracy of the method).

The availability of organic phosphates to support microbial, plant and animal growth depends on the rate of their degradation to generate free phosphate. There are various enzymes such as phosphatases, nucleases and phytases that are involved in the degradation process. Some of the abiotic pathways involve hydrolytic and photolytic reactions. Enzymatic hydrolysis of organic phosphorus is an essential step in the biogeochemical phosphate cycle.<sup>75</sup> In biological systems, adenosine triphosphate (ATP) hydrolysis is the final link between the energy derived from food or sunlight and useful work. This enables the body to perform functions such as muscle contraction, the establishment of ion gradients across membranes and biosynthetic processes necessary to maintain life.<sup>76</sup> These reactions are monitored to give insight on energy transductions in biological systems. Biochemistry laboratories often use *in vitro* studies to explore ATP-dependent molecular processes. Enzyme inhibitors of ATP-dependent enzymes such as kinases are needed to examine the binding sites and transition states involved in ATP-dependent reactions. ATP analogs are also used in X-ray crystallography to determine a protein structure in complex with ATP, often together with other substrates. <sup>31</sup>P NMR studies have also been employed in the study of phosphates and phosphate containing compounds. These have substantially advanced the knowledge of phosphate content of soil, water and other environmental samples. Details of UV-Visible absorption spectroscopy and <sup>31</sup>P NMR are given below. These are followed by Ion Selective Electrode technique. This will rationalize why the quest for a phosphate sensitive electrode is an important undertaking.

## 2.1 COLORIMETRIC DETERMINATION OF PHOSPHATE

There is often a direct relationship between the intensity of the color of a solution and the concentration of the colored component (the analyte species) which it contains. This direct relationship forms the basis of the colorimetric technique. One might readily determine the concentration of a sample based on its color intensity, simply by comparing its color with those of a series of solutions of known concentration of the analyte species. In some cases, the color of the solution may be due to an inherent property of the analyte itself. For example, a potassium permanganate ( $\text{KMnO}_4$ ) solution has a natural purple color, the intensity of which can be readily measured. Most of the species in water do not have any color, meaning that the species do not absorb light in the visible region. To measure the absorbance of the colorless molecules, a reaction must be found which will produce color that can be monitored. Many approaches are available and the most widely used are:

- (1) Reaction between the species and a reagent to produce a new compound which has one or more chromophores.
- (2) Chelating the species to produce a complex with a different color than either the species or the original chelant.
- (3) Using a colored compound which is bleached by the species being analyzed.
- (4) Forming an intermediate compound that can be oxidized or reduced afterwards to give a colored compound.

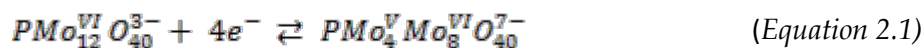
Developing a test solution for colorimetry includes finding the optimum pH for reaction, color development, masking of possible interferences and determination of optimum time for measurement. Intensity of coloured solutions is normally measured with a spectrophotometer. A beam of light of intensity  $I_0$  is focused on a sample, and a portion of the light,  $I$ , is absorbed by the analyte species. The amount of light absorbed may be mathematically expressed as  $A = \log I_0 / I$ . The absorbance,  $A$ , is related to concentration by the Beer-Lambert law:  $A = \epsilon cl$ , which states that the absorbance of a solution is directly proportional to its concentration,  $C$ , as long as the solution path length,  $l$ , and the wavelength of measurement are constant. Once the Beer-Lambert law is obeyed, a plot of absorbance against concentration will give a straight line, the slope of which is the molar absorptivity,  $\epsilon \times$  path length.<sup>77</sup>

Phosphates readily react with ammonium molybdate in the presence of suitable reducing agents to form coloured complexes. The phosphomolybdate complexes obey Beer's law and hence can be used for quantitative determination of phosphates in the analyte.

### 2.1.1 METHODS FOR MEASURING ORTHOPHOSPHATE: THE PHOSPHOMOLYBDATE COMPLEX ROUTE

Earlier methods of orthophosphates measurements are given by Strickland and Parsons<sup>78</sup>. Standard methods<sup>75,77,79</sup> are based on reaction of orthophosphates with acidic molybdate, to form 12-molybdophosphate ( $PMo_{12}O_{40}^{3-}$ ). A good example is the yellow ammonium phosphomolybdate,  $(NH_4)_3PMo_{12}O_{40}$ .<sup>118</sup> The phosphorus atom in the anion

is termed the hetero-atom,<sup>79</sup> and the heteropoly-molybdenum complexes are based on the *keggin* structure. The 12-molybdophosphate anion has a *α-keggin* structure.<sup>80</sup> It is reduced by ascorbic acid (C<sub>6</sub>H<sub>8</sub>O<sub>6</sub>) or tin(II) chloride (SnCl<sub>2</sub>) to form a strongly blue colored molybdophosphate species with uncertain concentration ratio of Mo(IV) and Mo(VI). The blue color arises because the near colorless molybdophosphate anion,  $PMo_{12}O_{40}^{3-}$  can accept more electrons (to be reduced) to form an intensely colored mixed valence complex. Literature cited that the blue color is probably due to partial reduction of the peripheral molybdenum atoms. Reduction of these peripheral molybdenum atoms is not complete, only about 20-25% is generally reduced.<sup>81</sup> This can occur in one electron or two electron steps. The reduction process is reversible and the structure of the anion is essentially unchanged. The blue complex produced is a *β-keggin* ion  $PMo_{12}O_{40}^{7-}$  with maximum UV-Visible absorption at 880 nm.<sup>82</sup>



The anion  $PMo_4^V Mo_8^{VI}O_{40}^{7-}$  has been determined in solid state and is a *β-isomer* i.e. with one of the four groups of edge shared octahedra on the *α-keggin* ion rotated through 60 degrees.<sup>82,83</sup>

Molybdophosphate reactions were first reported by Osmond in 1887 and have been the subject of considerable empirical scrutiny.<sup>84</sup> The absorbance of the colored species has been examined as a function of; known interferences, volumes of sample and reagent, acidity, molybdate and reductant concentrations, time, reagent temperature and the



stoichiometry of the molybdophosphate.<sup>85</sup> Formation of 12-molybdophosphate is still the basis for many colorimetric methods of phosphate determination. Several modifications of this method have been reported. These usually involve the use of different reductants and acid strength in attempts to improve selectivity and stability of the blue chromophore produced.<sup>86,87</sup> The methods widely used for batch and some automated analyses are based on the work of Murphy and Riley.<sup>88</sup> They utilized ascorbic acid as a reductant with a catalyst of potassium antimonyl tartrate. This method is preferred because of its relative stability to temperature and salt concentration in the analyte.<sup>89</sup> Detection is achieved at either 660-690 nm or 880 nm depending on the nature of the molybdophosphate blue species being measured.<sup>85</sup> Positive interference may arise from arsenates whereas hexavalent chromium and nitrite interfere at low concentrations.<sup>87</sup> In natural waters, silicate is the most likely interfering anion. However, the proportion of acid and molybdate in the test solution are normally adjusted to minimize silicate interference.<sup>90</sup> Condensed phosphates do not form molybdophosphate; they must be subjected to prior hydrolysis. Therefore, preliminary hydrolysis step is included when total phosphates concentrations are required.

Methods based on spectrophotometric measurements as molybdophosphate suffer two main disadvantages; low sensitivity and interference from several anions. Solvent extraction using solvents such as 1-pentanol (amyl alcohol), 2-methyl-1-propanol (isobutanol), Butyl ethanoate (acetic acid) and benzene<sup>91</sup> either before or after the

reduction step is an obvious procedure for curbing interferences. Extraction with 2-methyl-1-propanol is relatively efficient in eliminating silicate interference<sup>90,91</sup> whilst enhancing sensitivity about ten-fold compared with methods not incorporating an extraction step. Unfortunately liquid-liquid extraction procedures are tedious and time consuming and are not widely used. The molybdophosphate species interacts with a number of basic dye compounds (e.g., malachite green, crystal violet and rhodamine 6G) in acidic solution to form extractable ion association complexes.

The extracted complexes may be quantified by either spectrophotometry or spectrofluorimetry. For example, a spectrophotometric method for sea water analysis has been described<sup>92,93</sup> based on extraction of a molybdophosphate-malachite green complex. Similarly, the ion association complex of vanadomolybdophosphate and malachite green has been used<sup>94</sup> to determine phosphate in river water. Ions commonly found in river water did not interfere and, in the case of silicate, interference was less than that found in the corresponding malachite green molybdophosphate procedure. The detection limit for both malachite green procedures is about  $0.0001 \text{ mgL}^{-1}$  of phosphate. Stability of the ion association complex is a problem unless stabilized by addition of a surfactant. The difficulty here relates to the availability of a suitable phosphate-free surfactant although poly-vinyl alcohol appears to be satisfactory. Malachite green methods are very sensitive and interference by co-existing ions is minimal, but they are tedious in routine operation due to the need for extraction. Colored molybdophosphate chromophores in solution are usually quantitatively

determined by absorption spectroscopy. In most cases the UV-Visible absorption spectrophotometer is utilized. A brief discussion is provided below.

### 2.1.2 UV-VISIBLE ABSORPTION SPECTROSCOPY

UV-Visible absorption spectroscopy (spectrophotometry) is usually employed as a quantitative and qualitative analytical technique for monitoring the colored phosphomolybdate complexes. For most absorbing species, absorption peaks do not appear as sharp lines at highly differentiated wavelengths, but rather as bands of absorption over a range of wavelengths. A typical explanation for this is that an electronic transition is frequently accompanied by vibrational transitions between electronic levels. This is the so called 'vibrational fine structure'. Thus, a photon with a little too much or too little energy to be accepted by the molecule for a pure electronic transition can be utilized for a transition between one of the vibrational levels associated with the lower electronic state to one of vibrational levels of a higher electronic state. For example, if the difference in electronic energy is  $E$ , and the difference in vibrational energy is  $e$ , then photons with energies  $E$ ,  $E + e$ ,  $E + 2e...$ ,  $E - e$ ,  $E - 2e...$  etc. will be absorbed.<sup>95</sup>

Furthermore, each of the many vibrational levels associated with the electronic states also have a large number of rotational levels associated with it. Thus, a transition can consist of a large electron component, a smaller vibrational element, and an even smaller rotational change. The rotational contribution to the transition has the effect of filling in the gaps in the vibrational fine structure. In addition, when molecules are

closely packed together as they normally are in solution, they exert influences on each other which slightly disturb the already numerous, and almost infinite energy levels, and blur the sharp spectral lines into bands.<sup>95</sup>

The effect on the absorption spectrum of a compound when diluted in a solvent will vary depending on the chemical structures involved. Generally speaking, non-polar solvents and non-polar molecules show the least effect. However, polar molecules exhibit quite dramatic differences when interacted with polar solvent. Interaction between solute and solvent leads to absorption band broadening and a consequent reduction in structural resolution and  $\epsilon_{max}$ . Ionic forms may also be created in acidic or basic conditions. Thus, care must be taken to avoid an interaction between the solute and the solvent. The conditions under which the sample is examined are chosen to keep reflection, scattering, and fluorescence to the minimum. In the ultraviolet and visible regions of the electromagnetic spectrum, the bands observed are usually specific enough to allow a positive identification of an unknown complex in solution. The absorption spectrum of a compound is one of its most useful physical characteristics, both as a means of identification (qualitative analysis) and of estimation (quantitative analysis).<sup>96</sup>

In theory, sample analysis using UV-Visible absorption spectroscopy involves the reading of the  $\epsilon$  values from already documented literature tables. In practice, values of  $\epsilon$  depend on instrumental characteristics. To circumvent this difficulty, a calibration curve study using standards of known concentrations are done. Plot of absorbance

readings versus standard concentrations are obtained and concentrations of the actual samples are read directly from the calibration graph.

UV-Visible absorption spectroscopy can also be used to study the kinetics of a reaction. The rate studies involve the measurement of the change in concentration of the different complexes formed in solution as a function of time. Spectrometric rate measurements involve the measurements of a fall or rise in absorption at a fixed wavelength. These measurements provide information on the change in concentration of either the reactant or product. Sample analysis using UV-Visible absorption spectroscopy is a very quick process compared to other techniques such as High Performance Liquid Chromatography (HPLC). The UV-Visible technique is non-destructive to the sample and has a high sensitivity for detecting organic and bio-inorganic compounds. However, stray light can be a problem for UV-Visible spectroscopy. A brief description of the principles and applications of UV-Visible absorption spectroscopy will be discussed in the next paragraph.

#### **2.1.2.1 PRINCIPLES OF UV-VISIBLE ABSORPTION SPECTROSCOPY**

The principles of UV-Visible spectroscopy center on the fact that molecules have the ability to absorb ultraviolet or visible light. This absorption corresponds to the excitation of outer electrons in the molecules concerned. These interactions of electrons are brought about by the selective absorption of electromagnetic radiation by the analyte molecules. When a molecule absorbs energy, an electron is promoted from the Highest Occupied Molecular Orbital (HOMO) to the Lowest Unoccupied Molecular

Orbital (LUMO). It should be noted that occupied molecular orbitals with the lowest energy are the sigma ( $\sigma$ ) orbitals, and then at a slightly higher energy are the pi ( $\pi$ ) orbitals and non-bonding orbitals (those with unshared pair of electrons but still at a higher energy). This is depicted in Figure 2.2 below.<sup>97</sup>

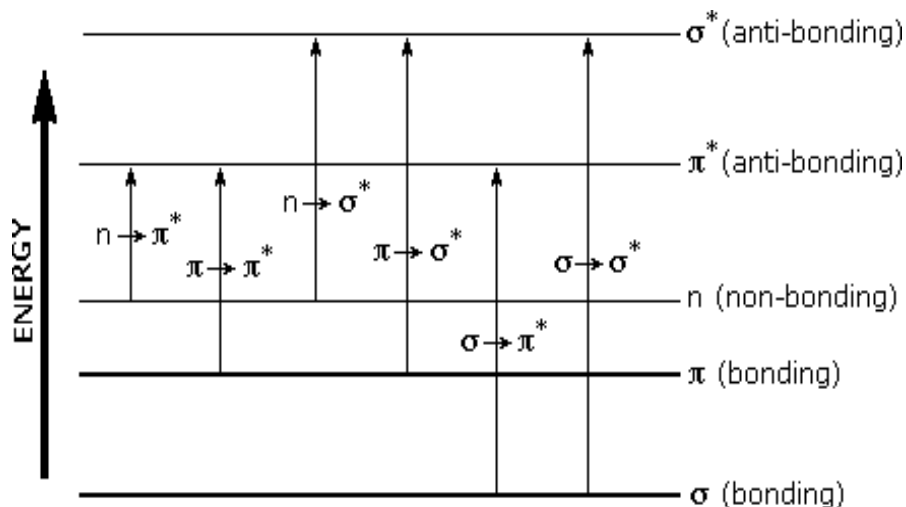


Figure 2.2 Electronic energy levels and transitions.

The highest energy orbitals belong to the  $\pi^*$  and the  $\sigma^*$ . The figure above shows  $\sigma \rightarrow \sigma^*$  and  $n \rightarrow \sigma^*$  transitions require relatively high energy, and are therefore associated with shorter wavelength radiation (ultraviolet). Lower energy  $n \rightarrow \pi^*$  and  $\pi \rightarrow \pi^*$  are ultraviolet or visible induced transitions. Peaks resulting from  $n \rightarrow \pi^*$  transitions are shifted to shorter wavelengths (*blue shift*) with increasing solvent polarity. This arises from increased solvation of the lone pair, which lowers the energy of the  $n$  orbital. Often (but not always), the reverse (i.e. *red shift*) is seen for  $\pi \rightarrow \pi^*$  transitions. This is caused by attractive polarization forces between the solvent and the absorber, which lower the energy levels of both the excited and unexcited states. This effect is greater for

the excited state. Hence, the energy difference between the excited and unexcited states is slightly reduced resulting in a small red shift. This effect also influences  $n \rightarrow \pi^*$  transitions but is overshadowed by the blue shift resulting from solvation of lone pairs. The probability that transition (and therefore absorption) will occur is closely related to molecular orbital structure. If the configuration of the molecular orbital is accurately known, the probability can be calculated with some degree of certainty. An estimate of the energy intensity made (relative to other transitions), and so is an indication of approximate value for the theoretical molar absorptivity of the species.<sup>98,99</sup>

Sometimes, the internal structure of a molecule may respond to radiant energy by more than just electronic transitions. In some molecules, the bonding electrons also have natural resonant frequencies that give rise to vibration while others exhibit rotation. This is because the difference in energy levels associated with vibration and rotation are much smaller than those involved in electronic transitions. Excitations will occur at corresponding longer wavelengths.<sup>100,101</sup>

### **2.1.2.2 FACTORS THAT AFFECT ACCURACY IN UV-VISIBLE ABSORPTION SPECTROPHOTOMETRY**

The ability of a spectrophotometer to measure accurately throughout its absorption range is impaired by a number of factors, chief of which is the inherent noise in the detector. It can be shown that instruments equipped with photo emissive detectors (phototube or photomultiplier) have minimum relative error when absorbance is 0.86. In practice the error will not be significant for any absorbance, except where light levels

are low e.g. at the extreme limits of any of the components of the system. If it is required to adjust the sample to bring absorbance within the preferred range, it is normally better to change the sample path-length rather than the concentration, e.g. by diluting. Note that spectrophotometers equipped with silicon diode detectors do not suffer from this limitation. In such instruments performance limits are usually dependent on stray light. A good instrument will measure absorbance up to 3 absorbance units with accuracy and reliability.<sup>96</sup>

There has been an increase in laboratory requirements to conform to good laboratory practice techniques. These require that results obtained can be traced back to an instrument and that the instrument can be proved to be working correctly, for validation purposes. For optimum results, one must take into consideration the effects of all variables both in instrument and operation. The effect of solvent, sample concentration, pH, temperature and spectral bandwidth / slit width in UV-Visible absorption technique is discussed below.

#### **2.1.2.2.1 EFFECT OF SOLVENT, SAMPLE PREPARATION, CONCENTRATION, pH, AND TEMPERATURE**

The ideal solvent for the preparation of sample solutions would dissolve all types of compounds, would be non flammable and nontoxic, and would be completely transparent at all wavelengths. Distilled water approaches the ideal but is not suitable for many non polar organic compounds. A number of factors like solvent used, concentration, pH, and temperature of the sample can affect the position and intensity



of absorption bands of molecules. These parameters should be controlled to ensure maximum precision and when comparing spectra measured under different conditions. The polarity of a solvent can modify the electronic environment of the absorbing chromophore. In general, the magnitude of the shift can be correlated with solvent polarity. Thus, for example, the absorption maximum of acetone can vary from 259 to 279 nm, depending on the solvent used. For comparative analysis, a single solvent should be used for all measurements.<sup>101</sup>

Concentration normally affects only the intensity of bands. At higher concentrations, however, molecular interactions (for example, dimerization) may cause changes in the shape and position of the absorbance band. These changes in turn affect the linearity of the concentration versus absorbance relationship and may lead to inaccurate quantitative results.<sup>246</sup>

The effects of pH on absorbance spectra can be very large and result primarily from the shifting of equilibrium between two different forms. For example, pH indicators visually change color at different pH values. If the spectrum of the sample under study is found to be affected by pH, a buffer should be used to control this parameter. Note, however, that most buffers themselves exhibit significant absorbance, which may affect the wavelength range over which measurements can be performed.<sup>247</sup>

Temperature can also affect UV-Visible absorption measurements. Simple expansion of the solvent, especially for some organic solvents, may be sufficient to change the apparent absorbance and thereby the accuracy of quantitative results. In addition,

temperature may affect equilibria, which can be either chemical or physical. A good example of a physical equilibrium is the denaturation of nucleic acids as temperature is increased, which changes absorptivity. Finally, notably for organic solvents, changes in refractive index with temperature can be significant. When convection currents cause different temperatures to occur in different parts of the cell, the resulting Schlieren (variations in the medium's density leading to variations in refractive index) effect can change the apparent absorbance. If temperature is found to have a significant effect on the measurements, the sample temperature should be controlled using a thermostated cell holder. This cell holder may be a simple water-jacketed holder used in conjunction with a circulating water bath, or a temperature controller. With organic solvents, it is advisable to use a stoppered cell to minimize the Schlieren effect.<sup>96,98-101</sup>

#### **2.1.2.2.2 EFFECT OF SPECTRAL BANDWIDTH AND BAND SLIT WIDTH**

The resolution of a spectrophotometer (i.e. the minimum separation between narrow absorption bands that can be observed) is usually limited by the spectral purity and intensity of the monochromator light output and the detector sensitivity at that wavelength. In some instruments the control of the energy level reaching the detector is achieved by adjusting the aperture of the slit at the monochromator exit. As the exit slit defines the spectral bandwidth (the range of wavelength) at the detector, it is important to realise that both photometric accuracy and wavelength accuracy may be affected. In general, narrower slit widths will reduce error provided the overall energy level remain adequate and electronic noise levels are insignificant. Most instruments using

diffraction gratings take advantage of the linear dispersion and provide fixed slit widths to give known and controlled bandwidth at the exit slit of the monochromator. More than one slit width may be available to give the user a means of trading energy against spectral sensitivity.<sup>102</sup>

### **2.1.2.2.3 OTHER METHODS FOR THE ANALYSIS OF ORTHOPHOSPHATE AND COMBINED PHOSPHATE.**

Over the years so many instrumental methods have been developed and utilized in the analysis of free orthophosphates and combined phosphates. Chromatographic method with gradient elution using an automated eluent generator has been developed for the simultaneous determination of orthophosphate, pyrophosphate, polyphosphate, trimetaphosphate and phytate in food products.<sup>103</sup> Indirect determination of inorganic phosphate in environmental samples has also been performed by Atomic absorption spectroscopy.<sup>104</sup> Electrophoresis method has been utilized by Dusek in the determination of phosphates in meat products.<sup>105</sup> Also, Wavelength Dispersive X-ray fluorescence (WDXRF) determination of phosphorus in food samples has been documented.<sup>106</sup> The use of visible (VIS), near infrared spectroscopy (NIRS) and Inductive Coupled Plasma Mass Spectroscopy (ICP-MS) to measure the concentration of phosphorus and other elements in wines,<sup>107</sup> and post mortem <sup>31</sup>P NMR study on meat done by Betram et al.<sup>108</sup>

The next section describes Phosphorus-31 Nuclear Magnetic Resonance (<sup>31</sup>P NMR) Spectroscopy as technique in monitoring phosphates. This technique identifies

phosphorus in a complex as a result of the chemical shift arising from the resonating phosphorus in the complex.

## 2.2 <sup>31</sup>P NMR SPECTROSCOPY

Phosphorus occurs predominantly as the isotope <sup>31</sup>P, which has a nuclear spin value of ½ and is therefore visible in nuclear magnetic resonance (NMR) spectrometry. It is 100% naturally abundant and reasonably good natural receptivity, 391 times larger than <sup>13</sup>C. Although 23 isotopes of phosphorus are known (all possibilities from <sup>24</sup>P to <sup>46</sup>P), only <sup>31</sup>P is stable. Phosphorus compounds (organic and inorganic) are found with phosphorus oxidation states ranging from -3 to +5. The most common oxidation states are +5, +3 and -3.<sup>109</sup> Phosphorus NMR (<sup>31</sup>P NMR) has been in use since the development of multinuclear, high-field Fourier-transform instruments in the late 1970s. The <sup>31</sup>P NMR method is widely used, with both one dimensional (1D) and multidimensional techniques, in such diverse areas as the characterization of organic and inorganic molecular structures, the analysis of biological fluids, the determination of intracellular pH, the noninvasive study of intact tissues and organs, and quantitative assays of industrial products.<sup>110</sup>

### 2.2.1 <sup>31</sup>P NMR CHEMICAL SHIFTS

The <sup>31</sup>P NMR chemical shift ( $\delta$ ) is a sensitive indicator of the chemical environment around the phosphorus atom. It relates closely to the molecular structure, and under some circumstances even facilitates stereo-chemical identification. It can be further

explained that this represents a change in resonance frequency of the nucleus, for a given value of its external magnetic field due to shielding from its environment. The unique chemistry of phosphorus is partially attributable to its variable oxidation state, the participation of d orbitals in bonding, and the ability of the phosphorus atom to vary its coordination number between 1 and 6. Phosphorus compounds give resonances in characteristic ranges depending primarily on the oxidation state and coordination number of the phosphorus atoms present. The chemical shift originates when a spinning charge generates a magnetic field that results in a magnetic moment proportional to the spin. In the presence of an external magnetic field, two spin states exist (for a spin  $\frac{1}{2}$  nucleus); one spin up and one spin down. One aligns with the magnetic field and the other opposes it. The difference in energy ( $\Delta E$ ) between the two spin states increases as the strength of the field increases. This excited state (paramagnetic contribution to shielding tensor) accounts for the observed phenomenon. The  $^{31}\text{P}$  NMR chemical shift has been extensively done by Gorenstein and Table 2.1 below elucidates his findings. The table shows chemical shifts obtained for selected inorganic compounds, organophosphorus compounds and biological compounds.<sup>110-112</sup>

Table 2.1 Chemical shifts ( $\delta$ ) ranges of selected phosphates and their derivatives.

Compounds/Class	General Structure	$\delta$ (ppm)	Comments
<b>Inorganic compounds</b>			
Orthophosphate		0.0	85% H <sub>3</sub> PO <sub>4</sub>
Protonated sodium tripolyphosphate		$\alpha = -11.5$	
[O <sub>3</sub> P <sub><math>\alpha</math></sub> OP <sub><math>\beta</math></sub> (O <sub>2</sub> )OP <sub><math>\alpha</math></sub> O <sub>3</sub> ] <sup>5-</sup> + 5H <sup>+</sup>		$\beta = -23.9$	
Protonated tetrapolyphosphate		$\alpha = -11.5$	
[O <sub>3</sub> P <sub><math>\alpha</math></sub> OP <sub><math>\beta</math></sub> (O <sub>2</sub> )OP <sub><math>\beta</math></sub> (O <sub>2</sub> )OP <sub><math>\alpha</math></sub> O <sub>3</sub> ] <sup>6-</sup> + 6H <sup>+</sup>		$\beta = -23.9$	
Phosphorus halides	PX <sub>3</sub>	97.0	X = F
		220	X = Cl
		178	X = I
H <sup>+</sup> + PF <sub>6</sub> <sup>-</sup>		-144	
[(CH <sub>3</sub> ) <sub>3</sub> Si] <sub>3</sub> C—P=As—C[Si(CH <sub>3</sub> ) <sub>3</sub> ] <sub>3</sub>		688	Coord. 2
(CH <sub>3</sub> ) <sub>3</sub> CP[Cr(CO) <sub>5</sub> ] <sub>2</sub>		1362	
P(NCO) <sub>6</sub> <sup>-</sup>		-388.4	Coord. 6
Gaseous P <sub>4</sub>		-552	
(CH <sub>3</sub> ) <sub>3</sub> SiC≡P		96	Coord. 1
FC≡P		-207	Coord. 1
<b>Organophosphorus compound</b>			
Aliphatic phosphate triesters	(RO) <sub>3</sub> P=O	2.1	R = CH <sub>3</sub>
		1.0	R = C <sub>2</sub> H <sub>5</sub>
		-0.7	R = <i>n</i> -C <sub>3</sub> H <sub>7</sub>
		-3.3	R = <i>i</i> -C <sub>3</sub> H <sub>7</sub>
		-1.0	R = <i>n</i> -C <sub>4</sub> H <sub>9</sub>
		-13.3	R = <i>i</i> -C <sub>4</sub> H <sub>9</sub>
Acyclic phosphonates	(RO) <sub>2</sub> RP=O	323.4	R = OCH <sub>3</sub>
		30	R = OC <sub>2</sub> H <sub>5</sub>
		27.4	R = C <sub>3</sub> H <sub>7</sub>
Acyclic phosphites	P—(OR) <sub>3</sub>	139.7	R = CH <sub>3</sub>
		137.6	R = C <sub>2</sub> H <sub>5</sub>

		137.5	R = <i>i</i> -C <sub>3</sub> H <sub>7</sub>
		138.1	R = <i>t</i> -C <sub>4</sub> H <sub>9</sub>
[CH <sub>2</sub> -P(C <sub>6</sub> H <sub>5</sub> ) <sub>2</sub> =P <sup>+</sup> -P(C <sub>6</sub> H <sub>5</sub> ) <sub>2</sub> -CH <sub>2</sub> ]		-232	Coord. 2
	R <sub>3</sub> P	-240	R = H
		-20.1	R = C <sub>2</sub> H <sub>5</sub>
		20.1	R = <i>i</i> -C <sub>3</sub> H <sub>7</sub>
		61.9	R = <i>t</i> -C <sub>4</sub> H <sub>9</sub>
<b><i>Biological compounds</i></b>			
Triose phosphates		4.13	
Adenosine 5-monophosphate (AMP)		3.44	
Orthophosphate		2.20	
Glycerol 3-phosphorylcholine		-0.13	
Phosphocreatine		-2.89	
Adenosine triphosphate (ATP)		$\alpha = -10.87$	
		$\beta = -20.50$	
		$\gamma = -6.19$	
Adenosine monophosphate (ADP)		$\alpha = -10.61$	
		$\beta = -6.33$	

All compounds listed are referenced to 85% H<sub>3</sub>PO<sub>4</sub> with downfield shifts defined as positive. Biological compounds are degassed perchloric acid muscle extracts at 37.7 ° C, pH 7.2, and K<sup>+</sup>counter ion. Co-ordination numbers are oxidation states are also listed.

Chemical shifts also depend on the pH, concentration and salt content of the solution, solvent effects, and the electronegativity of any substituent. Since the phosphorus atom is a comparatively reactive center, it can usually be found at or near an active site of interest. Phosphorus chemical shifts in general are referenced to a standard. This requires minor corrections to be made because of differences in the bulk properties of the samples. The primary <sup>31</sup>P NMR reference is 85% (H<sub>3</sub>PO<sub>4</sub>) phosphoric acid placed in a

sealed spherical container or cylindrical tube. Other external and internal standards have been utilized for specialized applications.<sup>110</sup>  $^{31}\text{P}$  NMR chemical shifts cover a wide range. Dissolved or gaseous diamagnetic phosphorus compounds span  $\sim 1900$  ppm. For dissolved paramagnetic phosphorus compounds, this range extends to  $\sim 2600$  ppm.<sup>113</sup> The  $^{31}\text{P}$  NMR chemical shift is not the only parameter available for probing the molecular environment of a phosphorus atom. The molecules can also be probed by their exhibition of spin-spin coupling.

### 2.2.2 $^{31}\text{P}$ NMR SPIN-SPIN COUPLING

$^{31}\text{P}$  NMR imparts spin-spin coupling ( $J$ ) information similar to a proton. Generally, coupling arises from the interaction of different spin states through the chemical bonds of a molecule and results in the splitting of NMR signals. This coupling provides detailed insight into the connectivity of atoms in a molecule. Pairs of phosphorus atoms can couple to each other and individual phosphorus atoms can couple to  $^{13}\text{C}$  and  $^1\text{H}$  atoms.  $^{31}\text{P}$ — $^{13}\text{C}$  and  $^{31}\text{P}$ — $^1\text{H}$  couplings are sensitive to the stereochemical relationship between the coupling nuclei. When used together with carbon chemical shifts, the conformation and stereochemical features of many chemical systems can be deduced. The  $^1\text{H}$ — $^{31}\text{P}$  couplings have been studied through one to four bonds and exhibit a dependence on the molecular conformation and geometry. Examples of the different types of couplings are shown in Table 2.2.<sup>111</sup>



Table 2.2 Typical <sup>31</sup>Phosphorus coupling constants

COMPOUND	PHOSPHORUS ATOM COUPLING CONSTANT (Hz, absolute value)
PH <sub>3</sub>	186 J <sub>PH</sub>
P(CH <sub>3</sub> ) <sub>3</sub>	2.7 J <sub>PH</sub>
F—C ≡ P	182 J <sub>PH</sub>
K <sup>+</sup> PF <sub>6</sub> <sup>-</sup>	710 J <sub>PF</sub>
PF <sub>5</sub>	~1000 J <sub>PF</sub>
OP(CH <sub>3</sub> ) <sub>3</sub>	68 J <sub>PC</sub>
P(CH <sub>2</sub> CH <sub>3</sub> ) <sub>2</sub>	13.7 J <sub>PCH</sub> 0.5 J <sub>PCCH</sub>
[O <sub>3</sub> P <sub>α</sub> OP <sub>β</sub> (O <sub>2</sub> )OP <sub>α</sub> O <sub>3</sub> ] <sup>5-</sup> + 5H <sup>+</sup>	16.7 J <sub>P<sub>α</sub>P<sub>β</sub></sub>
[O <sub>3</sub> P <sub>α</sub> OP <sub>β</sub> (O <sub>2</sub> )OP <sub>β</sub> (O <sub>2</sub> )OP <sub>α</sub> O <sub>3</sub> ] <sup>6-</sup> + 6Na <sup>+</sup>	19.9 J <sub>P<sub>α</sub>P<sub>β</sub></sub> 16.7 J <sub>P<sub>α</sub>P<sub>β</sub></sub>
Mo(CO) <sub>5</sub> P(OCH <sub>3</sub> ) <sub>3</sub>	217 J <sub>PMo</sub>
(EtO) <sub>2</sub> P(O)—SeP <sup>+</sup> (NEt <sub>2</sub> ) <sub>3</sub> —O(Se)P(OEt) <sub>2</sub>	17 <sub>2</sub> J <sub>PP</sub> 420 <sup>1</sup> J <sub>PP</sub>

The use of homonuclear and heteronuclear coupling constants and multinuclear (e.g., <sup>31</sup>P, <sup>1</sup>H and <sup>13</sup>C) NMR data allows the structure of monophosphorus and polyphosphorus compounds to be determined fully.<sup>114,115</sup> A good spin-spin coupling pattern of any <sup>31</sup>P NMR spectra will be expected to give rise to following:<sup>116</sup>

- (1) Each chemically different magnetic nucleus or set of nuclei will produce a peak or multiplet in a <sup>31</sup>P NMR spectrum. The multiplet will be symmetrical about its centre. E.g. in PF<sub>5</sub>, the <sup>31</sup>P nucleus will give rise to a multiplet and the equivalent (under thermal conditions) <sup>19</sup>F nuclei will give rise to a second multiplet.

- (2) Coupling of a magnetic nucleus  $A$  to  $N$  equivalent nuclei with spin  $I$  will split the signal from  $A$  into a multiplet consisting of  $2NI + 1$  peaks. For examples; Coupling to a single  $^1\text{H}$  nucleus will split the signal into  $2 \times 1 \times \frac{1}{2} + 1 = 2$  peaks. Coupling to 3 equivalent  $^1\text{H}$  nuclei (e.g. the protons in a methyl group) will give a multiplet consisting of  $2 \times 3 \times \frac{1}{2} + 1 = 4$  peaks. Coupling to 2 equivalent deuterium ( $^2\text{H}$ ) nuclei ( $I = 1$ ) will split the signal into  $2 \times 2 \times 1 + 1 = 5$  peaks.
- (3) The relative peak intensities for multiplet peaks arising from spin-spin coupling of a nucleus to  $N$  equivalent nuclei can be determined using Pascal's triangle.
- (4) To work out the multiplet pattern for the signal from a given type of nucleus, splitting from spin-spin coupling with surrounding nuclei must be applied consecutively. As an example let us consider the analysis of  $\text{CH}_2\text{FCH}_2\text{CH}_3$ . The  $\text{CH}_2\text{F}$  protons will be coupled to the F nucleus (spin  $-\frac{1}{2}$ ) through 2 bonds, and to the  $\text{CH}_2$  protons through three bonds. Four bond couplings to the  $\text{CH}_3$  protons can be ignored. Each of these  $\text{CH}_2\text{F}$  protons is spin-spin coupled to the other proton in the group, but this does not lead to a further splitting because the two protons have the same chemical shift. The F nucleus will split the signal into a doublet. The two equivalent  $\text{CH}_2$  protons will then split each line of the doublet into a triplet ( $2 \times 2 \times \frac{1}{2} + 1 = 3$ ). The  $\text{CH}_2\text{F}$  protons therefore give rise to a doublet of triplets in the spectrum. The  $\text{CH}_2$  protons will be coupled to the  $\text{CH}_2\text{F}$  protons, the F nucleus, and the  $\text{CH}_3$  protons. The peak will be split into 4 by the  $\text{CH}_3$  protons ( $2 \times 3 \times \frac{1}{2} + 1 = 4$ ). Each of these four peaks will be split into two by

the F nucleus, giving 8 peaks; and each of these 8 peaks will be split into three through coupling to the CH<sub>2</sub>F protons: there will be  $4 \times 2 \times 3 = 24$  peaks in total (note that there is no splitting due to coupling between the CH<sub>2</sub> protons because these have the same chemical shift). Finally, the CH<sub>3</sub> protons will give rise to a triplet through spin-spin coupling to the CH<sub>2</sub> protons. The relative peak intensities can be determined using successive applications of Pascal's triangle.

- (5) In general, spin-spin couplings are only observed between nuclei with spin  $-\frac{1}{2}$  or spin  $-1$ . Nuclei with  $I > \frac{1}{2}$  (e.g. Cl, Br) have nuclear electric quadrupole moments in addition to magnetic dipole moments. The reason that couplings involving these nuclei are often not observed is that quadrupole interactions with molecular electric field gradients provide a fast relaxation pathway, which means that other nuclei only ever 'see' these quadrupolar nuclei in their ground spin state (i.e. the nuclei are effectively decoupled). To understand the factors that determine whether or not coupling will be observed to such nuclei requires a little bit of theory about quadrupole interaction as given in the literature.<sup>116</sup>

### 2.2.3 TYPICAL <sup>31</sup>P NMR INSTRUMENTATION AND SAMPLE REQUIREMENTS

Many modern NMR spectrometers are capable of operating in multinuclear mode, and <sup>31</sup>P NMR can be performed in most cases simply by tuning the NMR probe to the phosphorus frequency and carrying out the necessary calibrations. The signal-to-noise ratio is dependent on many variables. These includes; the volume of sample, the magnetic field strength ( $B_0$ ), the magnetic probe design, spectral accumulation time,

relaxation times  $T_1$  and  $T_2$ , and sample concentration. Some of these variables can be controlled by the instrument operator. With the wide range of available instruments,  $^{31}\text{P}$  NMR can be performed on samples ranging in size from a few microliters ( $\mu\text{L}$ ), through a few tenths of a milliliter to several milliliters, using respectively a microprobe, a 5 mm probe, and a 10 mm probe.<sup>110</sup>

When the operation is limited to a given sample and a single type of instrument, the most sensitive probe for  $^{31}\text{P}$  measurements should be chosen. The sample should be concentrated as much as possible, since this helps to decrease accumulation time and improve sample throughput. Sample viscosity can be an issue if trying to dissolve too much material. This can cause broader signals and poor peak resolution. Nevertheless, reasonable spectra can be obtained with sample concentrations in the range of 1 mmol/L to 5 mmol/L. When faced with dilute samples, proper presentation of the sample and accurate spectrometer calibrations are particularly important. The sample should be mobile rather than bound, deoxygenated, and free of particulates. The removal of particulates by filtration makes a significant improvement to spectral quality.<sup>113</sup>

High-resolution solution work usually requires dissolution in a deuterated solvent for instrumental locking. However, excellent spectra can often be obtained in protonated solvents in the presence of a concentrically placed sealed capillary tube containing the deuterated solvent. This approach is unsuitable for intact biological samples where the NMR probe and coil assembly is designed around the specimen. As with other nuclei,

the highest  $^{31}\text{P}$  signal-to noise ratio is obtained when the following operations are performed:<sup>117</sup>

- (1) Optimization of magnetic field homogeneity (shimming).
- (2) Calibration of the observe coil  $90^\circ$  pulse width ( $\pi/2$ ).
- (3) Determination of the inherent relaxation times of the sample ( $T_1$ ) and the ensuing pulse repetition rate.
- (4) Choice of sufficient numbers of data points to digitize the data adequately.
- (5) Collection of sufficient time-averaged transients.

## 2.3 ION SELECTIVE ELECTRODES

An ion-selective electrode (ISE), also known as a specific ion electrode or ion sensitive electrode is a sensor that converts the activity of a specific ion dissolved in a solution into an electrical potential, which can be measured by a voltmeter or pH meter. The potential of an ion selective electrode is measured relative to a reference electrode when immersed in the sample solution that contains the analyte. This is conventional to potentiometric ionic determinations based on measuring the potential of electrochemical cells under no current flow. Potentiometric measurements are used to monitor titration reactions. However it is possible to use indicator electrodes (ISEs) to measure the analyte concentration directly (i.e. without titration) using a calibration

curve or standard addition approach. Under the negligible current flow, the measured potential is given by;<sup>77</sup>

$$E_{\text{measured}} = E_{\text{indicator}} - E_{\text{reference}} + \Sigma E_j \quad (\text{Equation 2.2})$$

Where  $\Sigma E_j$  is the sum of the potentials across all the liquid junctions in the circuit. Direct potentiometric determinations are mostly performed using ion selective electrodes.

Electrochemical reactions involve electron transfer among a metal electrode and species in solution. Under equilibrium conditions, such a process gives rise to a characteristic electrode potential which is dependent on solution composition and can, in principle, be used for analytical applications. However, if more than one redox systems are present in the solution, the potential-composition may be very intricate and of low analytical utility. In other words, electron-transfer reactions are, as a rule, not sufficiently selective for direct application in chemical sensors design. More selective response occurs when ion transfer among distinct phases occurs, for example,  $H^+$  transfer among a water sample and the surface of a pH-sensitive glass electrode. This is the key principle of the potentiometric membrane sensors. Such a sensor consists of an ion-selective membrane in contact with two solutions:

***Reference Electrode 1 | Solution 1 || Membrane || Solution 2 | Reference electrode 2***

For practical purposes, the membrane along with the reference electrode 2 and solution 2 (internal reference and solution, respectively) are assembled into a single body that represents the sensor itself. Such a device is often called an ion-selective electrode.

Although not rigorous, this term is still widely used. In other words, Ion selective electrodes are relatively simple potentiometric devices which are capable of accurately measuring the activity of ions in solution.

### 2.3.1 TYPICAL CONFIGURATION OF AN ION SELECTIVE ELECTRODE

Several types of ion selective electrodes are commercially available for the determination different ions in solution.<sup>118-123</sup> They are configured based on the ion of interest, the sensing materials and sensing methodology. A typical ion selective electrode (ISE) has a membrane that allows the passage of specific ions and is attached to a tube that contains an internal reference electrode. In some specifications, the membrane needs a binding agent. As shown in Figure 2.3 below;

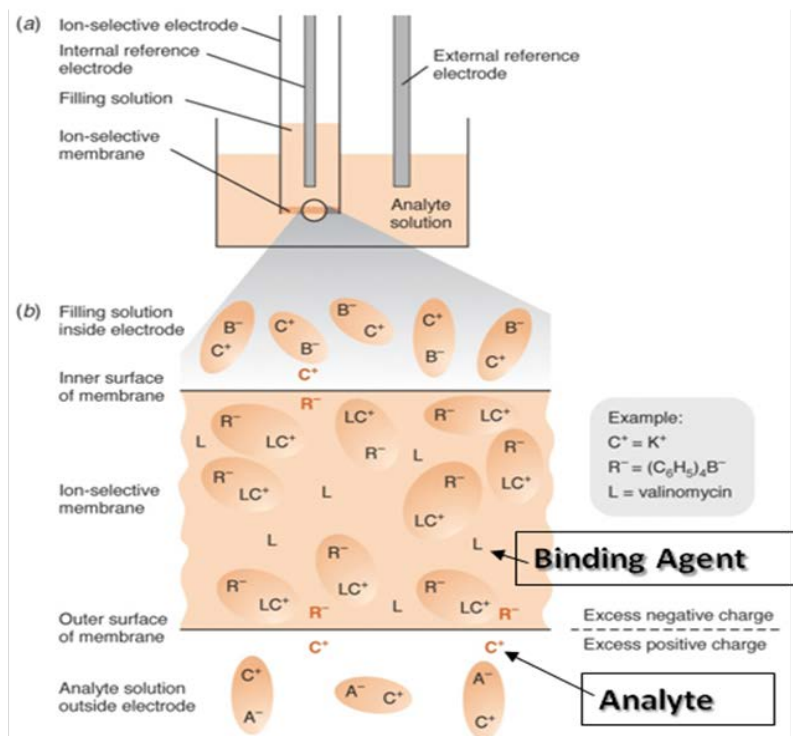
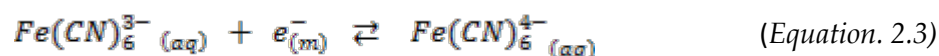


Figure 2.3 A cross section of a typical ion selective electrode.<sup>135</sup>

The nature of the membrane determines the selectivity of the electrode. A membrane is considered to be a material that separates two solutions. It is across this membrane that the charge develops. The term "membrane" is often confused as implying permeability. While this is true in many cases, the term here is used to denote a material where a charge can develop across. The measured potential is proportional to the activity of the ion in solution.<sup>124,125</sup> This potential is measured against a stable reference electrode of constant potential. The potential difference between the two electrodes will depend upon the activity of the specific ion which is related to the concentration of the specific ion in solution. Handheld or portable configurations allow ion selective electrodes to be used with ease in laboratories, where the operator may be testing several different samples. The electrodes may have many different types of membranes. Each type of membrane has its own unique characteristics that make it the best choice for a particular application. The most common choices for membranes are glass, solid state, liquid-ion exchange, PTFE/gas sensing (polytetrafluoroethylene), ISFET (ion-sensitive field effect transistor) and plastic.

### 2.3.2 ELECTRON TRANSFER AT THE SOLUTION-ELECTRODE INTERFACE

The ideas behind the development of electrode potentials at the solution–electrode interface can be examined considering the energy levels associated with the species involved in the potential determining equilibrium by using the following reaction as example.





Such an equilibrium can be established by preparing a solution containing both potassium hexacyanoferrate(II) ( $K_4Fe(CN)_6$ ), and potassium hexacyanoferrate(III) ( $K_3Fe(CN)_6$ ) dissolved in water and then inserting a wire (an electrode) made of platinum or another inert metal into the solution. The pertinent energy levels are shown in Figure 2.4 below.<sup>126,127</sup>

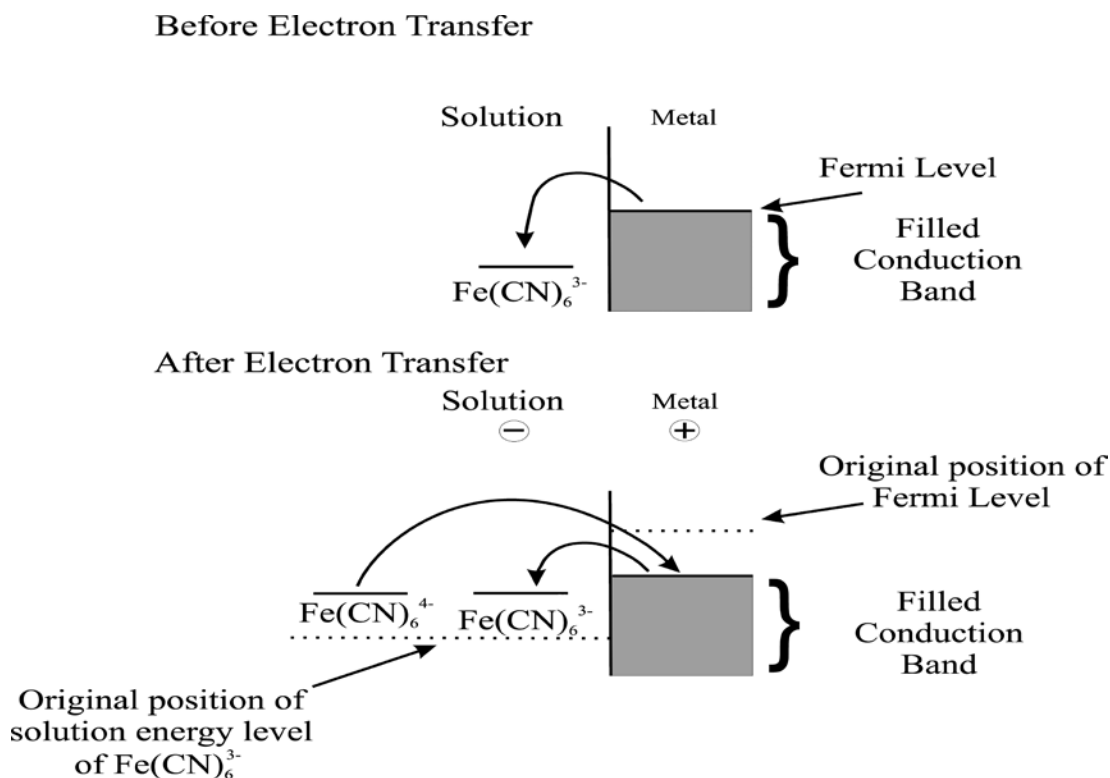


Figure 2.4 The energy of electrons in the ions in solution and in the metal wire.<sup>126</sup>

The electronic structure of a metal involves electronic conduction ‘bands’ in which the electrons are free to move throughout the solid, binding the (metal) cations together. The energy levels in these bands form an effective continuum of levels which are filled up to an energy maximum known as the Fermi level. In contrast, the electronic energy levels associated with the solution phase  $Fe(CN)_6^{3-} (aq)$  and  $Fe(CN)_6^{4-} (aq)$  ions are

discrete and relate to an unfilled molecular orbital in  $Fe(CN)_6^{3-}_{(aq)}$ , which gains an electron to form  $Fe(CN)_6^{4-}_{(aq)}$ . The addition of an electron to  $Fe(CN)_6^{3-}_{(aq)}$  alters the solvation of the ion so that the electron energy has a different value in the two complexes even though the same molecular orbital is involved. The figure above shows that the Fermi level is higher than the vacant orbital in the  $Fe(CN)_6^{3-}_{(aq)}$  ion before electron transfer takes place between the electrode and the solution. It is accordingly energetically favorable for electrons to leave the Fermi level and join the  $Fe(CN)_6^{3-}_{(aq)}$  species converting them to  $Fe(CN)_6^{4-}_{(aq)}$  ions in the process. This energy difference is the driving force of the electron transfer. As this electron transfer proceeds, positive charge must build up on the electrode (metal) and corresponding negative charge in the solution phase. The Fermi level becomes progressively lower as the electronic energy in the metal is lowered.

Correspondingly, the generation of negative charge in the solution must raise the (electronic) energy levels of the solution phase species. Ultimately, a situation is reached when the Fermi level lies in between the energy levels of the two ions, so that the rate at which electrons leave the electrode and reduce  $Fe(CN)_6^{3-}_{(aq)}$  ions is exactly matched by the rate at which electrons join the metal from the  $Fe(CN)_6^{4-}_{(aq)}$  ions which become oxidized. As we have noted before, this situation corresponds to dynamic equilibrium and once it is attained, no further net charge is possible. However, at the point of

equilibrium, there is a charge separation between the electrode and the solution, and this is the origin of the electrode potential established on the metal.<sup>127-130</sup>

### 2.3.3 THE NERNST EQUATION

It is a known fact that the position of chemical equilibrium is controlled by the chemical potentials of the reactants and products. The reason for this is that electrochemical equilibrium involves the transfer of a charged particle - the electron, between two phases (the solution and the electrode) which may have two different electrical potentials. Accordingly, the electrical energy of the electrons differs from one phase to another.

In a redox reaction, the energy released in a reaction due to movement of charged particles gives rise to a potential difference. The maximum potential difference is called the electromotive force (EMF),  $E$  and the maximum electric work  $W$ , is the product of charge  $q$  in Coulomb (C), and the potential  $E$  in Volt (= J/C) or EMF.<sup>77,131</sup>

$$W = q E \quad (\text{Equation 2.4})$$

The EMF ( $E$ ) is determined by the nature of the reactants and electrolytes, not by the size of the cell or amount of material in it. The amount of reactants is always proportional to the charge of the reactants. The change in Gibb's free energy is related to Work  $W$  as the negative value of maximum electric work.

$$\begin{aligned} \Delta G &= -W \\ &= -q E \end{aligned} \quad (\text{Equation 2.5})$$

A redox reaction equation represents definite amounts of reactants in the formation of definite amounts of products. The number ( $n$ ) of electrons in such a reaction equation is related to the amount of charge transferred when the reaction is completed. Since each mole of electron has a charge of 96,485 C (Faraday constant  $F$ );

$$q = nF \quad (\text{Equation 2.6})$$

And,

$$\Delta G = -nFE \quad (\text{Equation 2.7})$$

At standard conditions

$$\Delta G^\circ = -nFE^\circ \quad (\text{Equation 2.8})$$

The general Nernst equation correlates the Gibb's Free Energy  $\Delta G$  and the EMF of a chemical system. So for the reaction;



$$Q = \frac{[C]^c [D]^d}{[A]^a [B]^b} \quad (\text{Equation 2.10})$$

It has been shown that;

$$\Delta G = \Delta G^\circ + RT \ln Q \quad (\text{Equation 2.11})$$

Recalling *equations 2.7 and 2.8*, we have;

$$-nF\Delta E = -nF\Delta E^\circ + RT \ln Q \quad (\text{Equation 2.12})$$

Where  $R$ ,  $T$ ,  $Q$  and  $F$  are the gas constant ( $8.314 \text{ J mol}^{-1}\text{K}^{-1}$ ), temperature (in Kelvin), reaction quotient, and Faraday constant (96,485 C) respectively. Thus we have;

$$\Delta E = \Delta E^\circ - \frac{RT}{nF} \ln \frac{[C]^c [D]^d}{[A]^a [B]^b} \quad (\text{Equation 2.13})$$

For a typical ion selective electrode, if we describe the electric potential difference across the boundary between the membrane and analyte solution. The potential difference between the analyte solution and the solution inside the ISE is given as;

$$E = E_{out} - E_{in} = \frac{\Delta G_{solvation}}{nF} - \frac{RT}{nF} \ln \frac{[C]_{membrane}}{[C]_{out}} - E_{in} \quad (\text{Equation 2.14})$$

But most of the parameters in the equation are constants ( $\frac{\Delta G_{solvation}}{nF}$ ,  $[C]_{membrane}$ ,  $E_{in}$ ) for a particular electrode system, the Nernst equation can now be written as;

$$E = \text{constant} + \frac{RT}{nF} \ln [C]_{out} \quad (\text{Equation 2.15})$$

In practice, using the Nernst equation in potentiometric measurements involves at least one reference electrode whose composition and potential are fixed. Most measurements will include the use of a calibration plot for which only the magnitude of measured potential is related directly to analyte activity.<sup>77,131</sup>

### 2.3.4 CLASSIFICATION OF ION SELECTIVE ELECTRODES

It is quite important to note that ion selective electrodes come in different sizes and shapes. Each electrode has its own distinct characteristic feature depending on intentions of fabrication and manufacturer's interest. Though many texts may claim to clearly elucidate the internal construction of their electrode system, few actually give details of their composition and hence retain sole knowledge of their inventions. The

withheld information mostly controls the performance of the electrode. Nevertheless, there are certain features that are common to all. They consist of a cylindrical tube of each inventor's size and length specifications; an external membrane is fixed at one end so that the external solution can only come in contact with the outer surface and the other end is fitted with a low noise cable or a good conductive wire for connection to the millivolt measuring device. In some cases the internal connections are completed by a liquid or gel electrolyte, in others by an all solid state system.<sup>132</sup>

Several types of sensing electrodes are commercially available for various cations and anions. They are classified by the nature of the membrane material used to construct the electrode. It is this difference in membrane construction that makes an electrode selective for a particular ion. The major classifications of ion selective electrodes are metallic and membrane. Detailed discussion follows:

#### **2.3.4.1 METALLIC ELECTRODES**

There are four types of metallic electrodes: electrodes of the first, second and third kinds, and redox electrodes.<sup>77,133</sup>

##### **2.3.4.1.1 ELECTRODES OF THE FIRST KIND**

An electrode of the first kind is a pure metal electrode that is in direct equilibrium with its cation in the solution. A single reaction is involved. For example, the equilibrium between a metal X and its cation  $X^{n+}$  is;



For which,

$$E_{\text{ind}} = E_{X^{n+}/X}^{\circ} + \frac{0.0592}{n} \log a_{X^{n+}} \quad (\text{Equation 2.17})$$

Where  $E_{\text{ind}}$  is the electrode potential of the metal electrode and  $a_{X^{n+}}$  is the activity of the ion (or in dilute solution, approximately its molar concentration,  $[X^{n+}]$ ). The electrode systems of the first kind are not widely used for potentiometric measurement. They are not very selective. They respond not only to their own cations but also to other easily reduced cations. In addition, many first kind metal electrodes can only be used in neutral or basic solutions because they dissolve in the presence of acids. Furthermore, the surface of the metal itself can be oxidized in the presence of oxygen making it to give erroneous results at low ion activities. The use of certain hard metals like iron, chromium, cobalt, and nickel as electrodes of the first kind gives irreproducible potentials. The most widely used electrodes of the first kind in neutral solutions are Ag/Ag<sup>+</sup> and Hg/Hg<sup>2+</sup> electrodes. Although Cu/Cu<sup>2+</sup>, Zn/Zn<sup>2+</sup> and Pb/Pb<sup>2+</sup> electrodes are used in deaerated solutions.<sup>77</sup>

#### **2.3.4.1.2 ELECTRODES OF THE SECOND KIND**

An electrode of the second kind consist of a metal immersed in a saturated solution containing one of its sparingly soluble salts or coated with such a salt. This electrode is responsive to the anion of the metal salt despite the absence of direct electron transfer between the anion and the electrode. The activity of the free metal ion (to which the electrode does respond via a direct electron transfer) is controlled by complexation or

precipitation with the anion. Thus, the observed potential can be related indirectly to the activity of the anion. This type of electrode system has selectivity problems. Any other anion present that can form an insoluble salt or complex with the metal ion will interfere with the measurement of the targeted ion. A typical example is the Ag/AgCl electrode.<sup>133</sup>

#### **2.3.4.1.3 ELECTRODES OF THE THIRD KIND**

Electrodes of this kind depend also on solution equilibria, but in this case two solution equilibria are involved. These electrodes respond to a cation other than that of the electrode metal. In order for this electrode to respond properly, the complex between the metal cation and the anion must be more stable than the complex between the targeted cation and anion, and there must be an excess of uncomplexed cation in solution. One example of this type of electrode is the mercury electrode with ethylenediaminetetraacetic acid (EDTA) as the common anion that responds to calcium. Although this dual equilibria electrode is useful for pure samples, there are too many sources of interferences for electrodes of the third kind to function well in complex matrices.<sup>133</sup>

#### **2.3.4.1.4 REDOX ELECTRODES**

An electrode of the first kind or second kind develops a potential as the result of a redox reaction involving a metallic electrode. An electrode also can serve as a source of electrons or as a sink for electrons in an unrelated redox reaction, in which case we call



it a redox electrode. These types of inert metallic electrodes respond to redox systems. An inherent advantage of potentiometry is the ability to measure the activity of an analyte (rather than simply measuring molecular concentration). Hence, the determination of an analyte in various oxidation states is possible, as the potential depends on the ratio of activities of both species in a redox couple. Inert metals respond to redox systems. Examples are gold, palladium and platinum.<sup>133</sup> Note that a redox electrode's potential often responds to the activity of more than one ion, which can limit its usefulness for direct potentiometry.

#### **2.3.4.2 MEMBRANE ELECTRODES**

Membrane electrodes are sometimes called the p-ion electrodes because the data obtained from them are usually presented as p-functions, such as pH, pCa or pNO<sub>3</sub>. In this section, we will consider several types of p-ion membranes. However, it should be noted that most membrane electrodes are fundamentally different from metal electrodes both in design and in principle. A brief description of the general classes of membrane electrodes and their specific configurations are given below.

##### **2.3.4.2.1 CRYSTALLINE ELECTRODES**

These electrode types contain in their membranes mobile ions of one sign and fixed sites of opposite sign. They can be *homogenous* - in which the membrane is a crystalline material prepared from either a single compound of sparsely soluble salt incorporated in a suitable inert binder or a homogenous mixture of compounds, or *heterogeneous* - in

which they contain an active substance, or mixture of active substances, mixed with an inert matrix (silicone rubber or polyvinyl chloride, PVC) or placed in hydrophobized graphite or conducting epoxy resin to form a heterogeneous sensing membrane. In practice, these electrodes are applied in non saturated solutions, so that the insoluble membrane slowly dissolves. Insoluble inorganic materials as:  $\text{Ag}_2\text{S}$ ,  $\text{CuS}$ ,  $\text{CdS}$ ,  $\text{PbS}$ ,  $\text{LaF}_3$ ,  $\text{AgCl}$ ,  $\text{AgBr}$ ,  $\text{AgI}$  and  $\text{AgSCN}$  have all been tested as cation exchange membranes, incorporated into an electrode body in the form of single crystal or compressed powder discs. These materials are ionic conductors, though the conductivity is extremely small and mainly takes place through the migration of point defects in the lattice. The response time of these membranes can be increased by incorporating *aliovalent* (ions of different wavelengths) ions into the lattice (e.g. the fluoride-selective membrane, Lanthanum fluoride ( $\text{LaF}_3$ ) can be doped with Europium ( $\text{Eu}^{2+}$ ) ions).<sup>134</sup>

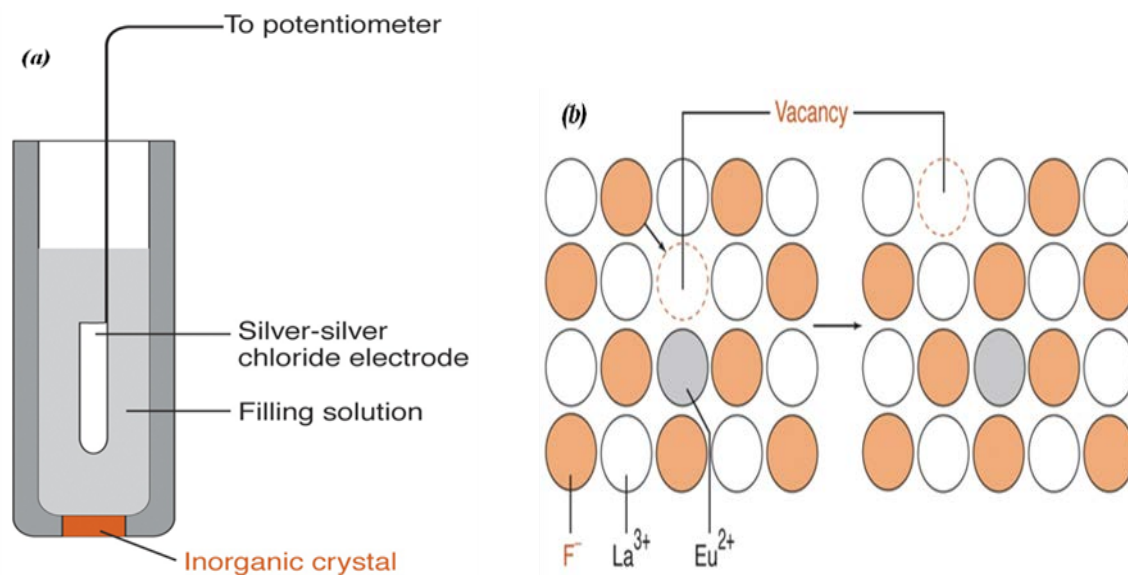


Figure 2.5 (a) A typical crystalline electrode. (b)  $\text{LaF}_3$  doped with  $\text{EuF}_2$ . This creates anion vacancies in the crystal and analyte, such as  $\text{F}^-$  can diffuse into the crystal and “jump” from one side to the other across the vacancies.<sup>135</sup>

Sensors for the detection of  $\text{Ag}^+$ ,  $\text{Cu}^{2+}$ ,  $\text{Cd}^{2+}$ ,  $\text{Pb}^{2+}$ ,  $\text{S}^{2-}$ ,  $\text{F}^-$ ,  $\text{Br}^-$ ,  $\text{I}^-$ ,  $\text{SCN}^-$  and  $\text{CN}^-$  ions can be constructed from such membranes. The sensitivity to ions of these electrodes arises from the dissolution equilibria at the membrane surface. The measurement ranges of such electrodes differ according to their real limits of detection. In some cases interference effects are frequently encountered. The fluoride electrode is a typical example of the crystalline electrode. The membrane consists of a single lanthanum fluoride crystal which has been doped with europium fluoride to reduce the bulk resistivity of the crystal.<sup>136-138</sup> It is claimed to be 100% selective for fluoride ions and is only interfered with by hydroxide. The hydroxide reacts with the lanthanum to form lanthanum hydroxide, with the consequent release of extra fluoride ions. This interference can be eliminated by adding a pH buffer to the samples to keep the pH in the range 4 to 8 and hence ensure a low hydroxide concentration in the solutions.

#### **2.3.4.2.2 NON-CRYSTALLINE ELECTRODES**

These electrodes have a support matrix containing an ion exchanger (either cationic or anionic), a plasticizer solvent and possibly an uncharged, selectivity enhancing species. This forms the ion-selective membrane which is usually interposed between two aqueous solutions. The matrix can be either macroporous (poly (propylene carbonate) filter, glass frit etc.) or microporous (e.g. "thirsty" glass or polymeric material like PVC) and the solvent, a solidified homogeneous mixture. Response of this type of electrode is due to the presence of the selectivity-enhancing species (which exhibit an ion-exchange property) in the membrane. The non crystalline electrodes are further categorized based

on the nature of their matrix and predominant charges on the matrix membrane. The first of these is the *Rigid-Self Supporting Matrix Electrodes* - A typical example of this type of non crystalline electrode is the glass electrode (a synthetic cross linked polymer). The sensing membrane is a thin polymer with fixed sites or a thin piece of glass. The chemical composition of the polymer or the glass determines the membrane selectivity. The pH glass electrode in Figure 2.6 falls within this category.<sup>135,139</sup>

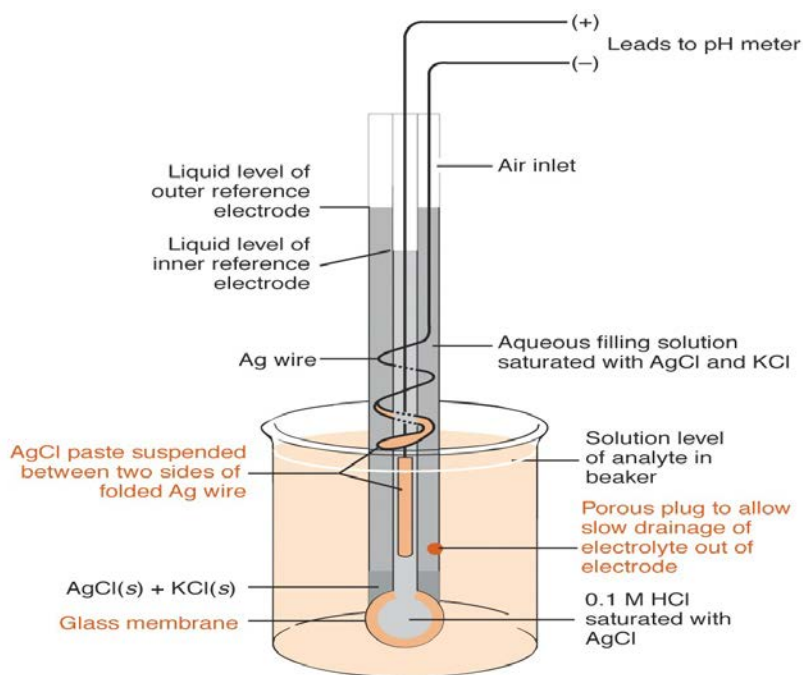
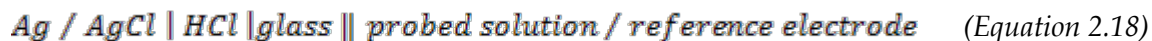


Figure 2.6 The pH meter (a glass electrode).<sup>135</sup>

A glass electrode is perhaps the most successful and ubiquitous electrochemical sensor. It provides information about the activity of hydronium ions,  $\text{H}_3\text{O}^+$ , in water. Water, which mildly dissociates to  $\text{H}_3\text{O}^+$  and  $\text{OH}^-$  ions, is the most common solvent medium, and chemical reactions in water largely depend on  $\text{H}_3\text{O}^+$  activity, the ability to measure it is essential. Conversely  $\text{H}_3\text{O}^+$  activity, or rather, its negative logarithm, the pH, is so

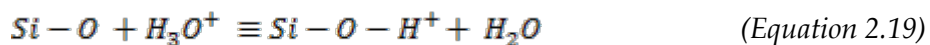
easy to measure, pH is the most commonly monitored and recorded parameter of liquid samples. A glass electrode consists of a glass bulb membrane, which gives it its name and an electrically insulating tubular body, which separates an internal solution and a silver/silver chloride electrode from the studied solution.<sup>140</sup>

The Ag/AgCl electrode is connected to a lead cable terminated with some connector that can hook up to a special voltmeter, the pH meter. The pH meter measures the potential difference and its changes across the glass membrane. The potential difference must be obtained between two points; one is the electrode contacting the internal solution. A second point is obtained by connecting to a reference electrode, immersed in the studied solution. Often, this reference electrode is built in the glass electrode (a combination electrode), in a concentric double barrel body of the device. It is a common misconception that the combination electrode requires only one lead, fostered because the round coaxial lead to the electrode looks like a single wire. This is not so. In any potentiometric measurement, and pH measurement is an example two inputs, one of which is a reference point. The completed glass electrode with a reference electrode cell is represented by the electrochemical shorthand;



The potential difference relevant to pH measurement builds up across the outside glass/solution interface marked ||. The key functional part, the glass membrane, is manufactured by blowing molten glass into a thin-walled bulb with a wall about 0.1 mm thick. The bulb is then sealed to a thicker glass or plastic tube, and filled, for

example, with a solution of HCl (0.1 mol/dm<sup>3</sup>). In this solution is immersed a silver/silver chloride electrode with a lead to the outside through a permanent hermetic seal. The filling solution has constant Cl<sup>-</sup> concentration, which keeps the Ag/AgCl inner electrode at fixed potential. The pH sensing ability of the glass electrode stems from the ion exchange property of its glass membrane. Glass is mostly amorphous silicon dioxide, with embedded oxides of alkali metals. When the surface of glass is exposed to water, some Si-O groups become protonated;

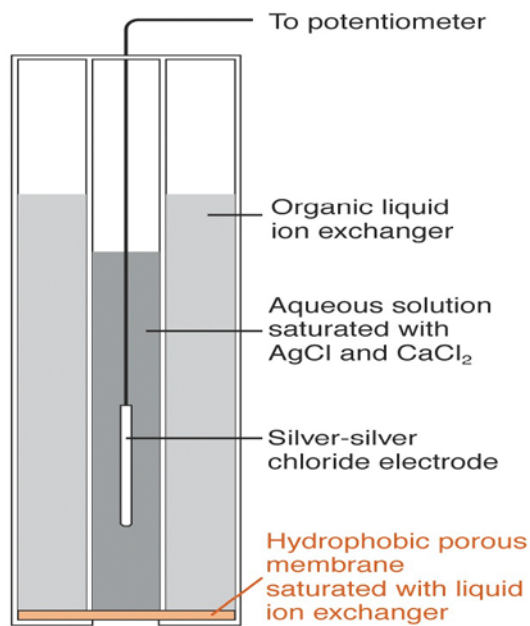


The exchange of hydronium (or written as proton, H<sup>+</sup>) between the solid membrane and the surrounding solution, and the equilibrium nature of this exchange, is the key principle of H<sub>3</sub>O<sup>+</sup> sensing. As with any interface separating two phases between which ionic exchange equilibrium is established, the glass membrane/solution interface becomes the site of a potential difference. The glass membrane has two wall/solution interfaces and there is potential buildup on each of them, with opposite polarity. But the pH inside the bulb is constant, because the internal solution is sealed. Therefore, the inner surface potential is constant, adding merely to an offset to the overall potential of the device. Additional contribution to the offset comes from potentials of the inner solution electrode, and the reference electrode, which are also constant. The changes in the device potential are therefore due entirely to the pH changes of the outside solution and the potential of the glass electrode/reference electrode setup is;

$$E_{\text{glass electrode}} = E_{\text{constant}} + \frac{2303 RT}{F} \log_a(H_3O^+) \quad (\text{Equation 2.20})$$

Where  $E^o$  represents the sum of the constant offset potentials of the inner glass surface/solution and the two Ag/AgCl electrodes.<sup>141</sup>

The second type of electrode under the non-crystalline electrodes is the group of *Electrodes with Mobile Charged Sites* also called the liquid membranes electrodes. They operate based on the classical ion-exchanger, neutral or charged carriers. These carriers are able to complex ions reversibly and transfer them through an organic membrane by carrier translocation. They are usually called ionophores or ion carriers. Among them are positively charged hydrophobic cations; quaternary ammonium cations or cations of substitutionally inert transition metal complexes of which when dissolved in suitable organic solvents and held in an inert support provide membranes which are sensitive to changes in the activities of anions. A good example is the  $Ca^{2+}$  electrode shown in Figure 2.7 below;<sup>135</sup>



*The membrane contains a hydrophobic species that is a chelator of Ca<sup>2+</sup>. Equilibration of Ca<sup>2+</sup> with the chelator establishes a voltage at the membrane-solution boundary related to Ca<sup>2+</sup>.*

Figure 2.7 The calcium electrode (a liquid based ISE).<sup>135</sup>

Negatively charged hydrophobic anions ( $(RO)_2PO_2^-$ ) also provide membranes which are sensitive to changes in cation activities. Uncharged carrier electrodes based on solutions of molecular complexing agents of cations (e.g. ion-dipole forming agents like antibiotics, macrocyclic compounds or other sequestering agents) and anions (e.g. adduct forming agents, such as organotin compounds, activated carbonyl compounds and porphyrins) are also known. The electrically neutral ionophores have found a wide field of application as components in ion selective liquid membrane electrodes. They are used in clinical chemistry,<sup>142,143</sup> electrophysiology<sup>144</sup> and as detectors in ion chromatography.<sup>145</sup>



#### 2.3.4.2.3 MULTIPLE MEMBRANES (MULTILAYER) ION SELECTIVE ELECTRODES (COMPOUND ELECTRODES)

Additional selectivity can be attained by using composite membranes, in which an enzyme present in the outer part of the membrane catalyses a specific chemical reaction to generate product ions. These ions can be detected by an internal ion-selective membrane. The well-known example is the selective detection of urea using urease as the enzyme catalyst. The ammonia generated, can then be detected by an ammonia or ammonium-selective electrode. Similarly, enzyme reactions generating protons can be followed with glass or other proton-selective membranes. There is a multiplicity of enzyme-electrodes that can be made in this way, with substrates including aliphatic alcohols, acetylcholine, amygdalin, asparagine, glucose, glutamin, penicillin and others.<sup>146</sup>

Compound or multiple membrane electrodes can be designed also as potentiometric gas sensors. The original concept was made for sensing carbon dioxide (*Severinghaus electrode*),<sup>147</sup> but the principle on which this electrode operates is general for other gas sensors for the detection of  $\text{NH}_3$ ,  $\text{SO}_2$ ,  $\text{NO}_2$ ,  $\text{HCN}$  etc. These electrodes are based on the measurement of local ion-activity variation, caused by permeation of gas molecules (through a hydrophobic gas-permeable membrane) to the inner electrode compartment and their subsequent interaction with an internal solution. In the case of  $\text{CO}_2$  electrode (Fig. 2.8) the mechanism can be described by series of equilibrium: the partitioning of the gas molecules between the sample and the electrode (solubility equilibrium) and

their hydrolysis inside the internal solution (e.g. 0.1 M NaHCO<sub>3</sub>), which influences on the pH of this solution. The pH change is detected by an internal pH electrode (a bicarbonate-selective electrode may also be applied). It is important to note, that if the detected species is hydrogen ion, then all acid/base species will interfere. Improved selectivity is obtained by an appropriate choice of the internal electrode and by the differential gas permeability of the hydrophobic membrane.<sup>135</sup>

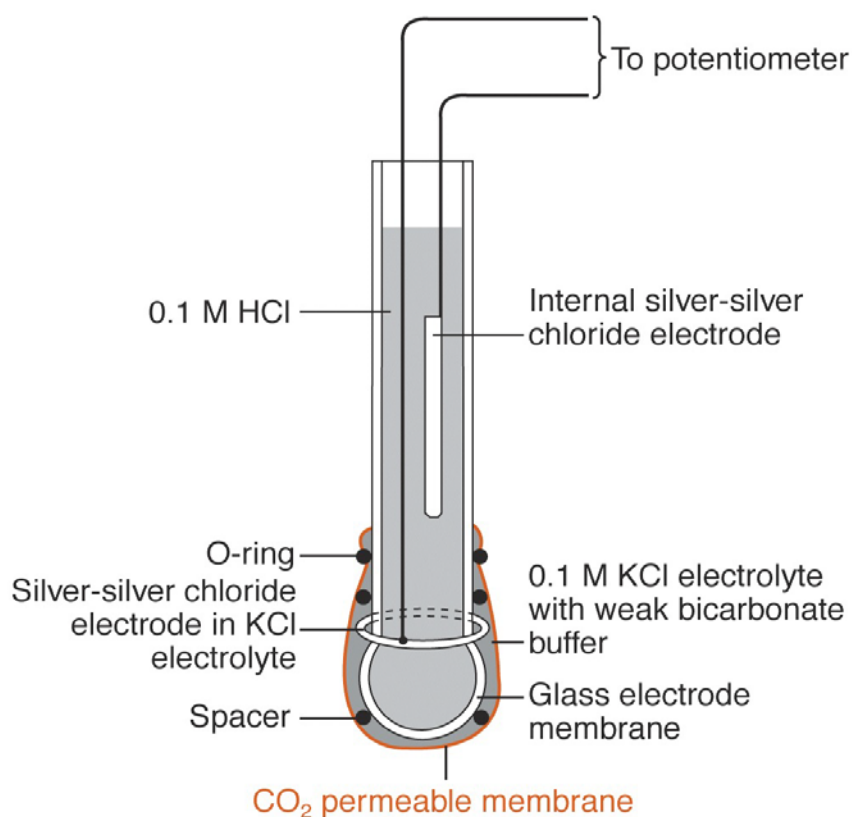


Figure 2.8 The CO<sub>2</sub> electrode. This compound ISE contain a normal electrode with a membrane to isolate the analyte.<sup>135</sup>

#### 2.3.4.2.4 METAL CONTACT OR ALL-SOLID-STATE ION SELECTIVE ELECTRODES

Recent developments in the areas of process, environmental and clinical analysis has led to a need for maintenance-free, robust and reliable sensors for different ions. One approach towards a maintenance-free ion sensor is to eliminate the inner filling solution and create all-solid-state electrode.<sup>148</sup> Also, miniaturization is easier for electrodes without any liquid components than for the more traditional ones with inner filling solution. In addition to the liquid in the filling solution, the liquid (plasticizer) in solvent polymeric membranes may leach out and limit the robustness of such electrodes. The transfer from ionic to electronic conductivity is provided by a solid contact (SC) layer having mixed ionic and electronic conductivity between the inner reference element and the sensing membrane. A good example is the all-solid-state sodium-selective electrode based on a calixarene ionophore in a poly-vinyl chloride membrane with a polypyrrole solid contact.<sup>149</sup> This configuration is in contrast to typical membrane usage in which electrolyte solutions are in contact with opposite membrane sites. Another example of the all solid state ion selective electrodes is the coated wire electrodes (CWE). Coated wire electrodes (CWEs) refer to a type of ion selective electrode in which an electroactive species is incorporated in a thin polymeric film coated directly on a metallic conductor. They generally involve electroactive species that are heterogeneously dispersed in the polymeric matrix.<sup>150</sup> Some solid state electrodes are built in such a way that there is a transducer layer that separates the sensing layer and the conducting element or wire.<sup>151,152</sup> Some have the conductive wires

directly attached to the sensing membrane improving its simplicity and robust nature.<sup>38,153</sup> Explained in details below are the characteristic features of an ion selective electrode.

### **2.3.5 CHARACTERIZATION OF AN ION SELECTIVE ELECTRODE**

The foremost properties characterizing the potentiometric electrodes based on ion sensitive membranes are their response to the ion they are intended to measure (the primary or principal ion) and their selectivity, i.e. their ability to discriminate the primary ion against other ions in solution. Interfering ions alter the response of an ion-selective electrode to an extent that depends on the nature of the intereferent and on its activity (or concentration). Quantifying this action was a problem of great concern since the beginning of ISE research. It was deemed necessary to suggest a set of requirements in outlining the development, assessment and applications of ISEs.

Recommendation and technical reports by International Union of Pure and Applied Chemistry (IUPAC) proposed some rules that should facilitate the correct communication on this subject. However IUPAC recommendation on some issues pertaining to ISE definitions has been criticized as unsatisfactory and even self contradictory; on the other hand, they are often applied carelessly. Many authors resort to variations which more or less divulge from the IUPAC criteria. Recently the interpretation of some concepts has been significantly improved, though most have not found their way into IUPAC documents.<sup>139,154-156</sup> Some of the criteria utilized for characterization of the electrodes as outlined by IUPAC are discussed below.

### 2.3.5.1 ACTIVITY VS CONCENTRATION

In solutions with a high concentration of ions, the inter-ionic interactions reduce the mobility of the ions, which in turn reduces the number of ions at the membrane surface. The measured voltage is less than what it should have been if it reflected the total number of ions in the solution. This results in errors and false estimate of concentration of samples that otherwise have high ionic concentrations. In order to avoid this, the maximum limit of detections must be found for the ion of interest, and solutions exceeding this concentration must be diluted down in order for proper concentrations to be read. The “effective concentration” at the membrane is called activity; it is the number of ions involved in a chemical reaction. In dilute samples, the activity is equal to concentration. Activity is related to ion concentration by:<sup>157</sup>

$$a = \gamma c \quad (\text{Equation 2.21})$$

Where;  $a$  = activity of ion in solution,  $c$  = concentration of ion in solution and  $\gamma$  = activity coefficient. The activity coefficient usually increases when concentration is increased. The relationship between the activity and concentration of a test solution can be graphically represented in Figure 2.9 below.

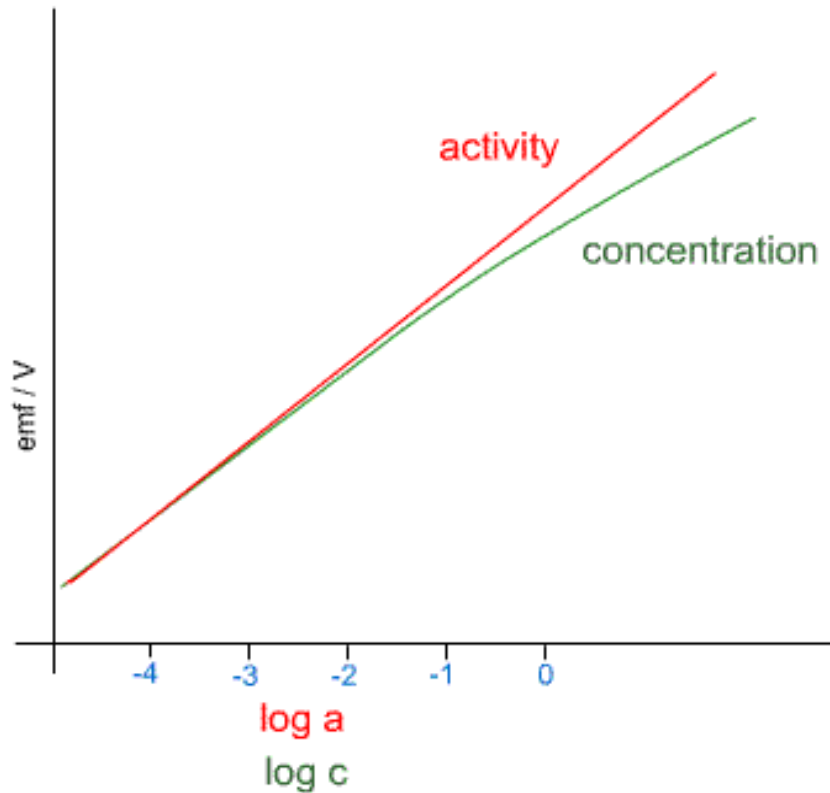


Figure 2.9 Calibration curve for electrode response to the logarithm of activity and stoichiometric concentration

The activity coefficient may be calculated using the *Debye-Hückel* equation.<sup>158,159</sup>

$$\log \gamma = -Az_i^2 \sqrt{\mu} \quad (\text{Equation 2.22})$$

Where,  $\gamma$  is the activity coefficient,  $\mu$  is the ionic strength of the solution and  $z_i$  is the charge on the ion. The key assumption is that the central ion is a point charge and that the other ions are spread around the central ion with a *Gaussian distribution*. Its range is limited to  $\mu < 0.01$ . This range does include the ionic strength of many freshwater environments.  $A$  is a constant that varies with temperature, relative permittivity and

nature of the solvent. This equation predicts that the log of the activity coefficient decreases linearly with the square root of the ionic strength. All ions of the same charge will have the same value. The *Debye-Hückel* equation has a limited range of application so chemists added a term to take into account that the central ion has a finite radius. Thus, the *Extended-Debye-Hückel* equation has a term called the ion size parameter  $b_i$ . This term is supposed to take into account the fact that ions have a finite radius and are not point charges.

$$\log \gamma = -Az_i^2 \frac{\sqrt{\mu}}{1+Bb_i\sqrt{\mu}} \quad (\text{Equation 2.23})$$

$B$  is a constant which varies with temperature. It should be noted that the equation is only accurate up to ionic strength of 0.6 M. At higher ionic strength, other factors come into play which makes calculation of the activity coefficient virtually impossible. Since the *Debye-Hückel* equation contains the charge and hydrated diameter of a specific ion, each ion in a solution could have a different calculated activity coefficient. (Experimental measurements give only an average activity coefficient for the ions that are present.) The ionic strength is a description of the solution and the same value of  $\mu$  is used for calculating the activity coefficients of each ion in solution.<sup>160,161</sup> These equations have seen modifications, each author improvising to suit his theoretical and experimental designs.<sup>159,162</sup>

### 2.3.5.2 SELECTIVITY OF ION SELECTIVE ELECTRODES

Ion selective electrodes are not entirely ion specific. This means that they may be sensitive to other ions to some extent in a system. In some situations where there are low ratio of interfering ion to the primary ion (ion of interest), interferences can be ignored. There are extreme cases where the electrode may be far more sensitive to the interfering ion than to the primary ion and can only be used if the interfering ions are only present in trace quantities or completely absent. The interfering ion can be removed by chemical complexation or precipitation.

The ability of an ion selective electrode to distinguish between different ions in same solution is expressed as the *Selectivity Coefficient*. The potentiometric selectivity coefficients are expressed according to the *Nicolsky-Eisenman* (N-E) equation as;<sup>139</sup>

$$E = E_{\text{constant}} + \frac{2.303RT}{z_A F} \log[a_A + K_{A,B}^{\text{pot}} (a_B)^{z_A/z_B} + K_{A,C}^{\text{pot}} (a_C)^{z_A/z_C} + \dots] \text{ (Equation 2.24)}$$

Where these parameters can be explained as follows;

$E$  = The experimentally observed EMF of an ISE (in Volts) when the only variables are activities in the test solution.

$E_{\text{constant}}$  = A constant that includes the standard potential of the electrode, the reference electrode potential and the junction potential.

$R$  = Gas constant and is equal to  $8.314510 \text{ K}^{-1} \text{ mol}^{-1}$ .

$T$  = Absolute temperature in Kelvin (K).

$F$  = Faraday's constant and is equal to  $9.6485309 \times 10^4 \text{ C mol}^{-1}$ .



$a_A$  = The activity of the primary ion  $A$ .

$a_B$  &  $a_C$  = The activities of the interfering ions  $B$  and  $C$  respectively.

$K_{A,B}^{pot}$  = The potentiometric selectivity coefficient for ion  $B$  with respect to the principal ion  $A$ .

$K_{A,C}^{pot}$  = The potentiometric selectivity coefficient for ion  $C$  with respect to the principal ion  $A$ .

$Z_A$  = The charge number: an integer with sign and magnitude corresponding to the charge of the principal ion  $A$ .

$Z_B$  &  $Z_C$  = These are charge numbers corresponding to the charge of interfering ions  $B$  and  $C$  respectively. Sign of these charge numbers is the same as that of the principal ion.

The theory predicts that if  $K_{A,B}^{pot}$  is larger than 1, the ISE responds to the interfering ions more selectively than to the primary ions. In most cases,  $K_{A,B}^{pot}$  is smaller than 1, which means that such ISEs responds to the primary ions more selectively than the interfering ions. The *Nicolsky-Eisenman* equation assumes a Nernstian response not only for the primary ion but for interfering ion as well.  $K_{A,B}^{pot}$  is assumed to be constant. Interference measurement can be obtained by using either the mixed solution method or the separate solution method. Mixed solution methods comprises of the following;<sup>155</sup>

(1) Fixed Interference method (FIM): this is a situation where we have a constant activity of the interfering ion,  $a_B$  and varying activity of the primary ion,  $a_A$ . The

EMF values obtained are plotted against the logarithm of the activity of the primary ion. The intersection of the extrapolated linear portions of this plot indicates the value of  $a_A$  that is to be used to calculate  $K_{A,B}^{pot}$  from the following equation;

$$K_{A,B}^{pot} = a_A / (a_B)^{Z_A/Z_B} \quad (\text{Equation 2.25})$$

Where,  $Z_A$  and  $Z_B$  have the same signs, positive or negative.

(2) Fixed primary ion method (FPM): This is the opposite of the fixed interference method. There is constant activity of the ion of interest,  $a_A$  and varying activity of the interfering ion,  $a_B$ . The intersection of the extrapolated linear portions of this plot indicates the value of  $a_B$  that is to be used to calculate  $K_{A,B}^{pot}$  from equation 2.24.

(3) Two solutions Method (TSM): this method involves measuring potentials of a pure solution of the primary ion,  $E_A$ , and a mixed solution containing the primary and the interfering ions,  $E_{A+B}$ . The potentiometric selectivity coefficient is calculated by inserting the value of the potential difference  $\Delta E = E_{A+B} - E_A$  into the following equation:

$$K_{A,B}^{pot} = a_A (e^{\Delta E Z_A F / (RT)} - 1) / (a_B)^{Z_A/Z_B} \quad (\text{Equation 2.26})$$

(4) Matched potential method (MPM): This method is independent of Nicolsky-Eisenman equation. The potentiometric selectivity coefficient is defined as the

activity ratio of primary and interfering ions that give the same potential change under identical conditions. First, a known activity ( $a'_A$ ) of the primary ion solution is added into a reference solution that contains a fixed activity ( $a_A$ ) of primary ions, and the corresponding potential change is recorded. Then, a solution of interfering ion is added to the reference solution until the same potential change ( $\Delta E$ ) is recorded. The change in potential produced at the constant background must be the same in both cases.

$$K_{A,B}^{pot} = (a'_A - a_A) / a_B \quad (\text{Equation 2.27})$$

In the separate solution method (SSM) the potential of cell comprising an ISE and the reference electrode is measured with two separate solutions, one containing the ion A of activity  $a_A$  (but no B), the other containing the ion B at the same activity  $a_A = a_B$  (but no A). If the measured values are  $E_A$  and  $E_B$  respectively, the value of  $K_{A,B}^{pot}$  may be calculated from the equation:

$$\log K_{A,B}^{pot} = \frac{(E_B - E_A)Z_A F}{2.303RT} + (1 - Z_A/Z_B) \log a_A \quad (\text{Equation 2.28})$$

This method is recommended only if the electrode exhibits a Nernstian response. It is less desirable because it does not represent the actual conditions under which the electrodes are used.<sup>156</sup>

For many years, it has largely been debated that the *Nicolsky-Eisenman* model for determining selectivity of primary ions and interfering ion lacks credibility when ions

of different charges are involved.<sup>163,164</sup> The  $K_{A,B}^{pot}$  value has been reported to be unrealistically large or small depending on whether the ion of higher charge is considered the primary or interfering ion. This suggests that the selectivity coefficient is not a physical constant but a value that depends on experimental conditions. Although the *Nicolsky-Eisenman* requires both the primary and the interfering ions to lead to Nernstian responses, few electrodes seem to exhibit a Nernstian behaviour for both the primary and interfering ions. As a result most reports have violated the prerequisite for the use of the *Nicolsky-Eisenman* equation. This is the major reason for the activity dependence of  $K_{A,B}^{pot}$  and the non-equality of  $K_{A,B}^{pot}$  values based on different methods. It was recommended that under the condition that both the primary ion and interfering ion leads to Nernstian responses, *Nicolsky-Eisenman* or its modification can be employed when ions of equal charge are involved. If Nernstian behaviour is not satisfied by one or both ions, the matched potential method is favoured even if the charges of the primary and interfering ions are equal.<sup>156</sup>

In complicated situations, it was duly suggested that the best representation and characterization of ion selective electrodes is to publish the response curves for the individual ion in question.<sup>165</sup> Modifications of the *Nicolsky-Eisenman* equation have also been attempted and the literary work proposed a relationship that allows the reliable description of the mixed ion response behaviour of ion selective electrodes with a single equation. The modified *Nicolsky-Eisenman* equations is claimed to be valid for any combination of mono-, di- or trivalent ions in solution.<sup>166</sup> The determination of

selectivity coefficients based on the practical slope of ion selective electrodes<sup>167</sup> and other parameters independent of the *Nicolsky-Eisenman* equation are ongoing.<sup>168-170</sup>

### 2.3.5.3 NERNSTIAN RESPONSE

Nernstian response occurs when an ion-selective electrode responds according to local thermodynamic equilibrium, over a given range of activity (or effective concentration). For Nernstian response a plot of the potential difference of the ISE cell (ISE with an outer reference electrode) versus the logarithm of the ionic activity of a given species is linear with a slope of  $2.303 RT/nF$  ( $59.16/n$  mV per unit change in the log of the activity of the measured sample at 298.15 K). Nernstian response implies ideal sensitivity, but not necessarily ideal selectivity since interfering ions may also give Nernstian response when present as the sole potential determining species.<sup>77,133,139</sup>

### 2.3.5.4 CALIBRATION THEORY

The operation of ion selective electrodes is based on the fact that there is a linear relationship between the electrical potential developed between an ISE and a reference electrode immersed in the same solution, and the logarithm of activity (or effective concentration) of the ions in the solution in accordance with the Nernst equation. Using a series of calibrating solutions the response curve or calibration curve of an ion-selective electrode can be measured and plotted as the signal (electromotive force) versus the activity of the analyte. Typical calibration curve of a potentiometric sensor determined in this way is shown in the Figure 2.10. The linear range of the calibration

curve is usually applied to determine the activity of the target ion in any unknown solution. However, it should be pointed out that only at constant ionic strength a linear relationship between the signal measured and the concentration of the analyte is maintained (because of the clear cut relationship between ion activity and concentration, occurring in such condition).

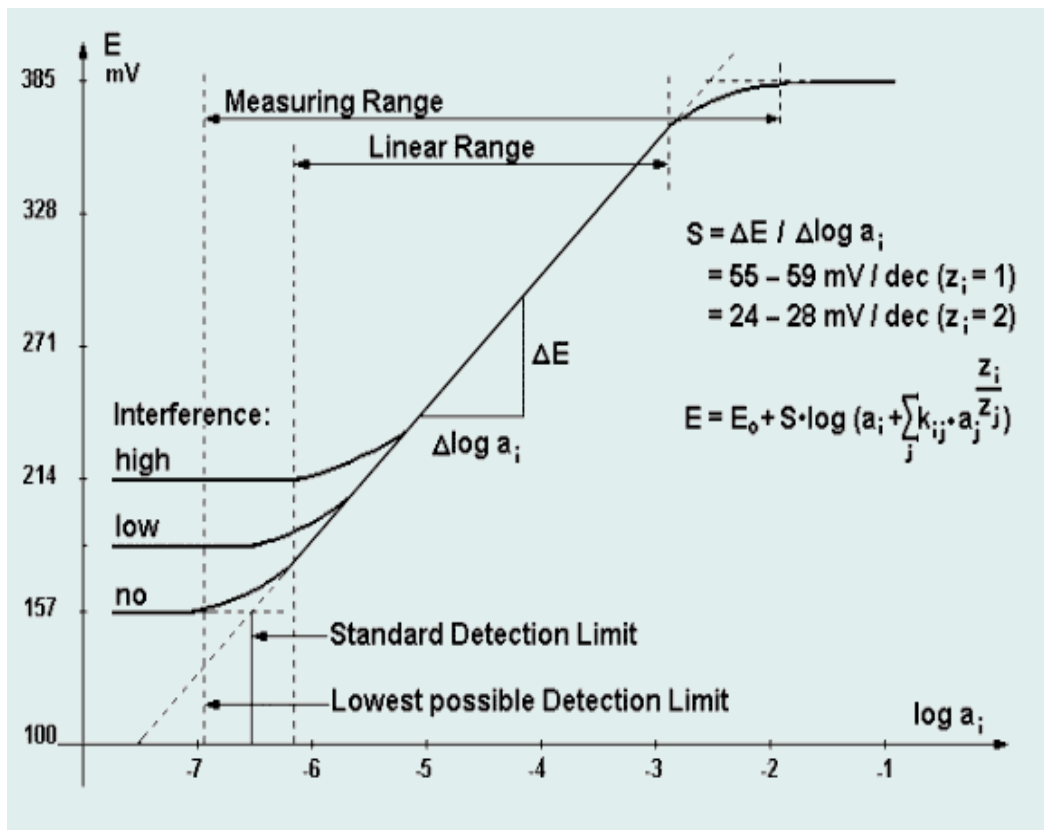


Figure 2.10 Typical calibration curve of an ion-selective electrode.<sup>171</sup>

Note that  $2.303RT/nF$  is the Slope ( $S$ ) of the line and this is an important diagnostic characteristic of the electrode. The slope gets lower as the electrode gets old or contaminated, and the lower the slope the higher the errors on the sample measurements. For example at  $S = 55$ , a 1 mV error in the reading will make about a 4%

difference in concentration; at  $S = 26$  the difference will be more like 8%. Due to the logarithmic relationship, the slope can easily be determined as the difference between the voltages measured in two solutions which differ by one order of magnitude, usually expressed as mV/decade. The theoretical value for the slope at 25° C is 59.2 for monovalent ions and 29.6 for divalent ions. In practice, these can vary considerably due to failure to meet "ideal" conditions. The critical factor is not so much the actual value of the slope, but that this should be as high as possible and remain constant over the range of concentrations and the time period required for the analyses.<sup>163,171</sup>

The linear range of the electrode is defined as that part of the calibration curve through which a linear regression would demonstrate that the data points do not deviate from linearity by more than 2 mV. For many electrodes this range can extend from about  $10^{-1}$  M down to  $10^{-6}$  M or even  $10^{-7}$  M. The total measuring range includes the linear part of the graph as shown in *figure 2.10* together with a lower curved portion where the response to varying concentration becomes progressively less as the concentration reduces. Samples can be measured in this lower range but it must be noted that more closely spaced calibration points are required in order to define the curve accurately and the percentage error per mV on the calculated concentration will be progressively higher as the slope reduces.

The IUPAC definition of limit of detection for monovalent ion is that concentration at which the measured potential differs from that predicted by the linear regression by more than 18 mV. The practical limit of detection can be calculated by plotting a calibration graph using several standards at the lower end of the concentration range,

and below it: say 100, 10, 1, 0.1, 0.05, 0.01 ppm - i.e. at least two to define the linear slope and two to show the position of the horizontal section below the limit of detection, where the electrode is unresponsive to concentration change. The limit of detection is then defined by the crossing point of the two straight lines drawn through this points.<sup>139</sup> In practice, frequent calibration of the electrode is encouraged. It is important to make one calibration graph before taking a series of sample measurement. For most precise result, it is best to measure samples soon after calibration. Ideally, each sample measurement must be preceded by recalibration; this is relatively easy if one point recalibration is used.

#### **2.3.5.5 IONIC STRENGTH AND TOTAL IONIC STRENGTH ADJUSTMENT BUFFERS (TISAB)**

Ionic strength ( $I$ ) is the measure of the total effect of all the ions in a solution. It is the sum of the molar concentration ( $c_i$ ) multiplied by the square of the valence ( $z_i$ ) of all the ions and can be denoted as;<sup>172</sup>

$$I = \frac{1}{2} \sum_{i=1}^n c_i z_i^2 \quad (\text{Equation 2.29})$$

This sum is taken over all ions in the solution. Multivalent ions contribute strongly to the ionic strength of a solution. The ionic strength plays a central role in the *Debye-Hückel* theory that describes the strong deviations from ideality typically encountered in ionic solutions.<sup>173</sup> Sample solutions may contain other ions in addition to the ion being measured and the ionic strength of the ions may be significantly higher than that of the standard (used in constructing a calibration graph). This brings a lot of disparity in the



linearity of the calibration graph. This problem may be solved by diluting the sample to a level that ionic strength is insignificant but making sure that the detected ion is within the linear range of the electrode. Another option is to bring the ionic strength of both the calibration standard and the samples to the same level by adding a suitable ionic strength adjustment buffers (TISAB). TISAB is used to adjust both the samples and standards to the same ionic strength and pH. This allows the concentration, rather than the activity, to be measured directly and often read directly off a meter. There are about four TISAB buffers that have been reported in the literatures.<sup>174</sup>

TISAB I - The composition of this TISAB includes 500 mL of water (H<sub>2</sub>O), 57 mL of glacial acetic acid, 58 g of sodium chloride (NaCl) and 0.30 g of sodium citrate dihydrate (dilute to 1 L). The solution is usually brought to a pH of about 5.0 - 5.5 by adding solutions of sodium hydroxide (NaOH). The standards and the unknown samples are both treated to a 1:1 ratio of TISAB and sample before electromotive force (EMF) measurements. They are used differently depending on the abundance of interfering components. For example, the TISAB 1 is usually utilized in fluoride measurements when magnesium, calcium, chloride, nitrate, sulphate and phosphates are present at high concentrations.<sup>175</sup>

TISAB II - This includes 500 mL of water, 170 g of sodium nitrate (NaNO<sub>3</sub>), 68 g of sodium acetate trihydrate and 92.4 g of sodium citrate dihydrate (dilute to 1 L). For fluoride measurements, this buffer is used when there are high iron(III) and silicate concentrations.<sup>176</sup>

TISAB III - This includes 17.65 g of 1,2 diaminocyclohexane N,N,N',N'-tetra acetic acid (CDTA), 500 mL of water, 40% sodium hydroxide, 300 g of sodium citrate dihydrate and 60 g of sodium chloride (dilute to 1 L). Again for fluoride measurements, this solution is utilized when aluminum ions are present in great quantity.<sup>177</sup>

TISAB IV - This consists of 500 mL of water, 84 mL of concentrated hydrochloric acid (37%), 242 g of tris(hydroxymethyl) methylamine (TRIS) and 239 g of disodium tartrate dihydrate. The whole solution is cooled, transferred in a 1 liter volumetric flask and made up to mark with water. 1:1 sample to TISAB ratio is also recommended for this buffer type.<sup>178,179</sup>

Total ionic strength adjustment buffers (TISAB) do not usually contain the ions to be measured or any likely interferent. They usually contain ionic strength adjusting salt, complexing ligand and pH buffer. The idea is to swamp the ionic strength effects of the host solutions and hence give a uniform ionic strength in all samples and standards. In the event of its success, the straight line calibration curve can be constructed using concentration units and the unknown concentrations can be read directly from the calibration graph. There is no need to recalculate the standard concentration after adding TISAB as long as all the standards and the samples are treated the same. Most recipes of TISAB possess ionic strength of about 0.1 M and thus will only be effective if the ionic strength of original sample is much lower than 0.1 M. They are usually employed in solution to reduce junction potentials. These potentials are developed due to different mobility of ions in solution. A charge (potential) develops when one ion

moves to an electrode more rapidly than the other ion. These special buffers are prepared according to experimental requirements and are used with fixed administration specifications to both standard and samples volumes.<sup>174</sup>

### **2.3.6 METHOD OF ANALYSIS USING ION SELECTIVE ELECTRODES**

The question often arises as to which determination method is most suitable for a particular sample. A number of techniques are available for determining the concentration of a sample even though the electrode may sense activity. They are;

- (1) Direct Potentiometry or Direct measurement: This is the most widely used method of analysis using ion selective electrodes. The electrodes are immersed in a test solution and the electrode potential is measured directly by a volt meter.<sup>180,181</sup> It requires the electrode to be calibrated first with standard solutions and its EMF values (with respect to a suitable reference electrode) plotted against the log of the concentration. The standard solutions used for calibration usually differ by a factor of ten and must be close to the expected activity or concentration of the sample. The sample solution can then be analysed by single direct potentiometric measurement by extrapolation from the calibration curve of the standards.
  
- (2) Incremental methods - This is the method of analysis whereby, instead of relating sample measurements to a pre-determined calibration graph, the concentrations of the unknown is determined by taking readings before and after

mixing known amounts of sample and standard. These methods help to minimise any differences in temperature and ionic strength between the standard and the sample. It also ensures that calibration and sample measurements are closely spaced in time. They are usually made under similar conditions without removing the electrodes from the solution, thus minimising any error due to drift and hysteresis. Under the incremental methods, two separate techniques are available.

The first is the Sample addition method or the standard addition method.<sup>180</sup> This method involves measuring the voltage in a relatively large volume (e.g. 25 - 100 mL) of sample (for standard addition) or standard (for sample addition) then adding a much smaller volume (e.g. 1 - 10 mL) of standard (or sample) and taking a second reading after the voltage has stabilized in the mixture. This method only works within the linear range of the electrode so it cannot be used for low-level samples. The volume and concentration of the standard and the volume of sample must be chosen carefully according to the following criteria;

- (a) The volume of the first solution must be large enough to cover the tips of both electrodes and allow room for a magnetic stirring rod to continuously stir the solution during measurement and mixing of the additive, whilst ensuring the electrodes remain immersed.
- (b) The concentration and volume of the additive must be sufficient to cause a significant and measurable increase in the measured voltage of the first solution (ideally 20 to 30 mV increase achieved by increasing

the original concentration by 5 to 10 times). (c) The volume of the additive must be small enough so that it does not cause a significant change in the ionic strength of the first solution. (d) The volume of the additive must be large enough so that volumetric errors are not significant. This can be averted by the use of gravimetric addition (i.e. add standard from a weighed dropping bottle then re-weigh).<sup>89,182,183</sup>

The second is the sample subtraction method. This involves adding a small amount of sample solution to a standard solution of an ion with which it will react stoichiometrically to form a complex or precipitate, thus reducing the concentration of both ions. The ISE used will be sensitive to the reactive ion in the standard, not the sample. This method is advantageous in the sense that it can extend the range of ions measurable by ISEs to others for which no ion sensitive membranes are available.

With the vast knowledge of potentiometry, ion selective electrodes and membrane technologies, one will be equipped with enough resources to venture into the research and fabrication of ion selective electrodes that can be selective to one's ion of interest. Based on this knowledge, fabrication of ion selective electrodes that will have maximum selectivity for phosphate ions in solution was achieved. The next chapter therefore, will specifically focus on all steps taken in the fabrication of the phosphate selective electrodes.

# *CHAPTER THREE*

## **DESIGN AND FABRICATION OF THE NEW SOLID STATE PHOSPHATE SELECTIVE ELECTRODES**

### **3.0 INTRODUCTION**

Ion selective electrodes are presumably the future of ion measurements. The rationale behind their recent application lies on their simplicity of design and cheap cost of production amongst others. Nonetheless, techniques such as UV-Visible absorption spectroscopy and  $^{31}\text{P}$  NMR spectroscopy are also good for ion analysis. However, ion analysis with the above mentioned techniques takes into consideration factors such as; cost, time, location and convenience as well as precision, accuracy and ease of analysis. The techniques' various shortcomings can be circumvented with the proper use of suitable ion selective electrodes. Selectivity of ion selective electrodes for one ion over another is determined by the nature and composition of the membrane materials used to fabricate the electrode. As an analytical tool, ion selective electrodes offer attractive advantages for direct measurement in complex samples. In many instances potentiometric measurements can be made in situ without interference from the chemical or physical properties of the sample (i.e. color, turbidity). They are inexpensive devices and when used in conjunction with commercially available high-

input impedance voltmeters, the entire method provides a low-cost yet effective means of performing a wide range of analyte determinations.

One approach towards a maintenance-free, robust and reliable sensor is to eliminate the inner filling solution and create an all-solid-state electrode.<sup>184</sup> The traditional barrel configuration of conventional electrodes (with internal filling solution) can prove cumbersome for some applications, so attempts at miniaturization brought about some new sensing systems, namely solid contact (SC) electrodes; such as solid crystal membranes, conducting filled polymer electrodes, and coated wire electrodes (CWE). This move to the total elimination of the internal filling solution of the conventional electrodes to the all-solid-state electrodes provides advantages such as; (a) simplicity of design, (b) mechanical flexibility, i.e. the electrode can be used horizontally, vertically, or inverted, and (c) the possibilities of miniaturization and micro fabrication. Also, the liquid (plasticizer) in solvent polymeric membranes may leach out and limit the robustness of such electrodes. The ionic conductivity is provided by a solid contact (SC) layer having mixed ionic and electronic conductivity between the inner reference element and the sensing membrane. A good example is the all-solid-state sodium-selective electrode based on a calixarene ionophore in a poly-vinyl chloride membrane with a polypyrrole solid contact.<sup>185</sup> This configuration is in contrast to typical membrane usage in which electrolyte solutions are in contact with opposite membrane sites.

Detailed description of the design and fabrication of the new solid state phosphate selective electrodes is given in this section. It also provides results obtained for pellets formation, electrodes construction, calibration curve studies, conditioning of the electrodes, effects of electrode composition, response time of the electrodes, pH effects, and interference studies done for various cations and anions.

### **3.1 EXPERIMENTAL SECTION**

#### **3.1.1 INSTRUMENTS AND REAGENTS**

All reagents used were either analytical reagent grade or the purest available commercially and were used without further purification. A digital screen Metrohm-781 pH/ion meter was used for potential measurements. The meter is capable of multi-point calibration with up to nine buffers (samples). Ion measurement can be by direct measurement or automatic standard addition or subtraction. The fabricated phosphate selective electrodes were utilized as our indicator electrodes. In order to measure the change in potential difference across the ion-selective membrane as the ionic concentration changes, it is necessary to include in the circuit a stable reference voltage which acts as a half-cell from which the relative deviations is measured. The reference electrode utilized was a Metrohm silver/silver chloride (Ag/AgCl) double junction reference electrode. The reference electrode utilizes 3 M potassium chloride (KCl) as its internal solution. The pH values of the reacting solutions were monitored with a Metrohm Aquatrode plus pH electrode. All measurements were performed with the



electrodes immersed in solutions and kept at ambient room temperature ( $25 \pm 3^\circ \text{C}$ ). The solutions were slowly stirred with a magnetic stirrer.

For the preparation of the phosphate standards at different pH, a mixture of dihydrogen and monohydrogen phosphate was used as given in Table 3.1.<sup>186</sup>

Table 3.1 Preparation of 0.1 M sodium phosphate buffer at  $25^\circ \text{C}$ .

pH	Volume of 0.1 M $\text{Na}_2\text{HPO}_4 \cdot 7\text{H}_2\text{O}$ (mL)	Volume of 0.1 M $\text{NaH}_2\text{PO}_4 \cdot 2\text{H}_2\text{O}$ (mL)
4.5	0.5	99.5
4.9	1	99
5.1	1.5	98.5
5.8	8.5	91.5
6.0	13.2	86.8
6.2	19.2	80.8
6.4	27.8	72.2
6.6	38.1	61.9
6.8	49.7	50.3
7.0	62.0	38.0
7.2	71.7	28.3
7.4	80.2	19.8
7.6	86.6	13.4
7.8	90.8	9.2
8.0	94.0	6.0
8.9	99.0	1.0

The pH values were calculated according to Henderson-Hasselbalch equation:<sup>187</sup>

$$\text{pH} = \text{pK}' + \log\left(\frac{[\text{HPO}_4^{2-}]}{[\text{H}_2\text{PO}_4^-]}\right) \quad (\text{Equation 3.1})$$

Where  $pK' = 6.86$  at  $25^\circ\text{C}$ . In dilute aqueous solutions, phosphate exists in four forms. In strongly basic conditions, the phosphate ion ( $\text{PO}_4^{3-}$ ) predominates, whereas in weakly basic conditions, the hydrogen phosphate ion ( $\text{HPO}_4^{2-}$ ) is prevalent. In weakly acid conditions, the dihydrogen phosphate ion ( $\text{H}_2\text{PO}_4^-$ ) is most common. In strongly acid conditions, aqueous phosphoric acid ( $\text{H}_3\text{PO}_4$ ) is the main form. For a neutral pH (pH 7.0), only  $\text{H}_2\text{PO}_4^-$  and  $\text{HPO}_4^{2-}$  ions are present in approximately equal amount. The above equation can be modified depending on the composition of the different phosphate species in the test solution which is pH dependent. The speciation diagram for phosphates is given in Figure 3.1 below.<sup>188,189</sup>

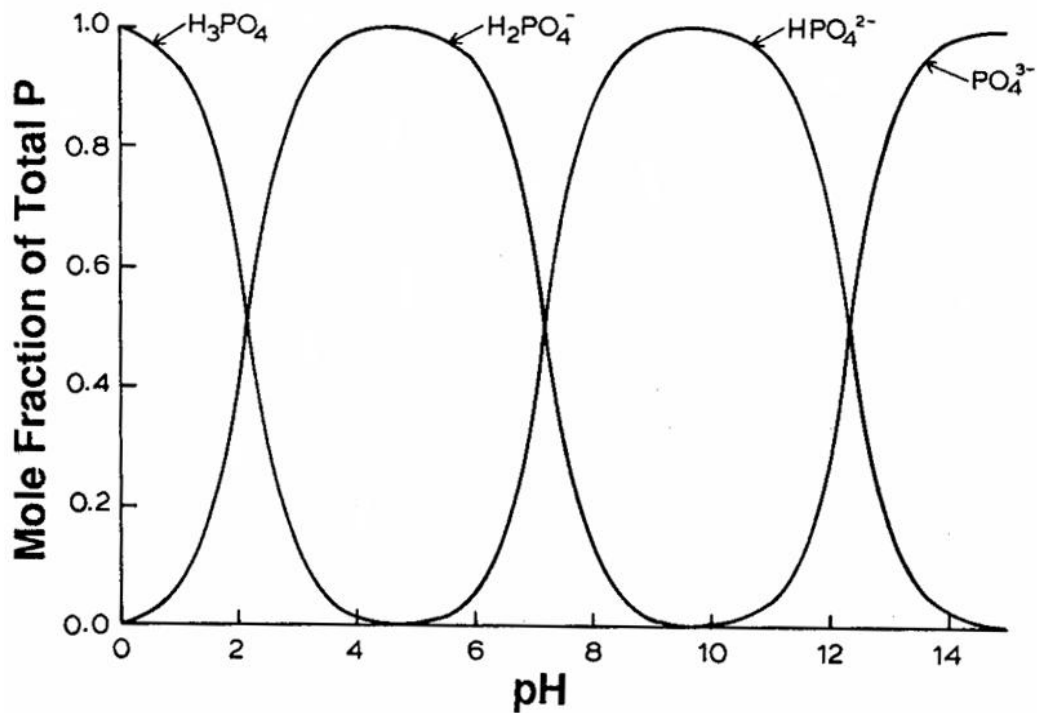


Figure 3.1 Phosphate ion speciation diagram.<sup>189</sup>

### 3.1.2 CHOICE OF MEMBRANE MATERIALS

The following chemicals were utilized in the formation of the membranes;

(1) Aluminium phosphate ( $\text{AlPO}_4$ ) - This slightly soluble metal salt is used as the main component. Electrodes manufactured with this metal detect ions via the type II electrodes mechanism. Type II electrodes do not have internal solutions and mobile ions of the chemical species to be sensed. Internal connection to the membrane is made with a suitable wire or conductor; in this case we utilized copper wire (99.9%).  $\text{AlPO}_4$  membranes have the capability to detect phosphate ions in solution. It is envisaged that aluminium and phosphates in solution will be simultaneously detected. Detection of aluminium ion concentration is obtained by the redox potential of aluminium metal. With the phosphate ion selective electrode of this invention, the dissolution equilibrium of aluminium phosphate is determined by phosphate. This also captures changes in the aluminium ion concentration at the same time.<sup>190</sup> If  $s'$  is the solubility of aluminium phosphate ( $\text{AlPO}_4$ ) and  $k'_{sp}$  is the solubility product ( $k'_{sp} = 9.84 \times 10^{-21}$  for  $[\text{Al}] [\text{PO}_4]$ ) at  $25^\circ \text{C}$ . In terms of detection limit in mole per litre,  $s'$  can be calculated to be  $9.92 \times 10^{-11}$ . Theoretically, ion detection down to a concentration of  $9.92 \times 10^{-11} \text{ molL}^{-1}$  is possible.<sup>191</sup>

(2) Aluminium (Al) - Pure aluminium possesses high electrical conductivity and resistance to corrosion. It is a relatively soft, durable, lightweight, ductile and malleable metal. It is easily machined, cast, drawn and extruded. The Aluminium

phosphates are held together in the membrane by this metal salt. It is important to state that there are possibilities of aluminium forming pseudo-complex formation with the phosphate moieties in solution. This denotes the principles of electrodes of the second kind (electrodes that responds to changes in ion activity through formation of complex). These changes in ion activities as a result of complexation are translated into electrical potential which relates to activity.

(3) Copper (Cu) – Some pores on the membrane surface caused a slow response to changes in ion activity. In order to prepare a more compacted membrane with increase in conductivity, powdered copper was added to the mixture of aluminium phosphate and aluminium metal. Effects of this on membrane compositions and efficiency are discussed in the experimental section in chapter 3. Also, discrete site chemisorption of transition-metal ion like Cu(II) has been identified on the surface of hydrous aluminium oxide ( $\delta$ -Al<sub>2</sub>O<sub>3</sub>).<sup>192-195</sup> This evidently suggests that copper may be used as a sensor that possesses sensing mechanisms similar to the coated wire electrodes (CWE). It has also been documented that orthophosphates readily form sparingly soluble precipitates with heavy metals. The solubility product of Cu<sub>3</sub>(PO<sub>4</sub>)<sub>2</sub> is characterized by  $\log K_s \approx -36.9$ <sup>33</sup>. More stable complexes are formed with the pyrophosphates and the triphosphates in solution ( $\log K_s \approx 7.6$  and  $\log K_s \approx 9.0$  respectively).<sup>194</sup> Adsorption of copper metal ions in the presence of organic ligands like phosphates has been attributed to ternary surface complex formation.

### 3.2 FABRICATION OF SOLID STATE MEMBRANE

The novel feature of the present solid state phosphate ion selective electrode is the use of Aluminium phosphate ( $\text{AlPO}_4$ ), Aluminium powder (Al) and powdered copper (Cu) as the membrane components (See section 3.1.2). They were mixed in various proportions as shown in table 3.2. The various mixtures were grounded in mortar and pestle and transferred into a die. The die was placed in a Paul Weber 30 hydraulic press attached to Edward (EDM2) high vacuum suction pump. The time allowed for each pellet formation was 20 minutes and the pressure of the press was set at 7,000 atmospheres ( $5.32 \times 10^6$  mmHg, 709,275 kPa). A DMM 15XP-A multimeter was used to measure electrical resistance across the thickness of each membrane. Readouts are obtained in digital form. The pellets obtained were grouped into binary pellets (those that contain only two of the membrane components) and ternary pellets (those that contain the three membrane components). Fifteen (15) different membrane pellets were prepared in all, while each composition was made in triplicates. The different membrane pellets were removed and stored in air and moisture controlled environment. The pellets compositions and properties are shown in Table 3.2 below.

Table 3.2 Properties of the fabricated membrane pellets.

COMPOSITION	EMPIRICAL FORMULA	MEMBRANE THICKNESS(mm)	RESISTANCE IN OHMS( $\Omega$ )	MASS OF THE DIFFERENT PELLETS (grams)
10% $\text{AlPO}_4$ + 90% Al	$\text{Al}_{41}\text{PO}_4$	1.61	0.6	0.05 + 0.45
20% $\text{AlPO}_4$ + 80% Al	$\text{Al}_{19}\text{PO}_4$	1.66	0.6	0.10 + 0.40
30% $\text{AlPO}_4$ + 70% Al	$\text{Al}_{11}\text{PO}_4$	1.74	0.7	0.15 + 0.35
40% $\text{AlPO}_4$ + 60% Al	$\text{Al}_8\text{PO}_4$	1.80	0.8	0.20 + 0.30
50% $\text{AlPO}_4$ + 50% Al	$\text{Al}_5\text{PO}_4$	1.86	1.2	0.25 + 0.25
60% $\text{AlPO}_4$ + 40% Al	$\text{Al}_4\text{PO}_4$	1.93	2.5	0.30 + 0.20
10% $\text{AlPO}_4$ + 90% Cu	$\text{Cu}_{17}\text{AlPO}_4$	0.70	0.6	0.05 + 0.45
20% $\text{AlPO}_4$ + 80% Cu	$\text{Cu}_8\text{AlPO}_4$	0.86	0.8	0.10 + 0.40
30% $\text{AlPO}_4$ + 70% Cu	$\text{Cu}_9(\text{AlPO}_4)_2$	1.00	0.9	0.15 + 0.35
10% $\text{AlPO}_4$ + 10% Cu + 80% Al	$\text{Cu}_2\text{Al}_{37}\text{PO}_4$	1.52	0.6	0.05 + 0.05 + 0.40
15% $\text{AlPO}_4$ + 15% Cu + 70% Al	$\text{Cu}_2\text{Al}_{22}\text{PO}_4$	1.49	0.6	0.075 + 0.075 + 0.35
20% $\text{AlPO}_4$ + 20% Cu + 60% Al	$\text{Cu}_4\text{Al}_{29}(\text{PO}_4)_2$	1.47	0.6	0.10 + 0.10 + 0.30
25% $\text{AlPO}_4$ + 25% Cu + 50% Al	$\text{Cu}_2\text{Al}_{10}\text{PO}_4$	1.45	0.6	0.125 + 0.125 + 0.25
30% $\text{AlPO}_4$ + 30% Cu + 40% Al	$\text{Cu}_2\text{Al}_7\text{PO}_4$	1.44	0.6	0.15 + 0.15 + 0.20
35% $\text{AlPO}_4$ + 35% Cu + 30% Al	$\text{Cu}_2\text{Al}_5\text{PO}_4$	1.43	0.7	0.175 + 0.175 + 0.15

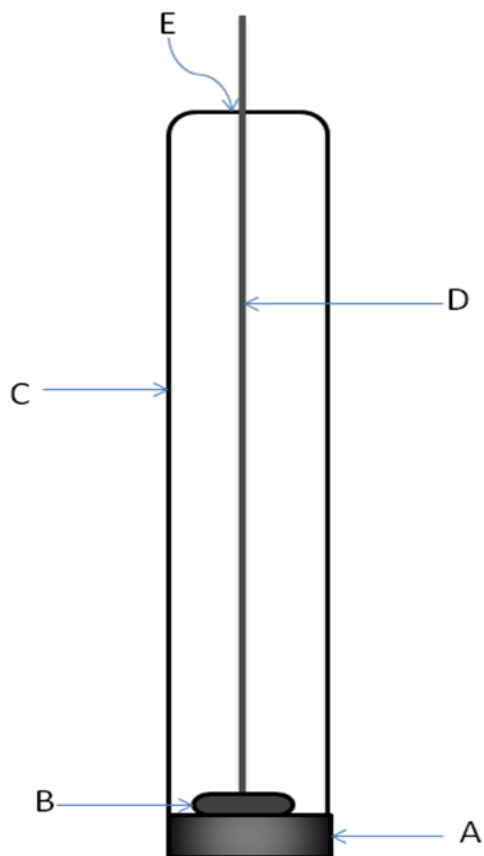
The mass of the membranes for all compositions is 0.5 g. The binary membranes ( $\text{AlPO}_4$  + Al and  $\text{AlPO}_4$  + Cu) exhibit similar physical and electrical characteristics in terms of

thickness (measured in mm) and the electrical resistance measured in ohms ( $\Omega$ ). The membrane thickness and electrical resistance increases as the amount of aluminium phosphate in each composition increases. It is observed that the binary membranes containing high amount of aluminium and copper are fairly strong with low electrical resistance. This may be due to high malleability, ductility and conductive properties of aluminium and copper. The final compositions attainable for the binary membranes are the 60%  $\text{AlPO}_4$  + 40% Al and 30%  $\text{AlPO}_4$  + 70% Cu, above which the membranes are unstable and break. The strength in the pellets observed for compositions containing more quantities of aluminium and copper may be attributed to proper linkage between the metals and the tetrahedral aluminium phosphate structure. The ternary membranes ( $\text{AlPO}_4$  + Cu + Al) did not differ from each in terms of membrane thickness and electrical resistivity throughout the composition prepared. Again, the final membrane composition that could be produced is 35%  $\text{AlPO}_4$  + 35% Cu + 30% Al.

### **3.3 ELECTRODE CONSTRUCTION**

Each electrode consists of a membrane pellet which is about 13.55 mm in diameter and varying thickness as shown in table 3.2, a glass test tube of about 13 mm diameter and 100 mm length, a 99.9% pure copper wire of 1 mm diameter and 200 mm length, and an epoxy resin. One end of the copper wire used was first coiled in spiral circles. The spiral end was firmly attached to one side of the pellet through pressure and held in place by epoxy resin. A tiny hole was created at the sealed end of the glass test tube that serves as the body of the electrode. The test tubes' open-end was attached to the

membrane and sealed with the resin as shown in figure 3.2. All openings were sealed airtight. To obtain a good sealing, the epoxy resin was applied to the edges of the tube from the inside and the outside. The loose end of the copper wire was connected to a voltmeter.



#### DESCRIPTION OF THE ION SELECTIVE ELECTRODE

A is the sensing membrane pellet as described in table 3.1.

B is the coiled end of the copper wire firmly contacting and connected to the membrane pellet by a conductive epoxy resin.

C is a supporting glass test tube that forms the body of the ion selective electrode.

D is the pure copper wire that serves as the conductor wire.

E is a small opening at the end of the glass tube from where the wire protrudes.

Figure 3.2 Overall arrangement of the phosphate solid state ion selective electrode.

### 3.4 CONDITIONING OF THE ELECTRODES

Similar electrodes having the same composition were separately kept in air, in distilled water and in  $1 \times 10^{-3}$  mol L<sup>-1</sup> solution of Na<sub>2</sub>HPO<sub>4</sub>·7H<sub>2</sub>O and their response to a



standard phosphate solution at a pH of 7 were duly noted. The results are shown in figure 3.3. The electrode that was immersed in  $1 \times 10^{-3}$  mol L<sup>-1</sup> solution of Na<sub>2</sub>HPO<sub>4</sub>·7H<sub>2</sub>O for about 6 hours showed quicker response and better regression for all the experiments conducted.

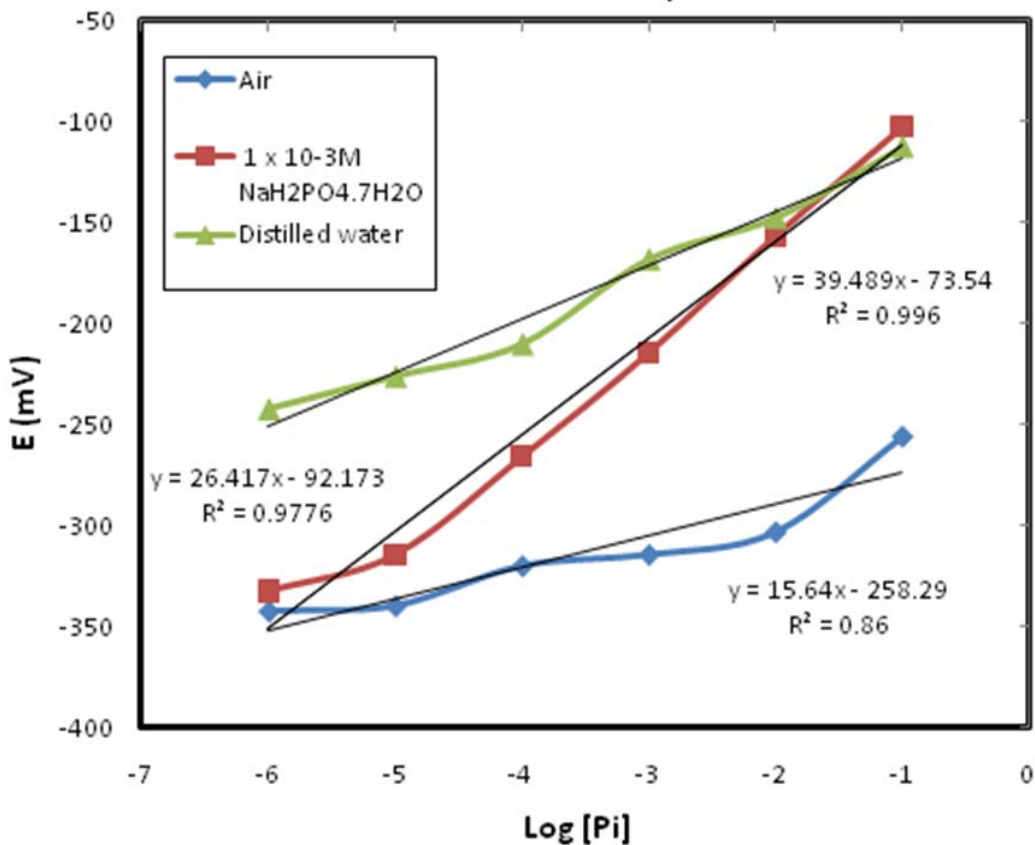


Figure 3.3 The effect of media on the performance of the electrodes. (it should be noted that the graph shown here is for the electrode with membrane combination 25% AlPO<sub>4</sub> + 25% Cu + 50% Al. Other electrodes discussed showed similar trend. Only this graph was shown to avoid repetition of similar data).

### 3.5 PROTOCOL OF THE STUDY

100 mL of each standard solution was measured out in a beaker and the electrodes potential values were measured in phosphate concentration ranges of  $1 \times 10^{-6}$  M to  $1 \times 10^{-1}$  M. The test phosphate selective electrode and a reference electrode (both connected to an ion meter) were inserted in the slowly stirred phosphate solution of known concentration, pH and temperature. The observed potential value displayed on the ion meter digital screen was recorded. The response time of the electrode was also noted and the potential value was only taken when the response is stable. The calibration curves were obtained by plotting the potential readings (in millivolt, mV) against the log of phosphate activity [Pi] (denoted in the graphs as Log A). A calibration curve was obtained for each electrode composition. The [Pi] responses were obtained in triplicates and the average value was used for the calibration curve. The electrodes are immersed in  $1 \times 10^{-3}$  mol L<sup>-1</sup> solution of Na<sub>2</sub>HPO<sub>4</sub>·7H<sub>2</sub>O for about 6 hours prior to use. The electrodes have been in use for about 3–4 times a week and have not deviated from their regression value in the past 12 months. The surface of the electrodes was polished with a soft paper before conditioning.

#### 3.5.1 CALIBRATION CURVE STUDIES

Calibration is carried out by immersing the electrodes in a series of solutions of known concentration and plotting a graph of the potential (mV) reading versus the log of the activity (or the actual activity on a logarithmic X axis). The concentration of the unknown is simply read off the calibrated standard graph. In many modern types of

equipment, the ion meter is fit with a memory with special computer graphics that calculates and plots this graphs while retaining the sequence or data of each calibrated series. This is much easier to use because once calibration is done, the concentration of the unknown can be displayed on the ion meter as the standard is stored in the systems memory. Recalibration generates another set of graph and one can easily calibrate the electrodes response as often as possible.

About 62 mL of  $1 \times 10^{-1}$  M sodium monohydrogen phosphate heptahydrate ( $\text{Na}_2\text{HPO}_4 \cdot 7\text{H}_2\text{O}$ ) solution was mixed with 38 mL of  $1 \times 10^{-1}$  M sodium dihydrogen phosphate dehydrate ( $\text{NaH}_2\text{PO}_4 \cdot 2\text{H}_2\text{O}$ ) to obtain a standard phosphate buffer solution with pH of 7. A known volume of this stock solution ( $1 \times 10^{-1}$  M) was serial diluted to obtain  $1 \times 10^{-2}$  M,  $1 \times 10^{-3}$  M,  $1 \times 10^{-4}$  M,  $1 \times 10^{-5}$  M and  $1 \times 10^{-6}$  M solutions.

### **3.6 RESULTS AND DISCUSSION**

The calibration curves obtained for the different phosphate selective electrodes are shown in Figures 3.4 to 3.18.

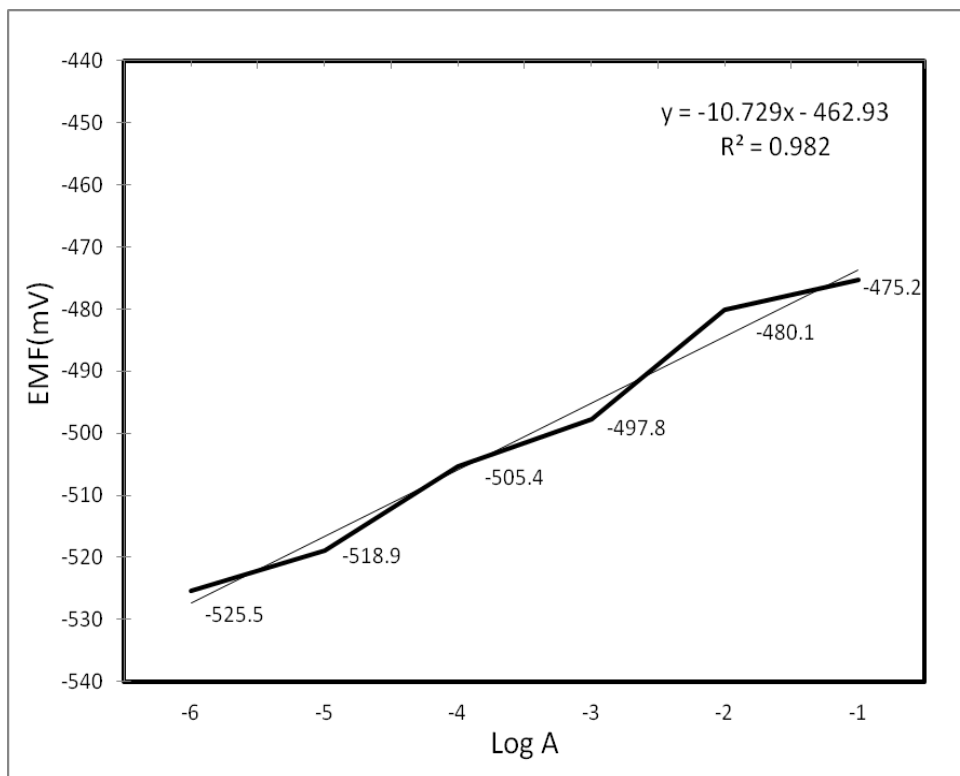


Figure 3.4 Calibration curve for the phosphate sensitive electrode combination 10%  $\text{AlPO}_4$  + 90% Al.

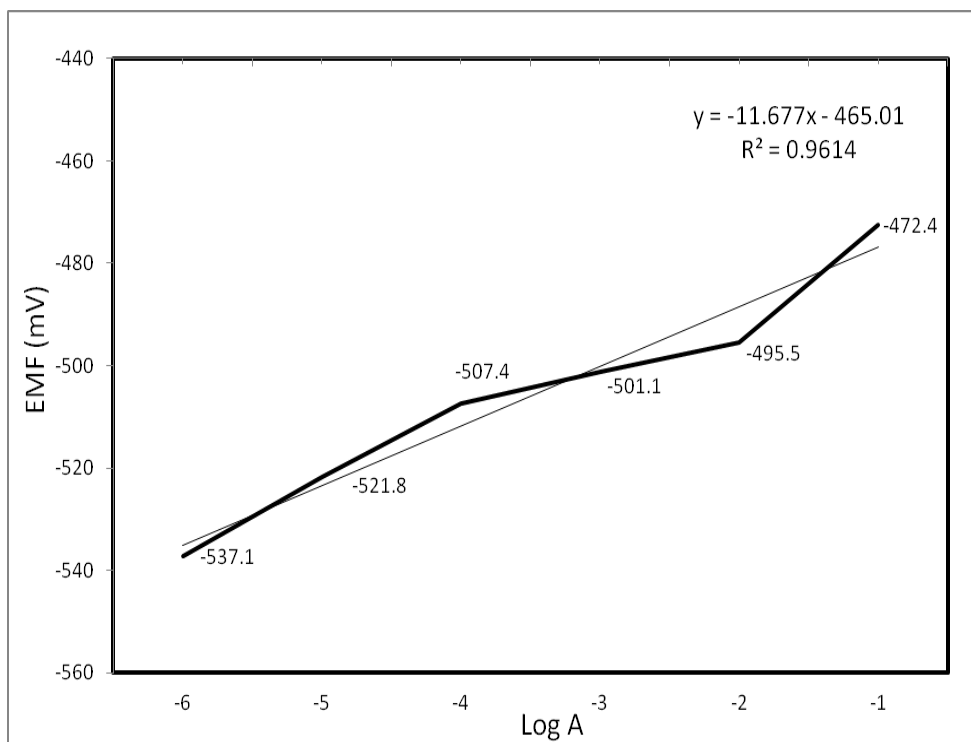


Figure 3.5 Calibration curve for the phosphate sensitive electrode combination 20%  $\text{AlPO}_4$  + 80% Al.

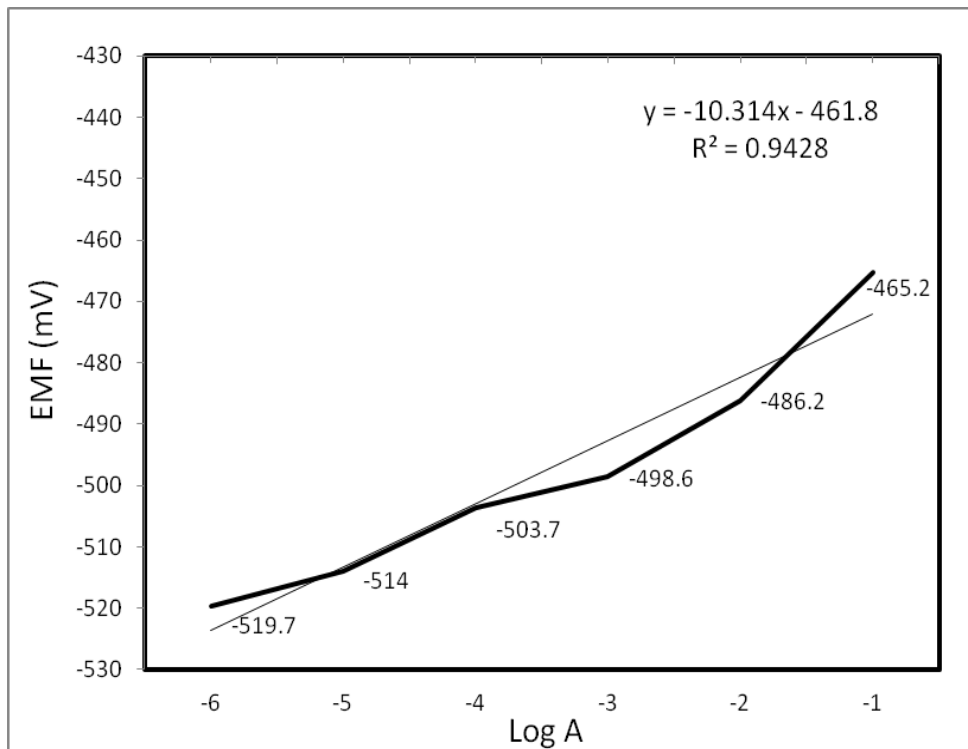


Figure 3.6 Calibration curve for the phosphate sensitive electrode combination 30%  $\text{AlPO}_4$  + 70%  $\text{Al}$ .

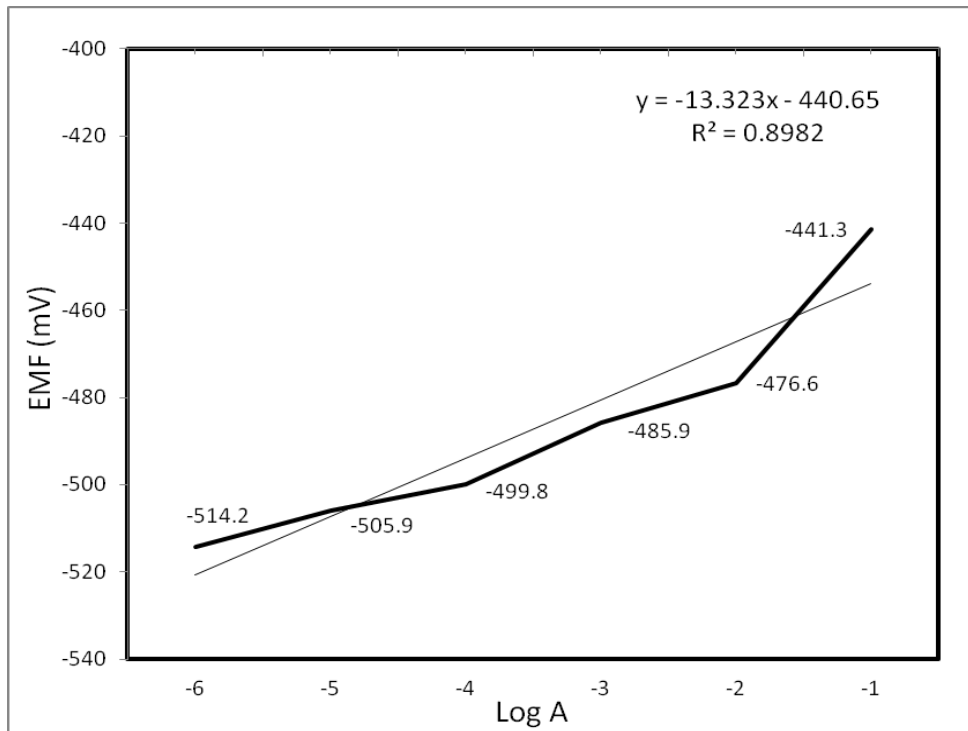


Figure 3.7 Calibration curve for the phosphate sensitive electrode combination 40%  $\text{AlPO}_4$  + 60%  $\text{Al}$ .

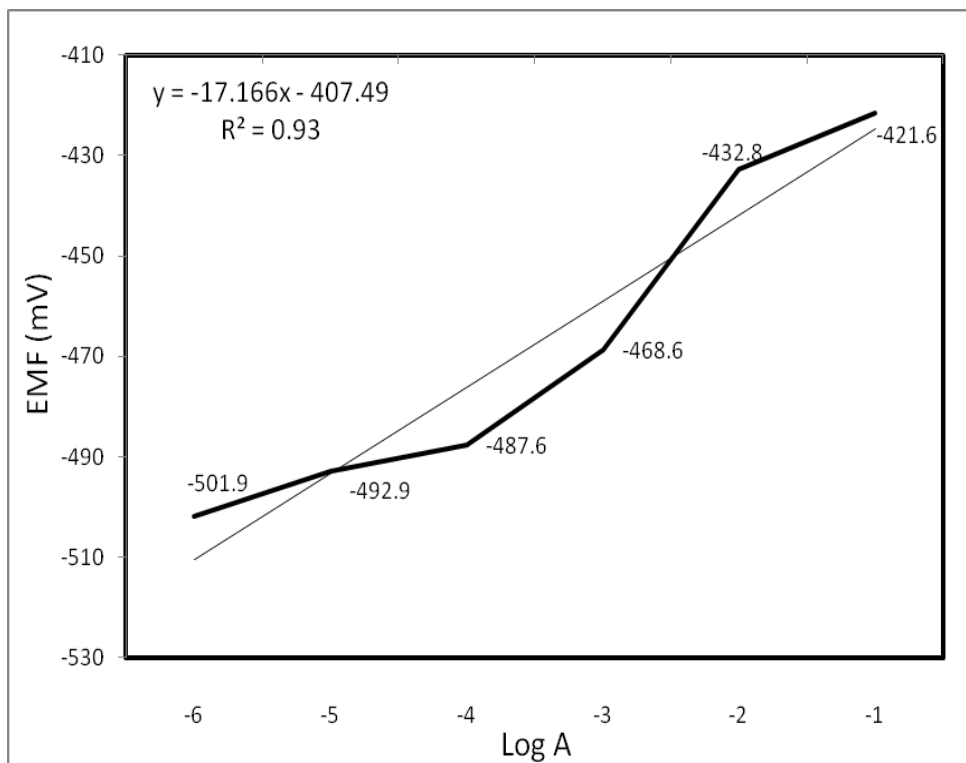


Figure 3.8 Calibration curve for the phosphate sensitive electrode combination 50%  $\text{AlPO}_4$  + 50%  $\text{Al}$ .

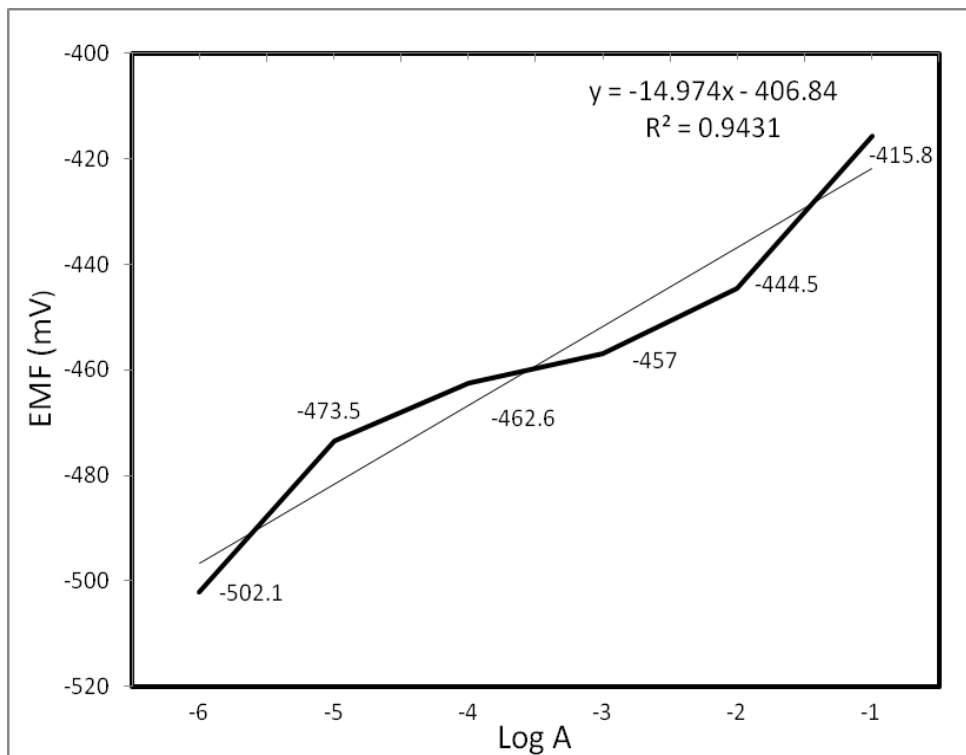


Figure 3.9 Calibration curve for the phosphate sensitive electrode combination 60%  $\text{AlPO}_4$  + 40%  $\text{Al}$ .

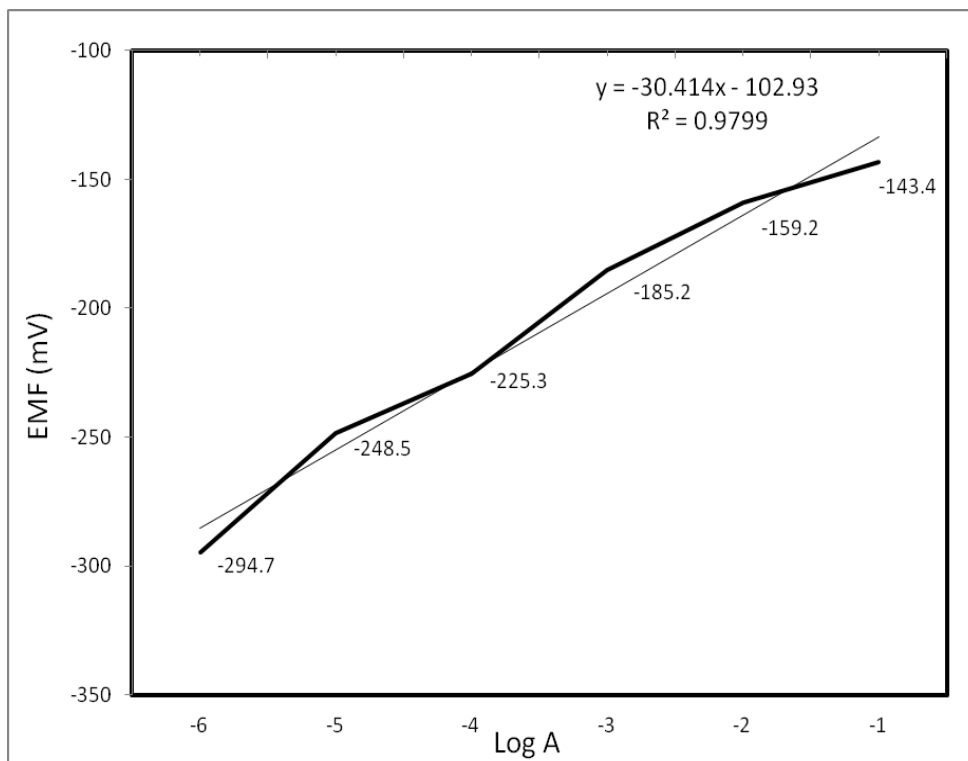


Figure 3.10 Calibration curve for the phosphate sensitive electrode combination 10%  $AlPO_4$  + 90%  $Cu$ .

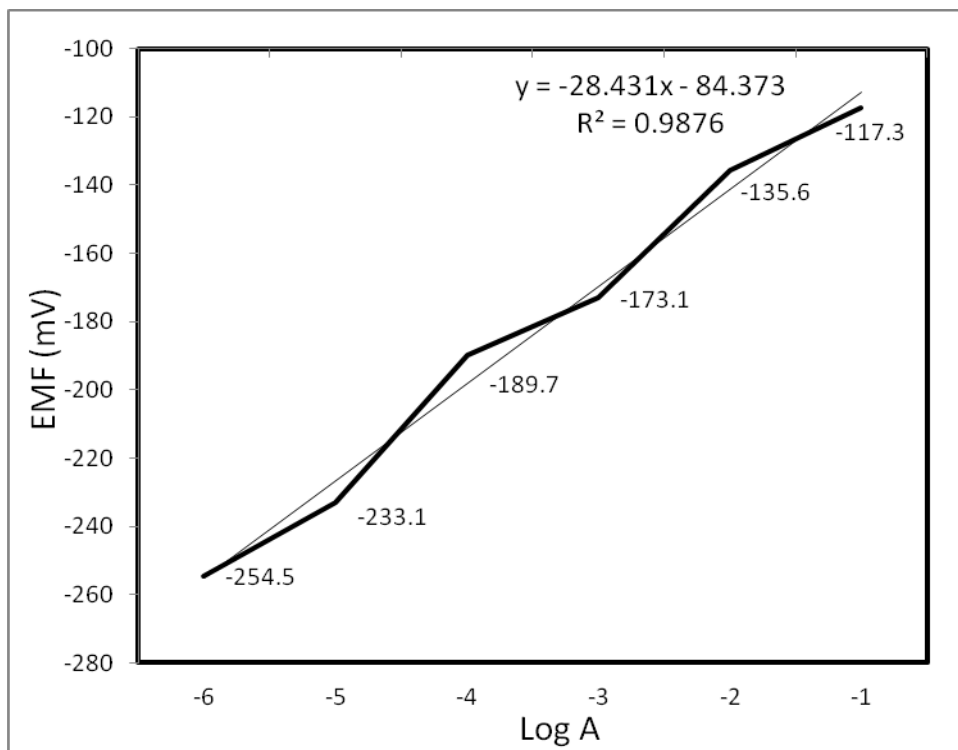


Figure 3.11 Calibration curve for the phosphate sensitive electrode combination 20%  $AlPO_4$  + 80%  $Cu$ .

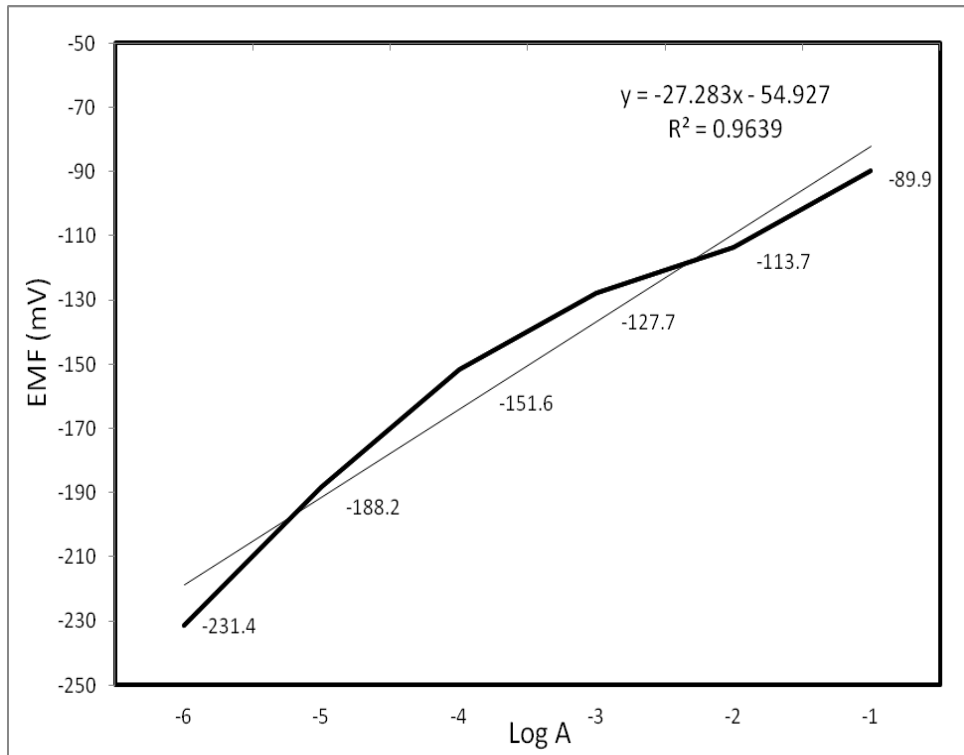


Figure 3.12 Calibration curve for the phosphate sensitive electrode combination 30%  $\text{AlPO}_4$  + 70%  $\text{Cu}$ .

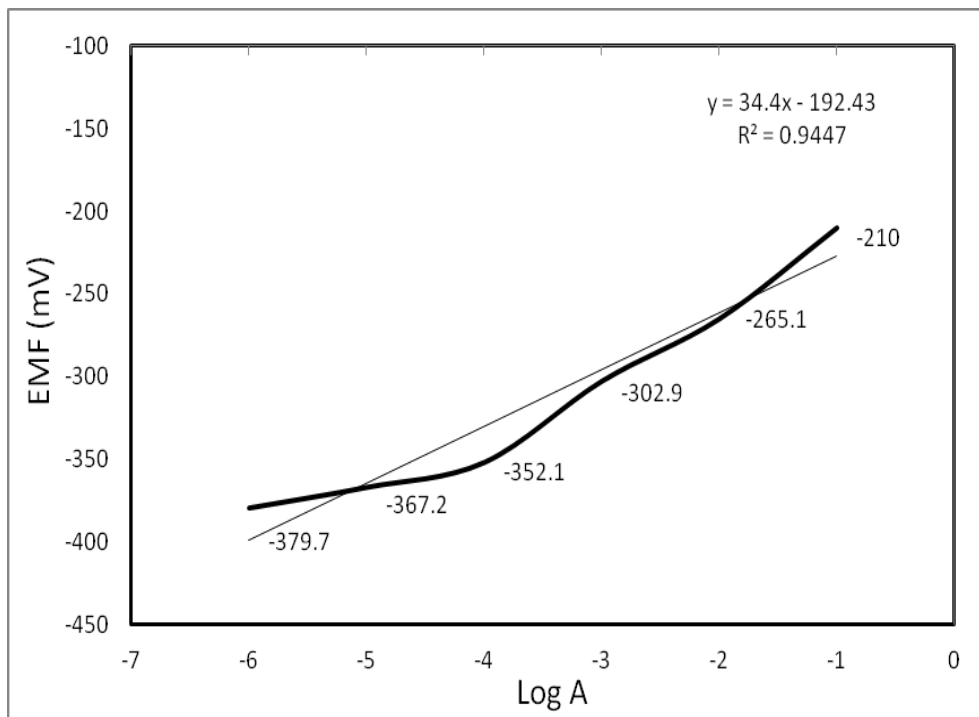


Figure 3.13 Calibration curve for the phosphate sensitive electrode combination 10%  $\text{AlPO}_4$  + 10%  $\text{Cu}$  + 80%  $\text{Al}$ .



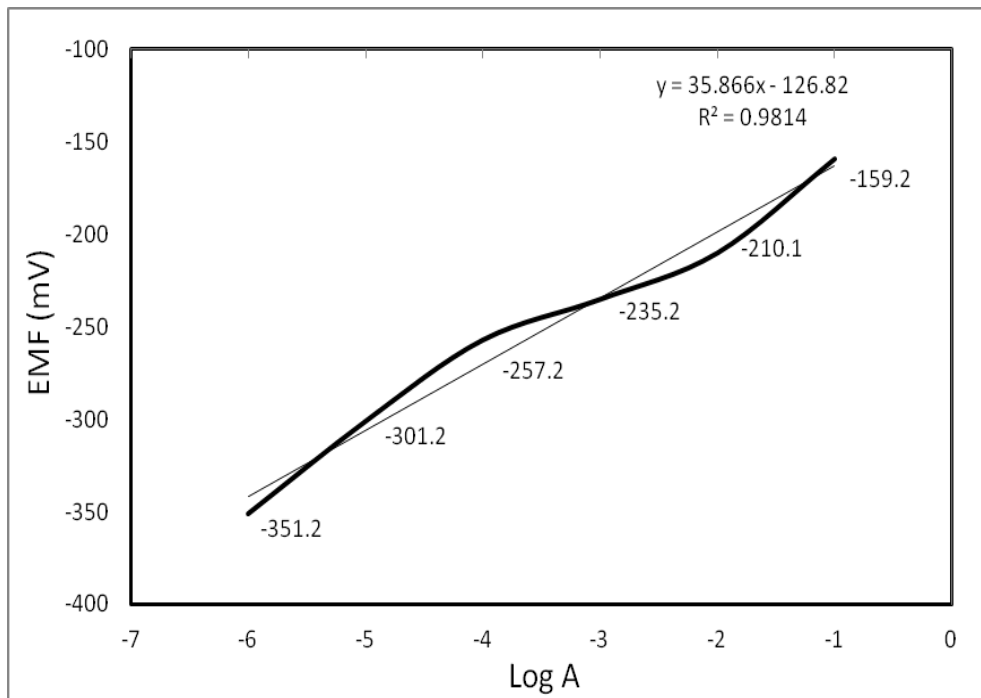


Figure 3.14 Calibration curve for the phosphate sensitive electrode combination 15%  $AlPO_4$  + 15% Cu + 70% Al.

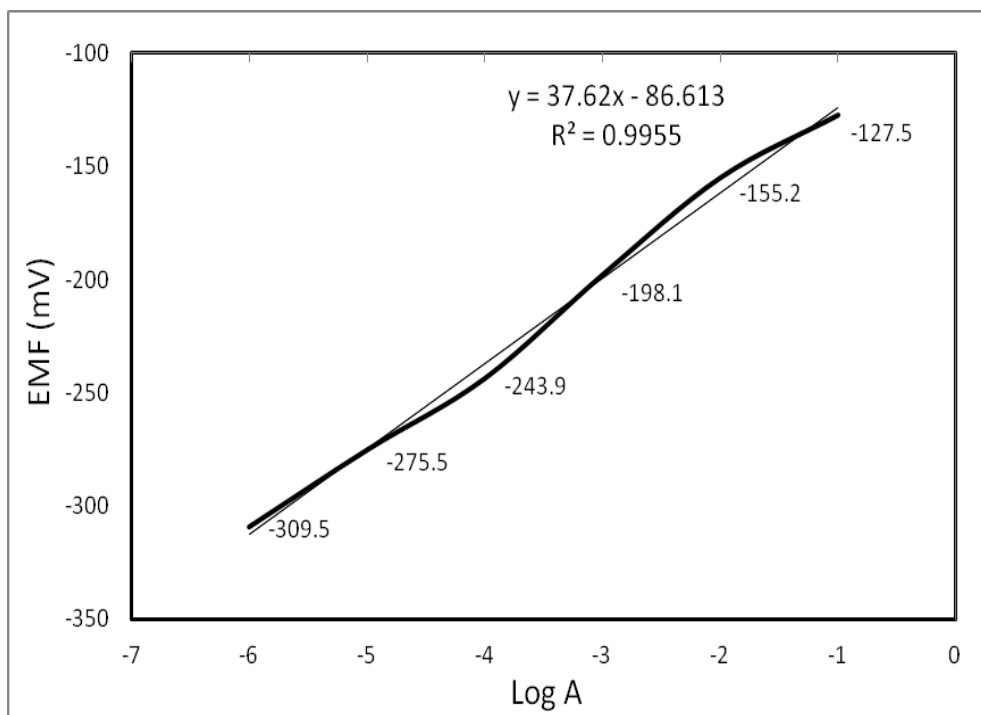


Figure 3.15 Calibration curve for the phosphate sensitive electrode combination 20%  $AlPO_4$  + 20% Cu + 60% Al.

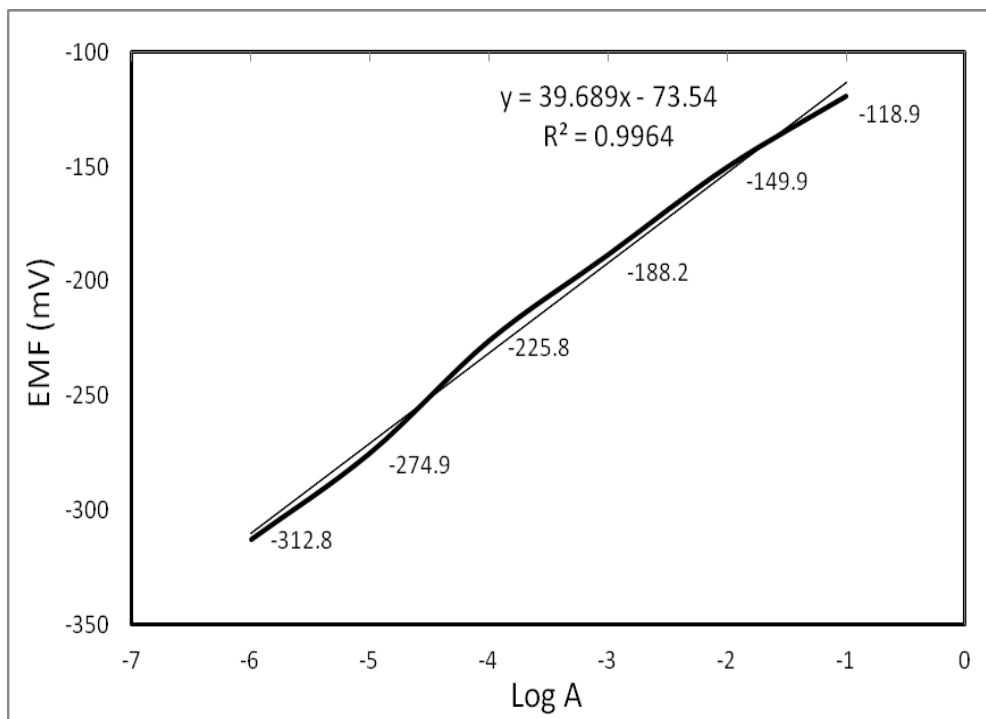


Figure 3.16 Calibration curve for the phosphate sensitive electrode combination 25%  $\text{AlPO}_4$  + 25% Cu + 50% Al.

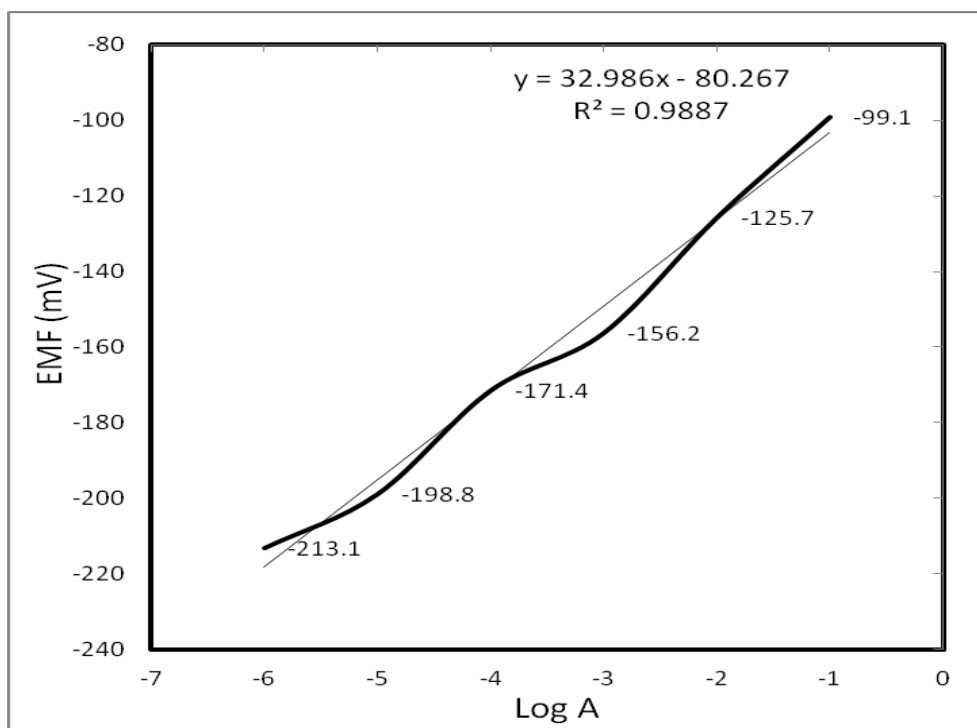


Figure 3.17 Calibration curve for the phosphate sensitive electrode combination 30%  $\text{AlPO}_4$  + 30% Cu + 40% Al.

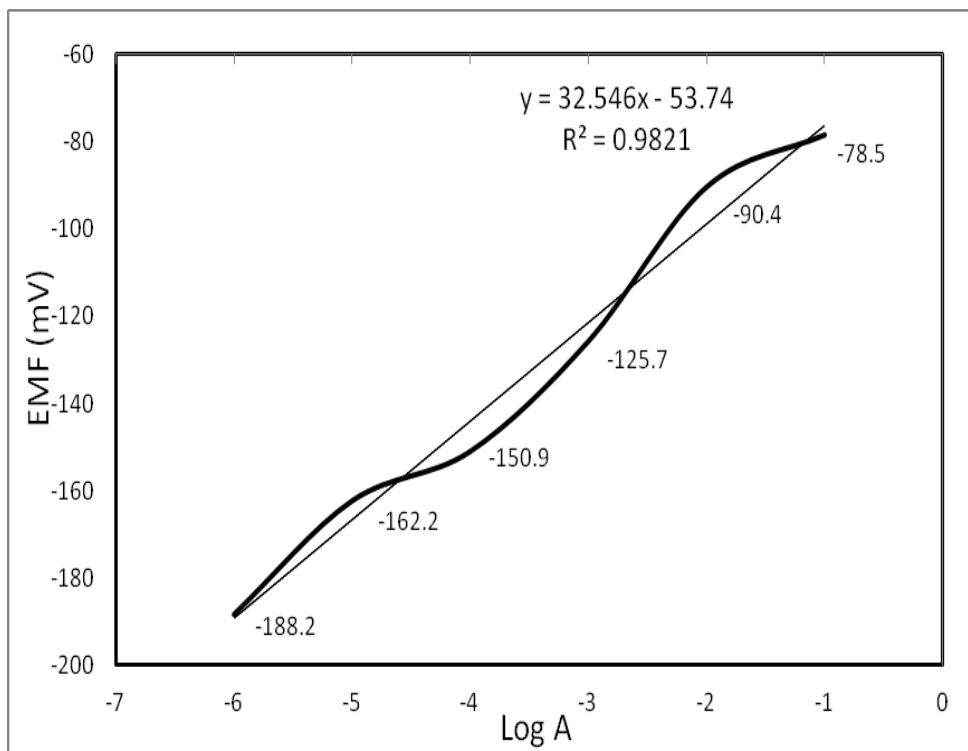


Figure 3.18 Calibration curve for the phosphate sensitive electrode combination 35%  $\text{AlPO}_4$  + 35% Cu + 30% Al.

The average Nernstian slopes for the different electrodes were determined and given in Table 3.3.

Table 3.3 Average Nernstian slopes for different phosphate sensitive electrodes.

Composition (%)	Average Slope ( $10^{-6}$ to $10^{-1}$ mol $\text{L}^{-1}$ )	$S = \sqrt{\frac{\sum(\bar{x} - x_i)^2}{N-1}}$	$CI^* = \bar{x} \pm \frac{t \cdot S}{\sqrt{N}}$
10 % $\text{AlPO}_4$ + 90% Al	10.729	0.183	$10.729 \pm 0.336$
20 % $\text{AlPO}_4$ + 80% Al	11.677	0.156	$11.677 \pm 0.284$
30% $\text{AlPO}_4$ + 70% Al	10.314	0.012	$10.314 \pm 0.022$
40% $\text{AlPO}_4$ + 60% Al	13.323	0.096	$13.323 \pm 0.176$
50% $\text{AlPO}_4$ + 50% Al	17.166	0.228	$17.166 \pm 0.419$
60% $\text{AlPO}_4$ + 40% Al	14.974	0.162	$14.974 \pm 0.297$

10% AlPO <sub>4</sub> + 90% Cu	30.414	0.104	30.414 ± 0.191
20% AlPO <sub>4</sub> + 80% Cu	28.431	1.307	28.431 ± 2.399
30% AlPO <sub>4</sub> + 70% Cu	27.283	0.869	27.283 ± 1.595
10% AlPO <sub>4</sub> + 10% Cu + 80% Al	34.400	0.982	34.400 ± 1.802
15% AlPO <sub>4</sub> + 15% Cu + 70% Al	35.866	0.659	35.866 ± 1.209
20% AlPO <sub>4</sub> + 20% Cu + 60% Al	37.620	0.599	37.620 ± 1.099
25% AlPO <sub>4</sub> + 25% Cu + 50% Al	39.689	0.762	39.689 ± 1.399
30% AlPO <sub>4</sub> + 30% Cu + 40% Al	32.986	0.995	32.986 ± 1.827
35% AlPO <sub>4</sub> + 35% Cu + 30% Al	32.546	0.458	32.546 ± 0.841

Note that there are three electrodes for each composition,  $N = 3$  and at 95% confidence interval,  $t$  is the deviation of a data point from the mean relative to one standard deviation (in this case  $t = 3.18$ ) and  $S$  is the calculated standard deviation.

The complete Nernst equation is composed of Nernst factor, sensitivity factor and selectivity factor. If one does not consider the sensitivity and selectivity factors (i.e. assuming 100% sensitivity and selectivity), the Nernst equation can be written as:

$E = E_o + 2.303 RT/nF$ . The fraction  $2.303 R/F$  can be replaced by 0.198 called the

Nernst factor. The factor  $0.198 T/n$  will ideally give a value of about 59 mV for a monovalent ion. The Nernst equation can be modified by the sensitivity of the electrode,  $S/100\%$ . Similarly the selectivity of an electrode is never 100%. Other ions may interfere. Hence selectivity factor has to be included to account for the interfering ions. Our ion selective electrodes are able to detect both the monohydrogen and dihydrogen phosphate ions which exist in the solution. This is in accordance with the

speciation diagram given in figure 3.1. Hence the value of  $n$  in the Nernst equation may be calculated by considering the concentration of the two species. For example, at a pH of 7.0, 62% of the dihydrogen phosphate and 38% of the monohydrogen phosphate anions are presumed to exist in the solution giving rise to a calculated  $n$  value of about 1.4. Hence, the ideal Nernstian slope is expected to be  $0.198 T/1.4$  which produces a value of 42 mV. This is evident in the Nernstian slopes obtained for the different phosphate sensitive electrodes in the calibration curves. The slopes obtained for the ternary electrodes agree more to the above than the binary ones.

From table 3.3, it can be seen that membrane composition affects the sensitivity and selectivity of the phosphate sensitive electrodes produced. The ternary electrode exhibits higher regression (less error in the slope). The electrode with the membrane composition of 25%  $\text{AlPO}_4$  +25% Cu + 50% Al was chosen for most of the analysis as it depicted analytical stability and better sensitivity in the phosphate concentration range under investigation. The Nernstian slope was found to be about 40 mV which is very close to the theoretical true value.

Ion selective electrodes measure the activity of ions in equilibrium at the membrane surface. In dilute solutions this is directly related to the total number of ions in the solution but at higher concentrations, inter-ionic interactions between all ions in the solution (both positive and negative) tend to reduce the mobility and thus there are relatively fewer of the measured ions in the vicinity of the membrane than in the bulk solution. Thus, the measured voltage is less than it would be if it reflected the total

number in the solution and this causes an erroneously low estimate of the concentration in samples with a high concentration and/or a complex matrix. The activity coefficient is always less than one and becomes smaller as the ionic strength increases; thus the difference between the measured activity and the actual concentration becomes higher at higher concentrations. This effect causes two main problems in ISE measurement. Firstly, when constructing a calibration graph using concentration units, the line is seen to curve away from linearity as the concentration increases (it remains straight, up to the highest concentrations if activity units are used). Thus, if concentration units are used, it is necessary to measure many more calibration points in order to define the curve more precisely and permit accurate interpolation of sample results. Secondly, it is most likely that the sample solutions will contain other ions in addition to the ion being measured and the ionic strength of the samples may be significantly higher than that of the standards. Thus, there will be an incompatibility between the calibration line and the measured samples leading to errors in the interpolated results. This is in line with literature evidence.<sup>139,171</sup>

If activity was directly proportional to concentration, the ISE response would be linear. If there is no ionic strength buffer, increasing the concentration changes the ionic strength, which changes the activity coefficient, which drives the activity away from the concentration, and, therefore, the ISE response becomes non-linear with concentration.

### 3.6.1 THE EFFECT OF pH ON THE DIFFERENT ELECTRODES

The effect of pH on the response of the electrodes in the calibration curve studies was undertaken by varying pH values as shown in table 3.1. For the experiment, standards of known concentration were prepared at different pH values and their EMF readings obtained for all the electrodes under investigation. The results obtained showed that there was no effect of pH on the response characteristics of all the electrodes constructed within pH range of 4.5 to 8.9. Since the solutions contain different compositions of the monohydrogen and the dihydrogen phosphate anions at the different pH values, it is indicative of the fact that the electrodes are sensitive to both anions without any particular preference. The measurements obtained correlates to the total phosphate species in the solution. However, the electrodes response was different at a pH above 9.0. This is due to the increase in the concentration of hydroxide ions in the solution which interferes with the electrodes responses. This effect was also noticed in the interference studies conducted. The graph shown here depicts the pH studies done for the electrode with membrane composition 25%  $AlPO_4$  + 25%  $Cu$  + 50%  $Al$  alone. Other electrodes showed similar trends too.

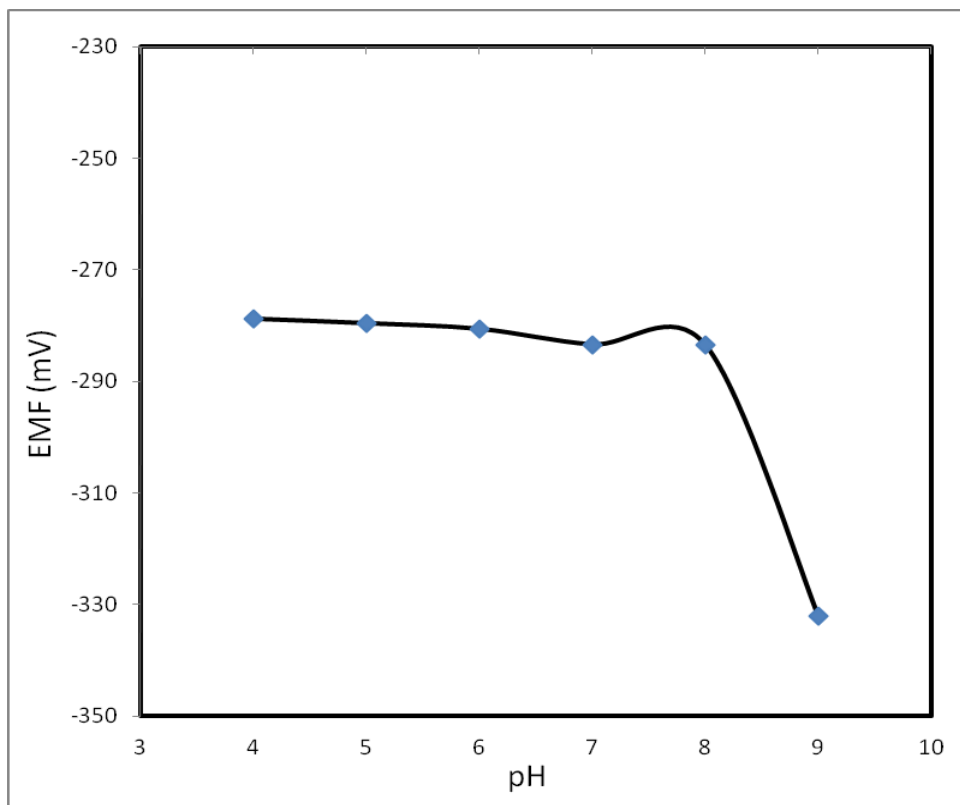


Figure 3.19 The pH dependence of the electrode with membrane composition of 25%  $\text{AlPO}_4$  + 25% Cu + 50% Al.

### 3.6.2 THE RESPONSE TIME OF THE ELECTRODES

The conventional IUPAC definition of response time for ISE is the time which elapses between the instant when an ISE and a reference electrode are brought into contact with the sample solution (or at which the activity of the ion of interest in a solution is changed). That is, the first instant at which the emf/time slope ( $\Delta E/\Delta t$ ) becomes equal to a limiting value selected on the basis of experimental conditions or requirements for accuracy.<sup>139</sup> The response time obviously is dependent on concentration change. In this study, the dipping method that gives static response was employed. The potential values were measured for each concentration change after 0 (point of electrode



immersion in solution), 30, 60, 90, 120, 150 and 180 seconds when Pi concentration was changed from  $1 \times 10^{-6}$  to  $1 \times 10^{-5}$ ,  $1 \times 10^{-5}$  to  $1 \times 10^{-4}$ ,  $1 \times 10^{-4}$  to  $1 \times 10^{-3}$ ,  $1 \times 10^{-3}$  to  $1 \times 10^{-2}$  and  $1 \times 10^{-2}$  to  $1 \times 10^{-1}$  M. The response was found to be stable in about 60 seconds. All these measurements were made at constant temperature. The dependence of response time with change of concentration of phosphate species is depicted in Figure 3.20.

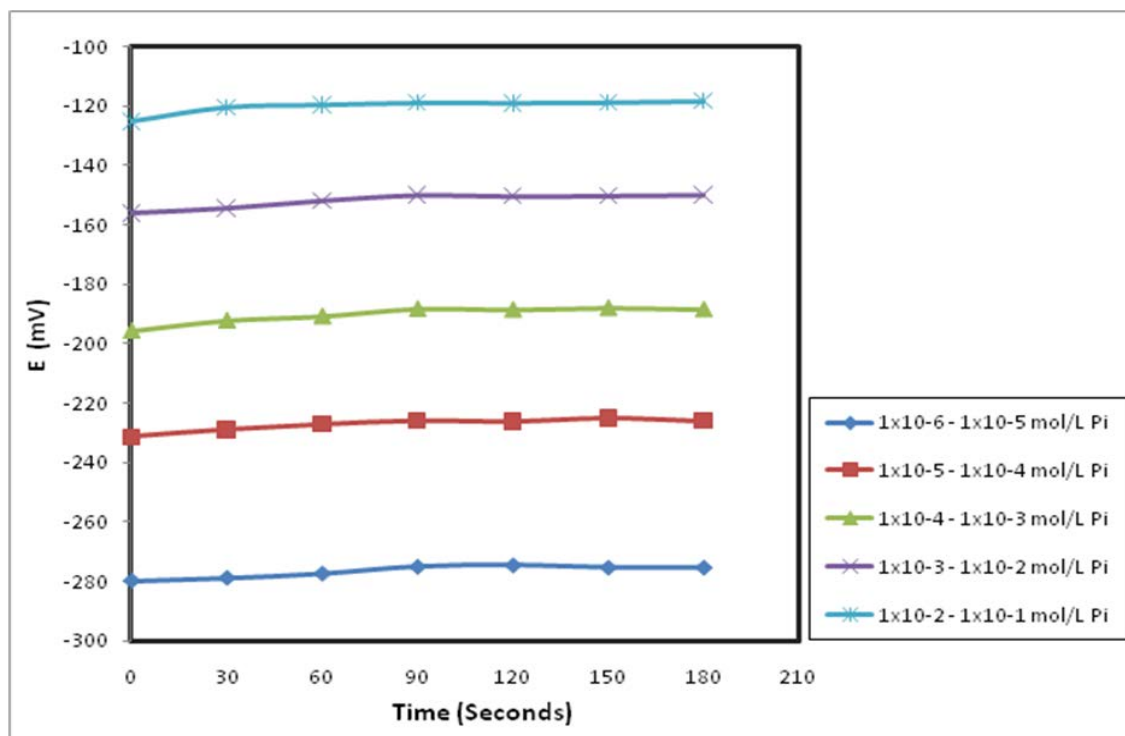


Figure 3.20 The dependence of response time with concentration (25%  $\text{AlPO}_4$  + 25%  $\text{Cu}$  + 50%  $\text{Al}$  membrane electrode).

### 3.6.3 INTERFERENCE STUDIES

All ion sensitive electrodes are sensitive to some other ions to some extent. For many applications these interferences are insignificant (unless there is a high ratio of interfering ion to primary ion) and can often be ignored. In some extreme cases,

however, the electrode is far more sensitive to the interfering ion than to the primary ion and can only be used if the interfering ion is only present in trace quantities or even completely absent. Hence it is important to study the effects of all other ions in the medium. The response of an ion selective electrode is the potential developed as a function of the ionic activity of the species in solution. Hence when activity increases the electrode potential is expected to become more positive if the electrode is sensing a cation and more negative if it is sensing an anion.

It should be worth mentioning that separate interference studies were conducted for all the electrodes produced in this study. The result shown in table 3.4 is only for the electrode combination 25%  $\text{AlPO}_4$  + 25% Cu + 50% Al. Again, this electrode was chosen for most of the analysis as it depicted analytical stability and better sensitivity in the phosphate concentration range under investigation. The Nernstian slope was found to be about 40 mV (see table 3.3) which is very close to the calculated theoretical true value. Solutions were prepared with a constant activity of the main ion (phosphate ion) and varying activity of interfering ion. The concentration of the stock solution of both the phosphate standard and the interferent was  $1 \times 10^{-2}$  M. They were mixed according to the results shown in Table 3.4.

Table 3.4 The effect of interfering ions on the electrode's response.

INTERFERENT SOLUTION	10 mL STANDARD + 10 mL INTERFERENT + 80 mL H <sub>2</sub> O	10 mL STANDARD+ 20 mL INTERFERENT + 70 mL H <sub>2</sub> O	10 mL STANDARD + 30mL INTERFERENT + 60mL H <sub>2</sub> O	10 mL STANDARD + 40 mL INTERFERENT + 50 mL H <sub>2</sub> O	10 mL STANDARD + 50 mL INTERFERENT + 40 mL H <sub>2</sub> O
KBr	-287.9	-296.7	-303.1	-310.2	-315.8
KCl	-280.1	-434.1	-459.2	-475.4	-483.5
KI	-296.5	-299.3	-309.5	-306.7	-303.5
KCN	-261.0	-357.7	-424.3	-466.1	-491.2
KOH	-253.0	-258.8	-273.1	-480.1	-579.2
KNO <sub>3</sub>	-210.4	-234.8	-218.0	-213.1	-206.5
NaCl	-282.6	-451.1	-483.0	-503.2	-521.2
NaOH	-263.2	-266.4	-293.0	-535.4	-644.2
NaF	-231.5	-253.5	-252.3	-231.4	-265.0
NaI	-236.4	-251.2	-264.1	-266.4	-265.1
Na <sub>2</sub> SO <sub>4</sub>	-226.5	-218.0	-209.1	-209.4	-208.5
Na <sub>2</sub> CO <sub>3</sub>	-213.7	-232.1	-216.0	-202.7	-217.8
CaCl <sub>2</sub>	-268.1	-401.0	-454.9	-473.7	-480.1
Ca(NO <sub>3</sub> ) <sub>2</sub>	-267.7	-273.7	-266.2	-279.8	-288.5
Ca(OH) <sub>2</sub>	-214.3	-306.3	-386.2	-570.8	-1061.2
CaCO <sub>3</sub>	-236.0	-252.0	-271.9	-248.0	-238.0
MgSO <sub>4</sub> .7H <sub>2</sub> O	-254.2	-242.0	-208.9	-200.6	-203.9
MgCl <sub>2</sub> .6H <sub>2</sub> O	-245.4	-490.4	-526.5	-553.8	-563.3
Mg(NO <sub>3</sub> ) <sub>2</sub> .6H <sub>2</sub> O	-287.7	-216.5	-202.6	-198.7	-191.8
Zn(CN) <sub>2</sub>	-256.0	-253.6	-254.6	-255.2	-259.8
ZnSO <sub>4</sub> .7H <sub>2</sub> O	-203.1	-181.7	-186.6	-186.9	-188.4
Zn(NO <sub>3</sub> ) <sub>2</sub> .4H <sub>2</sub> O	-189.9	-166.4	-168.0	-170.8	-171.8
CuSO <sub>4</sub>	-195.0	-86.8	-19.5	-10.1	-2.5
Cu(NO <sub>3</sub> ) <sub>2</sub>	-221.7	-119.5	-89.4	82.4	89.5
CuCl <sub>2</sub> .2H <sub>2</sub> O	-210.6	-321.7	-389.0	-461.0	-479.7
CoCO <sub>3</sub> .xH <sub>2</sub> O	-230.4	-278.4	-260.5	-240.0	-243.8

<b>Co(NO<sub>3</sub>)<sub>2</sub>.6H<sub>2</sub>O</b>	-234.9	-200.2	-216.8	-234.7	-248.9
<b>CoCl<sub>2</sub>.6H<sub>2</sub>O</b>	-212.6	-429.1	-474.4	-493.5	-510.0
<b>Ni(NO<sub>3</sub>)<sub>2</sub>.6H<sub>2</sub>O</b>	-243.0	-250.1	-244.9	-249.8	-258.1
<b>NiCl<sub>2</sub>.6H<sub>2</sub>O</b>	-251.0	-415.8	-445.9	-477.7	-491.2
<b>NaNO<sub>3</sub></b>	-215.1	-212.8	-208.2	-219.1	-225.4
<b>Pb(NO<sub>3</sub>)<sub>2</sub></b>	-206.2	-113.5	-135.5	-143.2	-177.3
<b>AgNO<sub>3</sub></b>	-241.0	-127.0	35.2	161.4	182.4
<b>V<sub>2</sub>O<sub>5</sub></b>	-237.6	-216.4	-186.7	-125.1	-53.6
<b>BaCl<sub>2</sub>.2H<sub>2</sub>O</b>	-235.8	381.0	-455.9	-492.8	-519.2
<b>HgCl<sub>2</sub></b>	-211.5	-391.2	-453.0	-457.9	-460.8
<b>NH<sub>4</sub>Br</b>	-308.0	-296.8	-299.6	-303.8	-311.7
<b>NH<sub>4</sub>Cl</b>	-261.4	-334.9	-410.7	-433.2	-465.5
<b>NH<sub>4</sub>ClO<sub>4</sub></b>	-260.9	-282.4	-286.6	-295.1	-298.0
<b>KClO<sub>3</sub></b>	-230.8	-245.3	-280.1	-299.8	-329.1
<b>Na<sub>4</sub>P<sub>2</sub>O<sub>7</sub>.10H<sub>2</sub>O</b>	-192.0	-191.3	-187.7	-184.7	-182.4

*The standard phosphate solution was  $1 \times 10^{-2}$  M constituted from 62% monohydrogen and 38% dihydrogen phosphates. The interferent species were also  $1 \times 10^{-2}$  M before mixing. The average EMF value of the phosphate standard was -274.9).*

It is generally accepted that the slope of ion sensitive electrodes increase by about 2 mV/decade with each  $10^{\circ}$  C rise in temperature.<sup>196,197</sup> The response of the electrode for selected anions and cations in the presence of  $1 \times 10^{-2}$  M phosphate is shown in Figures 3.21 and 3.22 respectively.

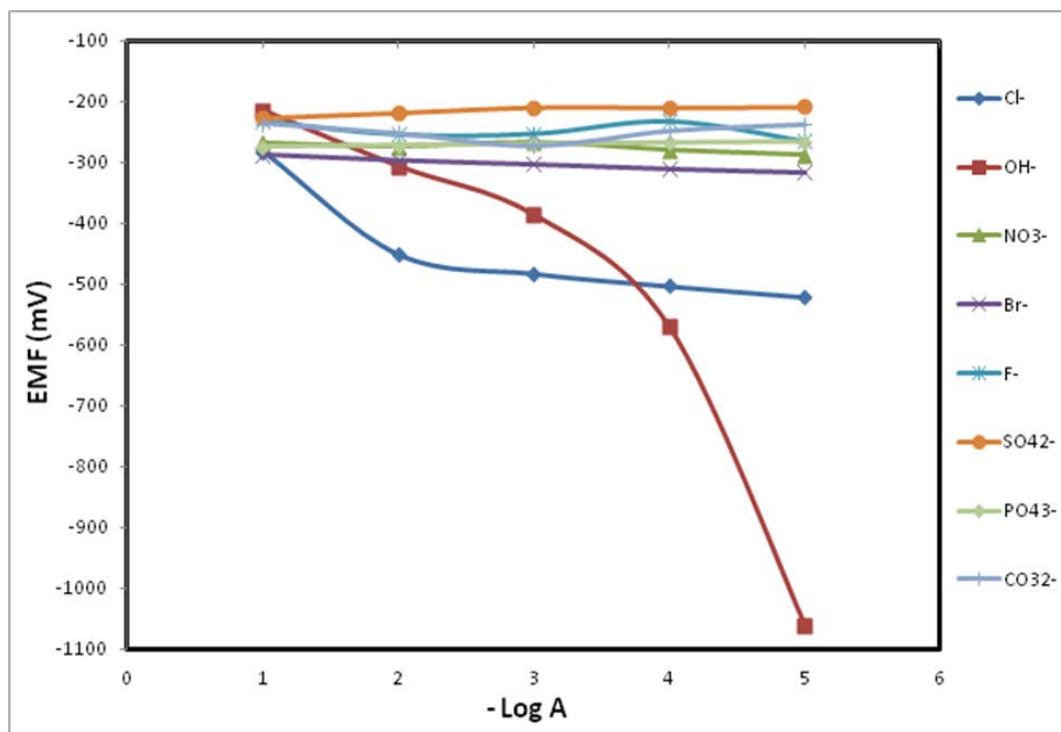


Figure 3.21 The response of the electrode against some anions in the presence of  $1 \times 10^{-2}$  M phosphate (25%  $AlPO_4$  + 25% Cu + 50% Al membrane electrode).

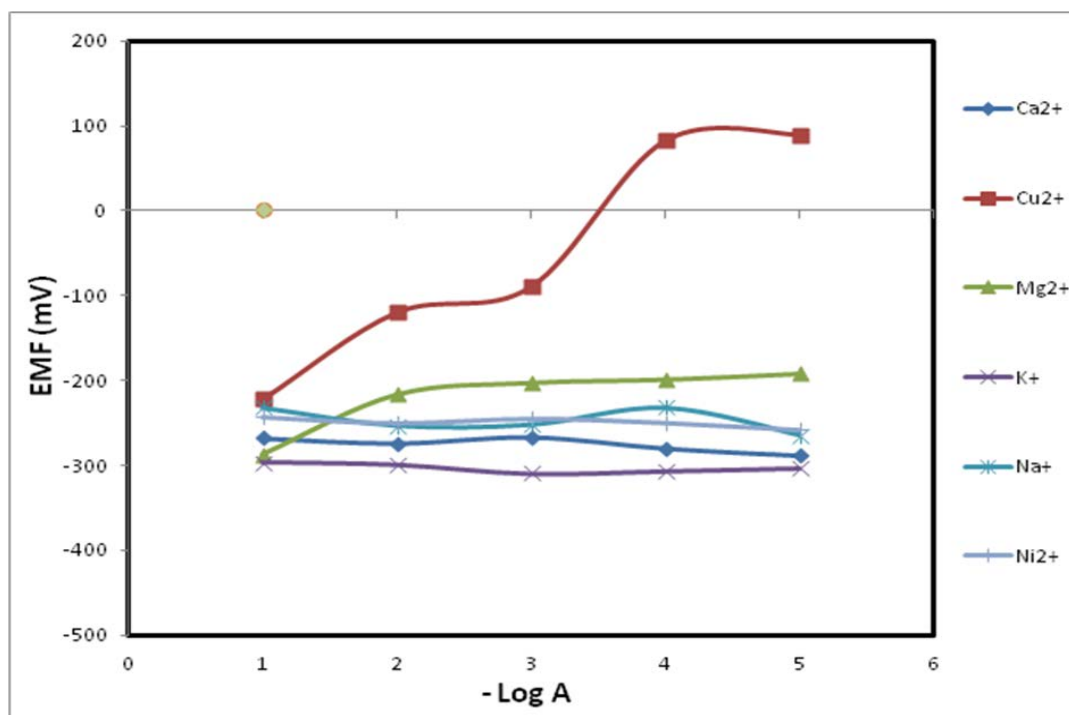


Figure 3.22 The response of the electrode against some cations in the presence of  $1 \times 10^{-2}$  M phosphate (25%  $AlPO_4$  + 25% Cu + 50% Al membrane electrode).

As can be seen from the table 3.4 and figures 3.21 and 3.22, no appreciable interference was observed for common anions such as sulphates, nitrates, carbonates, bromides and fluorides. The same can be said for the cations studied except for solutions that contain copper complexes. The electrode is found to be sensitive to chloride and hydroxide ions appreciably. Further studies on the use of the electrode to monitor chloride ions are under investigation. Determination of both chloride and phosphate ions simultaneously using our electrode for environmental samples is also under investigation. In order to achieve correct and sensitive results in analysis, it is important to know the effects of all the ions in the medium. The effect can be identified through selectivity coefficient. In this study, mixed solutions method<sup>39</sup> was used to determine selectivity coefficient  $k_{A,B}^{pot}$  as it usually corresponds more closely to the situation in samples. Selectivity coefficient values were calculated via making use of the below given equation:

$$k_{A,B}^{pot} a_B^{n_A/n_B} = a_A \left\{ \text{antilog} \left[ \frac{E_1 - E_2}{S} \right] \right\} - a_A \quad (\text{Equation 3.1})$$

Where  $S = 2.303RT/n_A F$  (the slope of the phosphate electrode),  $a_A$  is the activity of the primary ion,  $a_B$  the activity of the interfering ion,  $E_1$  is the potential measured when only  $A$  is present,  $E_2$  the potential responsive to the primary ion in the presence of interfering ion,  $k_{A,B}$  is the selectivity coefficient and  $n_A, n_B$  are the charges of  $A$  and  $B$  respectively. For the determination of the selectivity coefficients for each interfering ion, the  $a_B^{n_A/n_B}$  values in equation 3.1 are plotted against the values of right hand side of the

same equation ( $\alpha_A \left\{ \text{antilog} \left[ \frac{E_1 - E_2}{S} \right] \right\} - \alpha_A$ ) and the slope will be equal to the selectivity coefficient ( $k_{A,B}^{\text{pot}}$ ) of the interfering ion. The selectivity coefficients obtained for mentioned anions and cations are given in Table 3.5. The present phosphate electrode displayed very good selectivity for phosphate ions in solution.

Table 3.5 Selectivity coefficients ( $k_{A,B}^{\text{pot}}$ ) for the phosphate electrode (25%  $\text{AlPO}_4$  + 25%  $\text{Cu}$  + 50%  $\text{Al}$  membrane electrode) in mixed solutions (in the presence of  $1 \times 10^{-3}$  M phosphate) (B: interfering ion; A: phosphate ion).

IONS	$k_{A,B}^{\text{pot}}$
$\text{NO}_3^-$	$1.9 \times 10^{-1}$
$\text{F}^-$	$7.6 \times 10^{-2}$
$\text{SO}_4^{2-}$	$1.9 \times 10^{-1}$
$\text{Br}^-$	$2.1 \times 10^{-1}$
$\text{CO}_3^{2-}$	$2.9 \times 10^{-3}$
$\text{Cl}^-$	2.1
$\text{OH}^-$	16.4
$\text{Ca}^{2+}$	$3.5 \times 10^{-1}$
$\text{Cu}^{2+}$	1.9
$\text{Mg}^{2+}$	$4.2 \times 10^{-1}$
$\text{K}^+$	$5.7 \times 10^{-1}$
$\text{Na}^+$	$2.5 \times 10^{-1}$
$\text{Ni}^+$	$4.4 \times 10^{-2}$

Table 3.5 summarizes the results of measurements carried out in mixed solutions. It probably corresponds more realistically to practical samples where mixtures of ions are present. The electrode is relatively insensitive to most anions and cations but responds well to anionic solutions containing chlorides and hydroxides. Cationic interferences were also investigated and it was found that this electrode responds well to  $\text{Cu}^{2+}$  ions as

expected. A plot to show how the selectivity coefficient was obtained from the slope is shown for fluoride in Figure 3.23 below.

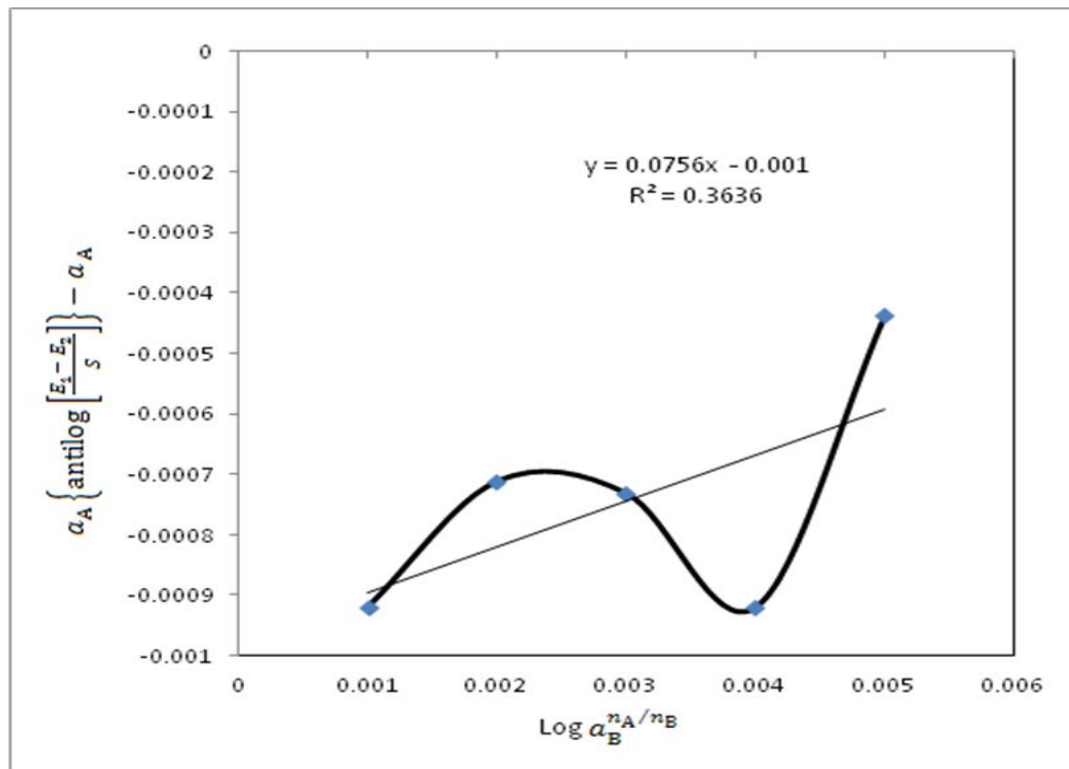


Figure 3.23. A plot showing selectivity coefficient for fluoride ion over the primary ion for the phosphate electrode (25%  $\text{AlPO}_4$  + 25% Cu + 50% Al).

Previous investigators<sup>39,40</sup> have employed the use of total ionic strength adjustment buffers (TISAB) to keep the ionic strength of the reacting solutions constant. In most cases they use 0.1 M  $\text{NaNO}_3$ . The effect of a change in ionic strength brought about by the concentrations of phosphate species in our working solution is evident. However, the effect of this change on the total electrode potential was found to be less important at solutions concentration less than  $1 \times 10^{-2}$  mol/L. Also, other TISAB formulations (see section 2.3.5.5) contain reasonable amount of hydroxide which will interfere in



phosphate ion determination with our electrode system. Hence in this study, no attempt was necessitated to keep the ionic strength constant as the main aim of our investigation is to produce robust phosphate selective electrodes that may be used in environmental samples without the need for ionic strength control. It should be worth mentioning that the determination of free phosphate in the presence of the pyrophosphate is possible using our fabricated electrodes, as there was no interference recorded in the experiments conducted.

The ternary membrane electrodes all show better analytical stability over the binary ones. The selected electrode from the ternary combinations (25%  $AlPO_4$  + 25%  $Cu$  + 50%  $Al$ ) was investigated in greater detail. Numerous tests were conducted as shown below. All solutions used were kept within the temperature range of  $25 \pm 3^\circ C$ .

- (a) Sensitivity: The response was Nernstian down to  $1 \times 10^{-6}$  M phosphate. It is quite interesting to note that the electrode is still sensitive to  $1 \times 10^{-7}$  M phosphate below which the sensitivity decreases and was not reproducible.
- (b) Precision: The within batch standard deviations of the response of the electrode to  $1 \times 10^{-3}$  M and  $1 \times 10^{-4}$  M phosphate were estimated from the differences between pairs of EMF readings on 5 separate days to be  $\pm 2.21$  mV and  $\pm 2.39$  mV respectively. The similarity in the calculated standard deviation indicates less drift in the standard potential of the electrode system.
- (c) Response time: The response time of the electrode to reach a steady EMF value when transferred from a  $1 \times 10^{-3}$  M to  $1 \times 10^{-4}$  M phosphate solutions was also

observed. The electrode took approximately 60 seconds to reach equilibrium after a tenfold change in the concentration.

- (d) Stability of standard potential: The electrode was immersed in a given solution tending to observe changes in EMF reading with age. It was kept in the solution for two weeks. No appreciable change was observed within the period under investigation. It has been in use for about 3-4 times a week and has not deviated from its regression value in the past 18 months.
- (e) Effect of pH and interferences: The electrode showed similar trend with other electrodes fabricated in terms of pH effect and interferences (see figure 3.19 and table 3.4 respectively).

The next chapter describes in details the application of the selected phosphate selective electrode in monitoring dephosphorylation and phosphorylation reactions utilizing model compounds.

# CHAPTER FOUR

## MONITORING PHOSPHORYLATION AND DEPHOSPHORYLATION REACTIONS USING A NOVEL PHOSPHATE SOLID STATE ION SELECTIVE ELECTRODE

### 4.0 PHOSPHORYLATION AND DEPHOSPHORYLATION REACTIONS

Phosphorylation and dephosphorylation processes play critical roles in mediating cellular responses to extracellular or intracellular stimuli. Multiple levels of protein phosphorylation and dephosphorylation reactions activate and deactivate specific carbohydrates and protein targets. Examples include, trans-cytoplasmic signalling to the nucleus by the nitrogen-activated protein kinase pathway,<sup>198</sup> cell cycle regulation mediated by the action of cyclin-dependent kinases,<sup>199</sup> and the regulation of metabolic enzymes such as glycogen phosphorylases, glycogen dephosphorylases, glycogen synthases and acetyl-CoA carboxylase through the second messenger cyclic adenosine monophosphate (cAMP)<sup>200</sup> produced in response to the binding of glucagon or epinephrine to  $\beta$ -adrenergic receptors. They link the process of respiration and fermentation with other cellular reactions. They are widely noticed in biological functions like the metabolism of cholesterol, DNA replication and RNA synthesis. These biochemical processes are accomplished by phosphorylases and dephosphorylases.<sup>201</sup>

The hydrolysis of ATP can also proceed with transfer of the terminal  $P_2O_7^{4-}$  moiety to water to yield the pyrophosphate ion and adenosine monophosphate (AMP).<sup>202</sup> This process is known as dephosphorylation. These processes have been widely studied and factors that give rise to phosphorylation and dephosphorylation processes elucidated. Among them is the involvement of metal ions in catalyzing these reactions. Metal ions aid this process by cleaving of the P-O-C bond linkage of the organophosphate esters. This is convenient due to the nucleophilicity of the phosphorus and the polar nature of P-O and C-O bonds. Metallohydrolases that contain dinuclear active sites are responsible for the degradation of neurotoxins, urea,  $\beta$ -lactam containing antibiotics and several toxic organophosphates.<sup>203</sup> In essence, enzymes appear to fully utilize the catalytic potential of the metal ions.<sup>204</sup> Metal ion containing enzymes (metalloenzymes) have been studied extensively and found to promote these reactions by one or more of the following effects;<sup>205-208</sup>

- (1) Electrophilic activation of the phosphorus centre: A metal ion bonded to the phosphate draws electron away from the phosphorus center. This increases the positive character of the phosphorus centre enabling nucleophilic attack by the nucleophiles in the system thereby cleaving the P-O linkage.
- (2) Charge neutralization or Shielding: Phosphate derivatives usually carry many negative charges so the approach of a negatively charged nucleophile such as a hydroxide ion is not favoured on electrostatic grounds, so the neutralization or shielding of these negative charges is very necessary for a nucleophilic attack at

the phosphorous centre. Metal ions are Lewis acids or electrophiles, so they serve as an acid catalyst for reactions catalyzed by protons.

- (3) Orientation of the substrate for hydrolytic attack by template formation: Metal ions enhance the optimal stereochemical orientation for intramolecular hydrolytic attack by the nucleophile. The bidentate coordination also results in the formation of a strained chelate activating the substrate for nucleophilic attack.
- (4) Provision of an effective nucleophile at biological pH: Hydroxide is a better nucleophile than water but its concentration would be low at a pH of 7.0. Simultaneous coordination of water and phosphate ester to a metal atom overcomes this problem. This is achieved because the conjugate base, hydroxide or alkoxide dissipates its charge through a binding interaction with the metal ion. Since these conjugate bases are better nucleophiles than their parent acids, attack on the electrophilic P atom is enhanced relative to the uncatalyzed reaction.<sup>201</sup>
- (5) Strain induction: the bidentate coordination of a phosphate to a metal ion could result in the formation of a strained chelate ring thus facilitating a nucleophilic attack at the phosphorus centre.

Irrespective of the contributions of the metalloenzymes in catalytic reactions involving phosphorylation and dephosphorylation, the mechanisms of these reactions proves elusive to general understanding. This is so because divalent metal ions are

substitutionally labile and form a variety of complexes in rapid equilibrium. As a result, it has been quite difficult to define the binding mode of any particular complex as being responsible for the rate enhancement observed.<sup>206</sup> It should be emphasized that lability of substitution is an essential requirement for efficient catalysis and it is for this reason that enzymes primarily contain the first row d-block metal ions as cofactors.

It has been suggested that enzyme complexation with a metal ion could change the mechanistic features of these biochemical processes. This change can be from a largely dissociative mechanism observed in the absence of a metal ion, to an associative mechanism. All reactions experiencing more nucleophilic involvement in the transition state.<sup>209-211</sup> A change from a dissociative to an associative mechanism would allow a larger potential advantage from catalysis by induced intramolecularity in an enzymatic reaction. This is because reactions with tight transition states have stricter requirements for alignment than reactions with loose transition states.<sup>212-214</sup> Additionally, a change to an associative mechanism (involvement of metal ions) would give a greater potential advantage from the general base catalysis. This is attributed to the increased bond formation to the nucleophile in the transition state and the concomitant anticipated charge transfer development on the nucleophile. The supposed mechanism has been suggested to vary individually for each enzyme between two limiting cases of fully dissociative and fully associative. Using ATP phosphorylation and dephosphorylation as an example, the phosphate group ( $\text{PO}_4^{3-}$ ) has to be cleaved from ATP before the new bond to the acceptor is formed. This is called a fully dissociative mechanism ( $\text{S}_\text{N}1$ -type

reaction). The fully associative mechanism ( $S_N2$ ) requires a trigonal planar transition state geometry, where the phosphorus is apically coordinated by oxygen of the  $\beta$ -phosphate group of adenosine diphosphate (ADP) and an electronegative atom of the acceptor group.<sup>215</sup>

Whether the mechanism is more associative or dissociative is usually based on the supposed P—O distances from x-ray crystallographic protein structures with bound ADP by assuming symmetrical transition-state geometry.<sup>216</sup> For example, a fully dissociative mechanism requires the P—O distances to be at least the sum of the Van Der Waals radii of both atoms ( $\geq 3 \text{ \AA}$ ) while a fully associative mechanism requires the distances to be in the range of a covalent P—O bond (around  $1.7 \text{ \AA}$ ).

In addition to the dissociative and associative mechanisms is the interchange or concerted mechanism. They can be either the interchange associative ( $I_a$  type) or the interchange dissociative ( $I_d$  type). Interchange mechanisms are characterized by the interchange of ligands X and Y between inner and outer coordination spheres of the metal. The associative and the interchange associative mechanisms ( $I_a$ ) are possible when the replacement rate of an outgoing ligand depends on the nature and concentration of the substituting ligand. If the replacement rate is independent of the nature of the substituting ligand, then the mechanisms are dissociative or interchange dissociative ( $I_d$ ). The dissociative and  $I_d$  mechanisms are difficult to distinguish because the differences depend on the energy well of the intermediate. If the intermediate is relatively stable (on the scale probably longer than  $10^{-10} \text{ s}$ ), to be able to distinguish the

substituting ligand, it will react with the ligands at different rates. This is a condition for dissociative mechanism. Thus, if two substituting ligands  $Y'$  and  $Y''$  are present (competitive reactions), the products will not be formed statistically (e.g. 50%  $MY'$  and 50%  $MY''$ ), but one of the products will predominate which strongly indicates that the dissociative mechanism is operative.

On the other hand, if the intermediate is exceedingly short lived (shorter than  $10^{-10}$  s); it cannot discriminate between the substituting ligands. The free coordination position is then occupied statistically, namely according to the substituting ligands' concentration. This is so called 'accidental bimolecularity'. Here the reaction rate depends on the substituting ligands concentration and not on its nature (this statement disregards the ligands solvation effect, steric effects and electric dipole charges effects, which usually ought not to be neglected). The leaving ligand X leaves the coordination shell and enters the solvation shell. The return from the solvation shell into the coordination shell is possible, but not if the entering ligand is in great excess and dominates the solvation shell. This is commonly the case because replacements are usually carried out under pseudo-first order conditions. (E.g. Y is in 10 to 100 fold excess over X). In such an  $I_d$  process, the reaction rate depends on the entering ligand concentration, but not on its nature.<sup>217</sup>

Probing phosphorylation and dephosphorylation reactions in biological systems is extremely difficult. Though most of the enzyme systems require metal ions for activity, some phosphorylases and dephosphorylases that contain no metal cofactor have



been reported.<sup>215</sup> Current efforts aimed at having a better understanding of phosphoryl transfer reactions employ *in vivo* techniques which mimic the real systems. These reactions can be monitored by several analytical techniques. Recent efforts are geared towards the use of relevant spectrophotometric techniques and ion selective electrodes as probes to ascertain these enzymatic functions. This project is aimed at the fabrication and utilization of a new solid state ion selective electrode for monitoring phosphorylation and dephosphorylation reactions in model systems.

Phosphate ester hydrolysis is an essential reaction process in both biological and environmental studies. Numerous model systems for the hydrolysis of phosphate esters exist in the literature.<sup>218,219-221</sup> A good understanding in their hydrolysis and related phosphoryl transfer involving cleavage within the P-O framework is of paramount importance. In biological systems, these reactions are catalyzed by enzymes which contain metal cations or require them as co-factors. In the absence of enzymic catalysis, hydrolysis reactions of 4-nitrophenylphosphate and polyphosphates such as pyrophosphate, linear triphosphate, adenosine diphosphate and adenosine triphosphate normally proceed extremely slowly in all but highly acidic media. It is known that the hydrolysis of free pyrophosphate at constant pH follows pseudo-first order kinetics.<sup>222</sup> Catalytic effects of metal ions on the hydrolysis of pyrophosphate have been widely reported and the effect of pH, ionic strength and temperature are well documented.<sup>223,224</sup> This section of our studies reports the monitoring of dephosphorylation and phosphorylation reactions reproduced in our laboratory using

our novel phosphate selective electrode. Model systems were utilized to mimic these enzymatic reactions.

## **4.1 EXPERIMENTAL SECTION**

### **4.1.1 INSTRUMENTS AND REAGENTS**

All reagents used were either analytical reagent grade or the purest available commercially and were used without further purification. The electrode with membrane combination 25%  $AlPO_4$  + 25%  $Cu$  + 50%  $Al$ , was used as an indicator electrode. The reference electrode utilized was a Metrohm Ag/AgCl (3 M KCl) double junction reference electrode. A digital screen Metrohm 781 pH/ion meter was used for potential measurements and pH. Although pH monitoring during reactions was simultaneously monitored with a Metrohm 635-pH meter equipped with a combination electrode. The pH electrode was conditioned prior to use in a pH range of 4 to 9. The pH of the reaction mixture was adjusted to 7 by glass stick dotting using 0.1 M, 0.01 M and 0.001 M of  $HClO_4$  acid. Since all reacting solutions tend to be basic, care was taken on adjustments to avoid the introduction of NaOH ( $OH^-$  interferent). The temperature of the reaction was controlled using a thermostated water bath, which allows the water to circulate via a jacketed reaction vessel maintained at 25° C.

### **4.1.2. CHOICE OF MODEL SYSTEMS**

Phosphorylation and dephosphorylation reactions have been successfully studied by using model compounds that mimic enzyme systems.<sup>202,205-207,225</sup> The advantages

inherent in the choice of the preferred tetraamminecobalt(III) as enzyme model is given below;

Model systems based on cobalt(III) complexes are especially advantageous in that metal coordination sites open for phosphate substitution can be limited. This permits studies of a type not readily available using labile metal centers.

- (1) They are exchange inert. This makes them thermodynamically stable, thus making their mechanisms and kinetics to be well understood.
- (2) The (-Co-N bonds in cobalt(III) amine and polyamine complexes retain their integrity in an aqueous medium for a long time.
- (3) They are easily synthesized and are kinetically robust, thereby permitting the characterization of all the species present in solution.
- (4) Cobalt(III) is a low spin  $d^6$  ion. It is diamagnetic and therefore enables  $^{31}\text{P}$  studies as a probe for monitoring the reactions.

#### **4.1.2.1 SODIUM PYROPHOSPHATE ( $\text{Na}_4\text{P}_2\text{O}_7 \cdot 10\text{H}_2\text{O}$ ) AND SODIUM TRIPOLYPHOSPHATE ( $\text{Na}_5\text{P}_3\text{O}_{10}$ ): SUBSTRATE MODELS FOR UNACTIVATED PHOSPHATE ESTER**

Polyphosphates are essential to life processes and understanding their hydrolysis and related phosphoryl transfer involving cleavage within the P-O-P framework is of paramount importance. In biological systems, these reactions are catalyzed by enzymes

which contain metal cations or require them as co-factors. In the absence of enzymic catalysis, hydrolysis reactions of simple polyphosphates such as pyrophosphate, linear triphosphate, adenosine diphosphate and adenosine triphosphate normally proceed extremely slowly in all but highly acidic media.<sup>222</sup>

It is known that the hydrolysis of free pyrophosphate at constant pH follows pseudo-first order kinetics.<sup>226</sup> Catalytic effects of metal ions on the hydrolysis of pyrophosphate have been widely reported and the effect of pH, ionic strength and temperature are well documented.<sup>227,228</sup> Studies<sup>222,226,229</sup> showed that in the presence of an excess bis(trimethylenediamine)hydroxoaquacobalt(III) ion  $[\text{CoN}_4(\text{OH})(\text{H}_2\text{O})]^{2+}$ , the degradation process is relatively rapid at 25° C and pH 7 for  $[\text{CoN}_4(\text{OH})(\text{H}_2\text{O})]_3^{2+}$  and substrate reactions at  $1 \times 10^{-2}$  molar concentration. Literature studies<sup>230</sup> have reported even greater rate of cleavage under the same conditions using  $[\text{CoN}_4(\text{OH})(\text{H}_2\text{O})]^{2+}$  with preformed  $[\text{CoN}_4\text{HP}_2\text{O}_7]$ . These studies were based on <sup>31</sup>P NMR analysis of quenched reaction aliquots where the cobalt(III) complex was decomposed and  $\text{PO}_4^{3-}/\text{P}_2\text{O}_7^{4-}$  were determined from the peak areas of their signals.

#### **4.1.2.2 4-NITROPHENYLPHOSPHATE (4-NPP): SUBSTRATE MODEL FOR ACTIVATED PHOSPHATE ESTER**

4-Nitrophenylphosphate (4-NPP) produces nitrophenolate ion and a phosphate moiety upon dephosphorylation. Rate of this reaction in the pH range of 4 to 9 is both essentially constant and very slow.<sup>229</sup> Spectrophotometric measurements on dephosphorylation are based on the different UV-Visible absorbance maxima of the

bright yellow nitrophenolate (400 nm) produced from cleavage of the phosphate moiety (310 nm). Ion selective electrodes detect the phosphate moiety produces as a result of same reactions.

#### 4.1.2.3 PREPARATION OF THE ENZYME MODEL

The diaqua complexes ( $[\text{CoN}_4(\text{H}_2\text{O})_2]^{3+}$ ) were prepared and characterized in solution from the carbonato complexes ( $[\text{CoN}_4\text{CO}_3]$ ) using protocols established by Bauer and Drinkard.<sup>231,232</sup> A 50 mL solution of 29.1 g of  $\text{Co}(\text{NO}_3)_2 \cdot 6\text{H}_2\text{O}$  (0.1 M) and 10 mL of 30% hydrogen peroxide (excess) was added drop wise with stirring to a cold slurry of 42.0 g of sodium bicarbonate (0.5 M) in 50 mL of  $\text{H}_2\text{O}$ . The mixture was allowed to stand at  $0^\circ \text{C}$  for 1 hour with continuous stirring. The olive product was filtered, washed on the filter with three 10 mL portions of ice cold water, and then thoroughly washed with absolute ethanol and dry ether. The  $\text{Na}_3[\text{Co}(\text{CO}_3)_3] \cdot 3\text{H}_2\text{O}$  complex obtained was 39.12 g and the percentage yield was calculated as 94.23%. It is important to mention that the number of base equivalents per mole of intermediate is six. Thus, the number of coordination positions per mole is equal to the number of base equivalents per mole.

A slurry of 3.6 g of  $\text{Na}_3[\text{Co}(\text{CO}_3)_3] \cdot 3\text{H}_2\text{O}$  (0.01 M) was mixed with 0.02 M of 1,3 diaminopropane and 0.04 M of perchloric acid and warmed in a steam bath for two hours. The mole ratio of the intermediate to ligand ( $\text{Na}_3[\text{Co}(\text{CO}_3)_3] \cdot 3\text{H}_2\text{O}$  : ligand) was 1 : 2, where ligand = bidentate ligand of 1, 3 diaminopropane. The reagent mixture was then filtered hot and the filtrate was saturated with absolute ethanol to precipitate an orange product, which is further recrystallized by placing it in the refrigerator for about

12 hours in an ethanol-water solution. It was observed that a pronounced improvement in both the quantity and quality of the yield was prominent when the reagents mixture was filtered hot and the filtrate reduced to about one-third of its original volume using rotavapour. After which further precipitation and recrystallization was carried out. The yield recorded was 3.28 g which was 87.46% of theoretical expected yield. It was dried in air and converted to the diaquo complex.

The conversion of the carbonato ( $[\text{CoN}_4\text{CO}_3]\text{ClO}_4\cdot\text{H}_2\text{O}$ ) to the diaquo  $[\text{CoN}_4(\text{OH}_2)_2]^{3+}$  complex was achieved by adding 2.5 mmol of 6 M perchloric acid to 1 mmol of finely divided carbonato specie. The solution was stirred in the dark under a vacuum aspirator for 30 minutes at 50° C. The pH was then adjusted to 7 and kept in a safe place free from UV radiations.

#### **4.1.2.4 PREPARATION OF THE SUBSTRATE MODELS**

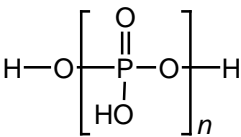
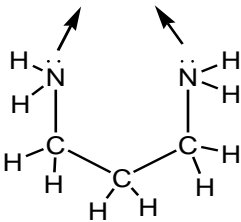
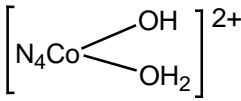
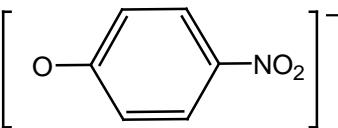
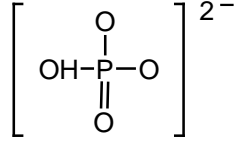
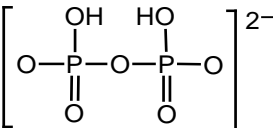
Aqueous solutions of  $5 \times 10^{-3}$  M sodium hydrogen phosphate ( $\text{NaH}_2\text{PO}_4$ ), 4-nitrophenyl phosphate ( $\text{C}_6\text{H}_4\text{NNa}_2\text{O}_6\text{P}\cdot 6\text{H}_2\text{O}$ ), sodium pyrophosphate ( $\text{Na}_4\text{O}_7\text{P}_2\cdot 10\text{H}_2\text{O}$ ), and sodium tripolyphosphates ( $\text{Na}_5\text{P}_3\text{O}_{10}$ ) were utilized as our substrate models. They were prepared in 100 mL and the pH adjusted to 7 at 25° C. The solutions were used on the same day to avoid deterioration from exposure to ultraviolet light.

#### **4.2 PROTOCOL OF THE STUDIES**

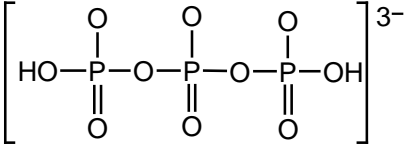
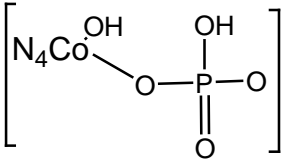
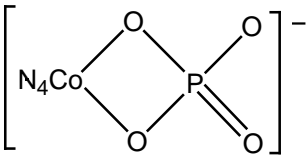
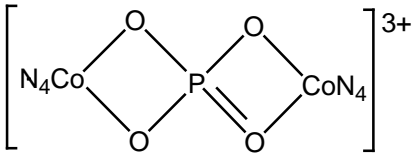
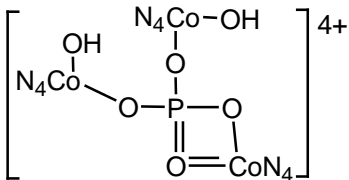
In the ensuing reactions, the assembly containing the phosphate selective electrode and the reference electrode were held in place halfway down the container of the

thermostated reaction vessel. Both electrodes were connected to the ion meter. The reaction solutions were slowly stirred during the reactions. A solution that contains  $1 \times 10^{-3}$  M cobalt(III)bis-trimethylenediamine and the phosphate substrate is prepared by mixing 20 mL of an aqueous solution of  $5 \times 10^{-3}$  M cobalt(III) bis trimethylenediamine diaqua complex ( $[\text{CoN}_4(\text{H}_2\text{O})_2]^{3+}$ ) with the same amount of  $5 \times 10^{-3}$  M substrate model in the thermostated reaction vessel at  $25^\circ\text{C}$ . 60 mL of deionized water was added to it and the pH maintained at 7 for the whole duration of the reaction under constant stirring. These reactions were monitored for possible hydrolysis or binding of the metal containing enzyme model to the phosphate substrate. Similarly, for a higher metal to substrate ratios hydrolysis, 40 and 60 mL of  $1 \times 10^{-3}\text{M}$  solutions of  $[\text{CoN}_4(\text{H}_2\text{O})_2]^{3+}$  producing a stoichiometric increase of  $[\text{CoN}_4(\text{H}_2\text{O})_2]^{2^{3+}}$  and  $[\text{CoN}_4(\text{H}_2\text{O})_2]^{3^{3+}}$  are added to a fixed volume of the substrates (20 mL) and making up the total volume to 100 ml with deionised water in the thermostated reaction vessel. Table 4.1 below shows the chemical and structural formula of the complexes encountered in this study along with pertinent explanation.

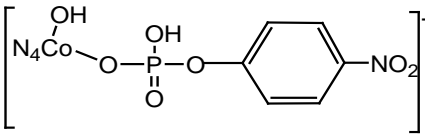
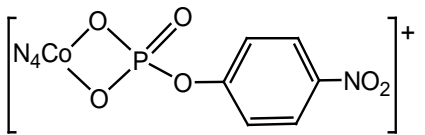
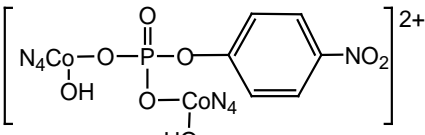
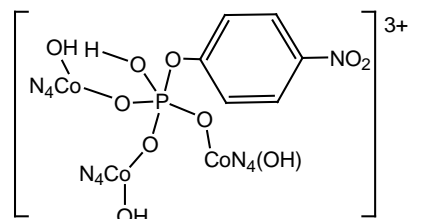
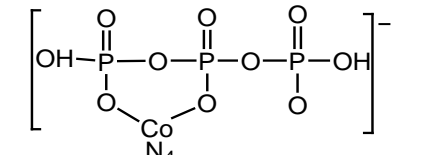
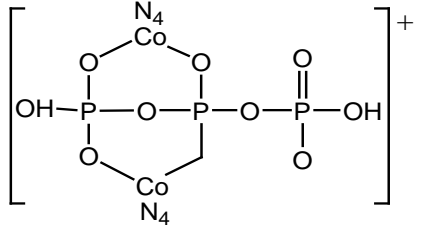
Table 4.1 Complexes encountered in the study

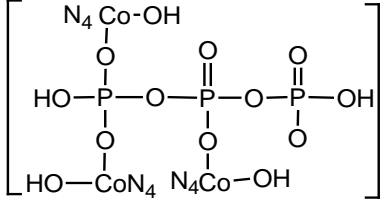
Structural Formula	Chemical /Condensed Formula	Comment
	$[\{\text{HO}(\text{PO}_2\text{OH})_n \text{H}\}]$	This is the accepted structural form of the polyphosphoric acids where $n$ can be 1, 2 or 3 for phosphoric, pyrophosphoric and triphosphoric acids respectively.
	$\text{NH}_2\text{CH}_2\text{CH}_2\text{CH}_2\text{NH}_2$	Trimethylenediamine (1,3 diaminopropane) normally abbreviated as tn. 2 molecules of tn are abbreviated as $\text{N}_4$ .
	$[\{\text{CoN}_4(\text{OH})(\text{OH}_2)\}]^{2+}$	The cis hydroxo/aquo complex is one of the reactive species in solution. <sup>231</sup>
	$[\text{O}_2\text{NC}_6\text{H}_4\text{O}]^-$ Abbreviated as 4NP	4-nitrophenolate anion is the predominant specie under the experimental condition.
	$[\text{HPO}_4]^{2-}$ $[\text{OH}(\text{PO}_2\text{O})]^{2-}$	The hydrogen phosphate anion is the predominant species in the middle pH region (pH region of 7-8) in the reacting solution.
	$[\text{H}_2\text{P}_2\text{O}_7]^{2-}$ $[(\text{OH})_2(\text{PO}_2)_2\text{O}]^{2-}$	The dihydrogen phosphate anion is the predominant specie in solution under the experimental conditions.



	$[\text{H}_2\text{P}_3\text{O}_{10}]^{3-}$ $[(\text{OH})_2(\text{PO}_2)_3\text{O}_2]^{3-}$	<p>The predominant triphosphate ion in solution under the experimental condition. The pyro- and triphosphate behave as typical polyprotic acids and thus protonation degree varies with pH. Between pH 2.3 and 6.5 triphosphates exists mainly as <math>[\text{H}_2\text{P}_3\text{O}_{10}]^{3-}</math> in solutions.<sup>233</sup></p>
	$[\{\text{CoN}_4(\text{OH})\text{O}_3\text{POH}\}]^-$	<p>Monocoordinated phosphate complex formed during the early stages of the reaction between <math>[\{\text{CoN}_4(\text{OH})(\text{OH}_2)\}]^{2+}</math> and <math>[\text{HPO}_4]^{2-}</math>.<sup>234</sup></p>
	$[\{\text{CoN}_4\text{O}_3\text{PO}\}]^-$	<p>It should be noted that the monocoordinated phosphates <math>[\{\text{CoN}_4(\text{OH})\text{O}_3\text{POH}\}]^-</math> and the bicoordinated phosphates <math>[\{\text{CoN}_4\text{O}_3\text{PO}\}]^-</math> exists in reaction solutions. The charge inherent on each depends on the degree of protonation. Example, the same complex can be positively charged, <math>[\{\text{CoN}_4(\text{OH})\text{OPO}(\text{OH})_2\}]^+</math>.</p>
	$[\{(\text{CoN}_4)_2\text{O}_3\text{PO}\}]^{3+}$	<p>Bicoordinated phosphate complex formed after 30 minutes of the reaction.<sup>234</sup> Monodentate species may also be depicted as <math>[\{(\text{CoN}_4(\text{OH})\text{O})_2\text{P}(\text{O})\text{OH}\}]^{2+}</math>.</p>
	$[\{(\text{CoN}_4)_3(\text{OH})_2\text{O}_3\text{PO}\}]^{4+}$	<p>A four membered phosphate ring complex formed from the reaction between <math>[\{\text{CoN}_4(\text{OH})(\text{OH}_2)\}]^{3+}</math> and <math>[\text{HPO}_4]^{2-}</math>. Monocoordinated chelate of this reaction can also be written as <math>[\{(\text{CoN}_4(\text{OH})\text{O})_3\text{P}(\text{O})\}]^{3+}</math>.<sup>234</sup></p>

	$\begin{aligned} & \{[\text{CoN}_4(\text{OH})\text{P}_2\text{O}_5(\text{OH})_2]\} \\ & \{[\text{CoN}_4(\text{OH})(\text{O})(\text{PO}_2)_2(\text{OH})_2]\} \end{aligned}$	<p>Monocoordinated pyrophosphate complexes formed during the early the early stages of the reaction between <math>\{[\text{CoN}_4(\text{OH})(\text{OH}_2)]\}^{2+}</math> and <math>[\text{H}_2\text{P}_2\text{O}_7]^{2-}</math>.<sup>205,222</sup></p>
	$\begin{aligned} & \{[\text{CoN}_4\text{P}_2\text{O}_7]\}^- \\ & \{[\text{CoN}_4(\text{O})_2(\text{PO})_2\text{O}_3]\}^- \end{aligned}$	<p>Six membered ring phosphate chelate formed after 30 minutes of reaction time. Different complexes have been reported in the literatures.<sup>205,222</sup></p>
	$\begin{aligned} & \{[(\text{CoN}_4)_2\text{P}_2\text{O}_7]\}^{2+} \\ & \{[(\text{CoN}_4(\text{O})_2)_2(\text{PO})_2\text{O}]\} \end{aligned}$	<p>A double six-membered ring phosphate chelate formed as a result of the reaction between <math>\{[\text{CoN}_4(\text{OH})(\text{OH}_2)]\}^{2+}</math> and <math>[\text{H}_2\text{P}_2\text{O}_7]^{2-}</math>. Other racemic and meso forms have been reported in the literatures.<sup>222</sup></p>
	$\{[(\text{CoN}_4)_3\text{P}_2\text{O}_7]\}^{2+}$	<p>A double four-membered and a single six-membered ring phosphate complex formed as a result of saturated reaction between <math>\{[\text{CoN}_4(\text{OH})(\text{OH}_2)]\}^{3^{2+}}</math> and <math>[\text{H}_2\text{P}_2\text{O}_7]^{2-}</math>. Other suggested structures can be found in the literatures.<sup>205</sup></p>
	$[\text{O}_2\text{NC}_6\text{H}_4\text{PO}_2(\text{O})(\text{OH})]^-$ Abbreviated as 4NPP	<p>4-Nitrophenylphosphate anion prevalent in the solution</p>
	Abbreviated as $\{[\text{CoN}_4(\text{OH})4\text{NP}]\}^+$	<p>This is the product of the reaction between <math>\{[\text{CoN}_4(\text{OH})(\text{OH}_2)]\}^{2+}</math> and <math>[\text{O}_2\text{NC}_6\text{H}_4\text{O}]^-</math>.<sup>235,236</sup></p>

	<p>Abbreviated as <math>[\{\text{CoN}_4(\text{OH})_4\text{NPP}\}]^+</math></p>	<p>Monocordinated 4-NPP complex formed during the early stages of the reaction between <math>[\{\text{CoN}_4(\text{OH})(\text{OH}_2)\}]^{2+}</math> and <math>[\text{O}_2\text{NC}_6\text{H}_4\text{PO}_2(\text{O})(\text{OH})]^-</math>.<sup>236</sup></p>
	<p>Abbreviated as <math>[\{\text{CoN}_4\text{NPP}\}]^+</math></p>	<p>A bicordinated phosphate complex attached to the 4-NPP formed after 30 minutes of reaction time.<sup>235,236</sup></p>
	<p>Abbreviated as <math>[\{(\text{CoN}_4(\text{OH}))_2\text{NPP}\}]^{2+}</math></p>	<p>The reaction between <math>[\{\text{CoN}_4(\text{OH})(\text{OH}_2)\}]^{2+}</math> and 4-NPP to produce <math>[\{(\text{CoN}_4)_2(\text{OH})_2\text{NPP}\}]^{2+}</math>. Other structural conformations can be found in the literatures.<sup>236</sup></p>
	<p>Abbreviated as <math>[\{(\text{CoN}_4(\text{OH}))_3\text{NPP}\}]^{3+}</math></p>	<p>The reaction between <math>[\{\text{CoN}_4(\text{OH})(\text{OH}_2)\}]^{3+}</math> and 4-NPP to produce <math>[\{(\text{CoN}_4)_3(\text{OH})_3\text{NPP}\}]^{2+}</math>.</p>
	<p>Abbreviated as <math>[\{\text{CoN}_4\text{P}_3\text{O}_{10}\}]^-</math></p>	<p>A bicordinated triphosphate complex formed after about 30 minutes of reaction between <math>[\{\text{CoN}_4(\text{OH})(\text{OH}_2)\}]^{2+}</math> and <math>[\text{H}_2\text{P}_3\text{O}_{10}]^{3-}</math>.</p>
	<p>Abbreviated as <math>[\{(\text{CoN}_4)_2\text{P}_3\text{O}_{10}\}]^+</math></p>	<p>A double six-membered ring phosphate chelate formed as a result of the reaction between <math>[\{\text{CoN}_4(\text{OH})(\text{OH}_2)\}]^{2+}</math> and <math>[\text{H}_2\text{P}_2\text{O}_7]^{3-}</math>. Other possible structures leading to complexation or hydrolysis can be referred to in the literatures.<sup>237</sup></p>

	<p>Abbreviated as  <math>[(CoN_4)_3P_3O_{10}]^+</math>  <math>[(CoN_4(OH))_3O_2(PO_2)_3(OH)_2]^+</math></p>	<p>A triple coordinated tripolyphosphate complexes formed during the early stages of the reaction between <math>[(CoN_4(OH)(OH_2))]^{2+}</math> and <math>[H_2P_3O_{10}]^{3-}</math>. A double four-membered, a single six-membered ring phosphate complex and an inorganic phosphate has been observed in the reaction that leads to hydrolysis.<sup>237</sup></p>
---	---	---

### 4.3 RESULTS AND DISCUSSION

The EMF response of the electrode for  $1 \times 10^{-3}$  M solutions of all the reagents at pH 7.0 is depicted in table 4.2. It is to be noted that the phosphate species show varying EMF (mV) readings indicating different levels of sensitivity by the electrode. These data are of paramount important as they provide a handle for comparison when discussing the results obtained from the experiments.

Table 4.2 EMF (mV) readings of all reagents used in the study

REAGENTS	EMF (mV) with Time		
	5 minutes	10 minutes	Average
H <sub>2</sub> O (water)	-353.8	-350.1	-351.9
CoN <sub>4</sub> (H <sub>2</sub> O) <sub>2</sub>	-307.5	-307.9	-307.7
NaH <sub>2</sub> PO <sub>4</sub> .2H <sub>2</sub> O	-243.1	-242.3	-242.7
4-NPP	-299.2	-297.6	-298.4
Na <sub>4</sub> O <sub>7</sub> P <sub>2</sub> .10H <sub>2</sub> O	-298.4	-297.0	-297.7
Na <sub>5</sub> P <sub>3</sub> O <sub>10</sub>	-304.4	-303.9	-304.1

The EMF (mV) readings of all reagents were recorded at intervals of 5 and 10 minutes (the duration allowed for complete hydrolysis if any). The average was obtained and shown in table 4.2.

### 4.3.1 RESULTS FOR COBALT(III)BIS-TRIMETHYLENEDIAMINE HYDROLYSIS OF PHOSPHATE COMPLEXES

The EMF values observed for the 1:1, 2:1 and 3:1 metal to substrate ratios for this reaction can be summarized in the tables 4.3, 4.4 and 4.5 below. All experiments were conducted in triplicates. The cobalt(III) bis-trimethylenediamine serves as the metal complex while  $\text{NaH}_2\text{PO}_4 \cdot 2\text{H}_2\text{O}$  was utilized as the substrate model.

Table 4.3 EMF (mV) values recorded for the reaction between  $[\{\text{CoN}_4(\text{OH})(\text{OH}_2)\}]^{2+}$  and  $[\text{HPO}_4]^{2-}$  for 1:1  $[\{\text{CoN}_4(\text{OH})(\text{OH}_2)\}]^{2+}$  to  $[\text{HPO}_4]^{2-}$  ratios.

Time (min)	DATA 1	DATA 2	DATA 3	MEAN
0.5	-350.5	-348.2	-350.7	349.8 ± 1.4
1	-357.7	-348.9	-351.1	352.5 ± 4.6
2	-358.1	-352.7	-351.6	354.1 ± 3.5
3	-357.3	-355.1	-351.9	354.7 ± 2.7
4	-354.4	-354.3	-351.2	353.3 ± 1.8
5	-353.6	-353.4	-350.6	352.5 ± 1.7
6	-350.9	-352.1	-350.3	351.1 ± 0.9
7	-349.2	-352.2	-350.5	350.6 ± 1.5
8	-347.8	-353.4	-351.1	350.7 ± 2.8
9	-348.1	-352.3	-351.5	350.6 ± 2.2
10	-347.2	-352.9	-351.4	350.5 ± 2.9

Table 4.4 EMF (mV) values recorded for the reaction between  $[\text{CoN}_4(\text{OH})(\text{OH}_2)]^{2+}$  and  $[\text{HPO}_4]^{2-}$  for 2:1  $[\text{CoN}_4(\text{OH})(\text{OH}_2)]^{2+}$  to  $[\text{HPO}_4]^{2-}$  ratios.

Time (min)	DATA 1	DATA 2	DATA 3	MEAN
0.5	-330.1	-328.9	-329.9	329.6 ± 0.6
1	-331.0	-330.1	-331.1	330.7 ± 0.6
2	-333.1	-331.4	-331.9	331.4 ± 0.4
3	-334.4	-332.5	-333.8	333.5 ± 1.0
4	-333.4	-332.5	-334.1	333.3 ± 0.8
5	-332.8	-332.6	-334.2	333.2 ± 0.9
6	-334.6	-332.9	-334.9	334.1 ± 1.0
7	-335.3	-332.4	-334.8	333.8 ± 2.0
8	-334.2	-332.0	-334.9	333.7 ± 1.5
9	-332.8	-331.8	-335.1	333.2 ± 1.7
10	-332.6	-331.9	-335.4	333.3 ± 1.9

Table 4.5 EMF (mV) values recorded for the reaction between  $[\text{CoN}_4(\text{OH})(\text{OH}_2)]^{2+}$  and  $[\text{HPO}_4]^{2-}$  for 3:1  $[\text{CoN}_4(\text{OH})(\text{OH}_2)]^{2+}$  to  $[\text{HPO}_4]^{2-}$  ratios.

Time (min)	DATA 1	DATA 2	DATA 3	MEAN
0.5	-322.7	-323.2	-321.9	322.6 ± 0.7
1	-328.2	-326.8	-322.1	325.7 ± 3.2
2	-327.4	-327.2	-323.5	326.0 ± 2.2
3	-327.5	-328.1	-324.4	326.6 ± 2.0
4	-326.9	-328.3	-324.8	326.6 ± 1.8
5	-326.4	-328.4	-325.1	326.6 ± 1.7
6	-326.5	-328.4	-325.0	326.6 ± 1.7
7	-325.5	-328.1	-325.4	326.3 ± 1.5
8	-325.1	-327.9	-325.9	326.1 ± 1.2
9	-324.4	-327.4	-326.4	326.0 ± 1.5
10	-323.8	-327.3	-326.0	325.7 ± 1.8

Reaction solutions which were 1:1 in  $[\text{CoN}_4(\text{OH})(\text{H}_2\text{O})]^{2+}$  to  $[\text{HPO}_4]^{2-}$  ratio, at pH 7.0 and  $25^\circ \text{C}$ , result in rapid water substitution to form the monodentate complex,  $[\{\text{CoN}_4(\text{OH})\text{O}_3\text{POH}\}]$  which can then form a four membered chelate  $[\{\text{CoN}_4\text{O}_3\text{PO}\}]$ . The formation of several mono and poly chelated phosphate species in reaction solutions have been documented in previous  $^{31}\text{P}$  NMR studies.<sup>238</sup> Formation of the complex results in a decrease of electron density on the phosphorous centre increasing its electrophilic character. Similarly, the addition of 2:1 and 3:1 molar ratio of  $[\text{CoN}_4(\text{OH})(\text{H}_2\text{O})]^{2+}$  and  $[\text{HPO}_4]^{2-}$  under the experimental condition is presumed to produce largely  $[\{\text{CoN}_4(\text{OH})\text{O}\}_2\text{P}(\text{O})\text{OH}]^{2+}$  and  $[\{\text{CoN}_4(\text{OH})\text{O}\}_3\text{P}(\text{O})]^{3+}$  respectively, as evidenced previously.<sup>234,238</sup> A double four membered ring phosphate complex formed after 30 minutes of the reaction has also been documented for a 2:1 reaction between  $[\text{CoN}_4(\text{OH})(\text{H}_2\text{O})]^{2+}$  and  $[\text{HPO}_4]^{2-}$  (see table 4.1).<sup>234</sup> The 3:1 reaction of this type presumably formed three monodentate coordinated phosphate chelate with the possibility of a four membered ring system as previously reported.

During the course of the reaction between the metal and the substrates, complex formation seems to be a fast process as the EMF reading changed instantaneous during mixing. The readings signify depletion of the phosphate in the solution as a result of complexation and gradually changes to readings obtained with deionized water. We attempted to determine the apparent value for the equilibrium constant for the formation of the complex by precipitating out the unreacted  $[\text{CoN}_4(\text{OH})(\text{H}_2\text{O})]^{2+}$  by using chelex 100. Chelex 100 is a chelating material that has the ability to bind or reduce

transition metal ions. The experiment proved that all chelated and unchelated cobalt species precipitated out. There is a reduction reaction of the metal from Co(III) to Co(II) as the solution became colourless. The EMF reading of the clear solution revealed the absence of any  $[\text{CoN}_4(\text{OH})(\text{H}_2\text{O})]^{2+}$  species in the solution. Hence we can conclude from the above observation that the reaction was complete and no unreacted phosphate exists in the solution after mixing and complex formation takes place readily to 100%.

#### **4.3.2 RESULTS FOR COBALT(III)BIS-TRIMETHYLENEDIAMINE HYDROLYSIS OF 4-NITROPHENYLPHOSPHATE**

The reactions between  $[\{\text{CoN}_4(\text{OH})(\text{OH}_2)\}]^{2+}$  and  $[\text{O}_2\text{NC}_6\text{H}_4\text{PO}_2(\text{O})(\text{OH})]^-$  (abbreviated as 4-NPP) for 1:1, 2:1 and 3:1  $[\{\text{CoN}_4(\text{OH})(\text{OH}_2)\}]^{2+}$  to 4-NPP ratios were conducted at 25° C and at a pH of 7. The EMF values observed for the 1:1, 2:1 and 3:1 reactions can be summarized in the tables 4.6, 4.7 and 4.8 below.



Table 4.6 EMF (mV) values recorded for the reaction between  $[\text{CoN}_4(\text{OH})(\text{OH}_2)]^{2+}$  and 4-NPP for 1:1  $[\text{CoN}_4(\text{OH})(\text{OH}_2)]^{2+}$  to 4-NPP ratios.

Time (min)	DATA 1	DATA 2	DATA 3	MEAN
0.5	-338.6	-340.2	-341.8	340.2 ± 1.6
1	-344.9	-342.8	-342.4	343.3 ± 1.3
2	-346.6	-343.1	-343.4	344.3 ± 1.9
3	-346.2	-345.6	-346.1	345.9 ± 0.3
4	-345.7	-345.7	-346.0	345.8 ± 0.2
5	-345.4	-346.1	-346.1	345.8 ± 0.4
6	-345.2	-346.0	-345.9	345.7 ± 0.4
7	-344.8	-346.2	-345.8	345.6 ± 0.7
8	-344.1	-345.9	-346.2	345.4 ± 1.1
9	-344.0	-345.5	-346.2	345.2 ± 1.1
10	-344.3	-345.9	-346.3	345.4 ± 1.2

Table 4.7 EMF (mV) values recorded for the reaction between  $[\text{CoN}_4(\text{OH})(\text{OH}_2)]^{2+}$  and 4-NPP for 2:1  $[\text{CoN}_4(\text{OH})(\text{OH}_2)]^{2+}$  to 4-NPP ratios.

Time (min)	DATA 1	DATA 2	DATA 3	MEAN
0.5	-323.4	-322.9	-324.2	323.5 ± 0.7
1	-323.7	-323.1	-324.8	323.8 ± 0.9
2	-324.8	-324.4	-325.1	324.7 ± 0.4
3	-326.9	-325.1	-325.8	325.9 ± 0.9
4	-328.6	-325.8	-326.1	326.8 ± 1.5
5	-326.7	-326.0	-326.4	326.3 ± 0.4
6	-327.7	-326.5	-326.5	326.9 ± 0.7
7	-328.1	-326.6	-327.0	327.2 ± 0.8
8	-328.0	-327.0	-327.8	327.6 ± 0.5
9	-328.1	-327.9	-328.4	328.1 ± 0.3
10	-328.2	-327.5	-327.9	327.8 ± 0.4

Table 4.8 EMF (mV) values recorded for the reaction between  $[\text{CoN}_4(\text{OH})(\text{OH}_2)]^{2+}$  and 4-NPP for 3:1  $[\text{CoN}_4(\text{OH})(\text{OH}_2)]^{2+}$  to 4-NPP ratios.

Time (min)	DATA 1	DATA 2	DATA 3	MEAN
0.5	-324.5	-320.2	-325.1	323.2 ± 2.7
1	-326.9	-323.1	-326.4	325.4 ± 2.1
2	-326.5	-323.9	-327.7	326.0 ± 1.9
3	-327.4	-324.1	-328.1	326.5 ± 2.1
4	-328.1	-325.8	-328.4	327.4 ± 1.4
5	-328.4	-326.2	-329.5	328.0 ± 1.7
6	-328.6	-327.9	-330.4	328.9 ± 1.3
7	-328.6	-328.8	-330.9	329.4 ± 1.3
8	-328.5	-329.1	-331.4	329.6 ± 1.5
9	-329.0	-330.8	-332.1	330.6 ± 1.6
10	-329.2	-331.2	-332.0	330.8 ± 1.4

The hydrolysis involving different metal ions and 4-NPP have been elaborately studied using UV-Visible absorption spectroscopy.<sup>236,239-241</sup> It is presumed that at pH around 6.5 to 7.0, the aquohydroxo species is predominant. The values for  $\text{pK}_1$  and  $\text{pK}_2$  as determined by potentiometric titration under conditions where cis-trans isomerism had proceeded to equilibrium are 4.94 and 7.20 for  $\text{N}_4$  complexes. Diaquabis-(ethylenediamine) cobalt(III) in solution will be a mixture of cis and trans isomers as reported by previous investigators.<sup>262</sup> However, diaquabis (trimethylenediamine) cobalt(III) will prevail as cis isomers in solution due to fast cis-trans isomerisation ( $t_{1/2} = 1$  sec at 25° C). Literature values of  $\text{pK}_1$  4.98 and  $\text{pK}_2$  7.22 for  $[\text{CoN}_4(\text{H}_2\text{O})_2]^{3+}$  support the above assumptions.<sup>242</sup> The pH corresponding to the rate maxima are all between the  $\text{pK}_1$

and  $pK_2$  of the acid-base equilibrium for the cobalt complex, indicating that the aquohydroxo form is the active species that promotes the dephosphorylation reactions. The enhanced reactivity for the aquohydroxo ions in comparison to the dihydroxo and diaquo species was noted for the system and this is in line with literature reports.<sup>243</sup>

Hence at pH 7.0, the  $[\text{CoN}_4(\text{OH})(\text{H}_2\text{O})]^{2+}$  and 4-NPP react to form a  $[\{\text{CoN}_4(\text{OH})4\text{-NPP}\}]^+$ . Addition of  $[\text{CoN}_4(\text{OH})(\text{H}_2\text{O})]^{2+}$  to 4-NPP results in the formation of a monodentate complex<sup>236</sup> which then undergo intramolecular attack by the coordinated water or hydroxide of the metal complex on the phosphorus centre, thereby effecting dephosphorylation of the phosphate ester. In previous reports,<sup>222,235,237,244</sup> the formation of a four membered chelate ring system ( $[\{\text{CoN}_4\text{-NPP}\}]^+$ , see table 4.1) has also been noted for related systems along with opened ring monodentate species resulting in the formation of 4-nitrophenol and the metal coordinated phosphate. The observed rise in the pH of the reaction reflects the second step which involves the intramolecular attack by the coordinated hydroxide on the phosphorus centre thereby promoting the dephosphorylation of 4-NPP. Since no free phosphate is detected by the electrode the reaction pathway leading to metal coordinated phosphate and 4-nitrophenol production is very plausible.

UV-Visible absorption studies<sup>205,235</sup> reported an enhancement in the rate of dephosphorylation in reaction solution that contained 2:1  $[\text{CoN}_4(\text{OH})(\text{H}_2\text{O})]^{2+}$  to 4-NPP ratio. This can be explained by the fact that the second metal ion coordinates to one of the available oxygen on the 4-NPP, thereby creating a possibility of intramolecular

attack on the phosphorous centre by coordinated water or hydroxide of the metal ion. Our electrode could not separate both reactions since there is no free phosphate produced in the solution to be detected.

No significant additional amount of dephosphorylation was observed for reaction solutions that contained 3:1  $[\text{CoN}_4(\text{OH})(\text{H}_2\text{O})]^{2+}$  to 4-NPP ratio. Since the reaction is presumed to be stoichiometric and not catalytic, it is anticipated that with an increase in the metal-to-phosphate ratio, the rate of dephosphorylation should increase. However, above 3:1,  $[\text{CoN}_4(\text{OH})(\text{H}_2\text{O})]^{2+}$  to 4-NPP ratio, the concentration of the hydroxo aqua species in the system becomes large, presumably triggering an oligation reaction resulting in unreactive dimeric species in the solution. This has been reported in similar studies.<sup>238</sup>

### **4.3.3 RESULTS FOR COBALT(III)BIS-TRIMETHYLENEDIAMINE HYDROLYSIS OF PYROPHOSPHATE**

The EMF values observed for the 1:1, 2:1 and 3:1 metal to substrate ratios for this reaction can be summarized in the tables 4.9, 4.10 and 4.11 below. All experiments were conducted in triplicates. The cobalt(III)bis-trimethylenediamine ( $[\text{CoN}_4(\text{OH})(\text{H}_2\text{O})]^{2+}$ ) serves as the metal complex while sodium pyrophosphate ( $[(\text{OH})_2(\text{PO}_2)_2\text{O}]^{2-}$  (abbreviated as  $[\text{H}_2\text{P}_2\text{O}_7]^{2-}$ ) was utilized as the substrate model. All experiments were done at 25° C and a pH of 7.

Table 4.9 EMF (mV) values recorded for the reaction between  $[\text{CoN}_4(\text{OH})(\text{OH}_2)]^{2+}$  and  $[\text{H}_2\text{P}_2\text{O}_7]^{2-}$  for 1:1  $[\text{CoN}_4(\text{OH})(\text{OH}_2)]^{2+}$  to  $[\text{H}_2\text{P}_2\text{O}_7]^{2-}$  ratios.

Time (min)	DATA 1	DATA 2	DATA 3	MEAN
0.5	-349.2	-348.7	-350.1	349.3 ± 0.7
1	-353.6	-349.1	-350.4	351.0 ± 2.3
2	-355.3	-349.4	-350.2	351.6 ± 3.2
3	-354.9	-350.2	-351.1	352.0 ± 2.5
4	-357.1	-350.8	-351.3	353.0 ± 3.5
5	-354.8	-351.4	-352.0	352.7 ± 1.8
6	-354.3	-352.1	-352.8	353.0 ± 1.1
7	-354.0	-352.8	-353.4	353.4 ± 0.6
8	-355.1	-353.1	-354.1	354.1 ± 1.0
9	-356.4	-354.8	-355.4	355.5 ± 0.8
10	-357.2	-353.8	-355.4	355.6 ± 1.7

In reaction solutions which were 1:1 in  $[\text{CoN}_4(\text{OH})(\text{H}_2\text{O})]^{2+}$  to  $[\text{H}_2\text{P}_2\text{O}_7]^{2-}$  ratio, the formation of six membered ring phosphate chelate,  $[\text{CoN}_4\text{P}_2\text{O}_7]^-$ , is predominant as reported in the literature.<sup>222</sup> No hydrolysis is expected due to the stability of the symmetrical ring system. Documented  $^{31}\text{P}$  NMR spectra for this reaction over the entire pH range give rise to signals at 0 to 5 ppm signifying a conclusive evidence of a bidentate six membered chelate. The EMF reading from those reaction solutions is consistent with the above observation. Tables 4.10 and 4.11 shows the data obtained for 2:1 and 3:1  $[\text{CoN}_4(\text{OH})(\text{H}_2\text{O})]^{2+}$  to  $[\text{H}_2\text{P}_2\text{O}_7]^{2-}$  ratios.

Table 4.10 EMF (mV) values recorded for the reaction between  $[\{\text{CoN}_4(\text{OH})(\text{OH}_2)\}]^{2+}$  and  $[\text{H}_2\text{P}_2\text{O}_{10}]^{2-}$  for 2:1  $[\{\text{CoN}_4(\text{OH})(\text{OH}_2)\}]^{2+}$  to  $[\text{H}_2\text{P}_2\text{O}_7]^{2-}$  ratios.

Time (min)	DATA 1	DATA 2	DATA 3	MEAN
0.5	-322.7	-335.1	-340.4	332.7 ± 9.1
1	-340.5	-338.4	-344.2	341.0 ± 2.9
2	-345.8	-339.2	-346.1	343.7 ± 3.9
3	-346.5	-340.4	-347.8	344.9 ± 4.0
4	-344.8	-341.1	-347.5	344.5 ± 3.2
5	-344.3	-342.0	-347.6	344.6 ± 2.3
6	-345.0	-342.8	-348.1	345.3 ± 2.7
7	-345.8	-342.9	-347.4	345.3 ± 2.3
8	-346.1	-344.4	-347.0	345.8 ± 1.3
9	-345.9	-344.7	-347.3	345.9 ± 1.3
10	-346.1	-344.3	-346.6	345.6 ± 1.2

Table 4.11 EMF (mV) values recorded for the reaction between  $[\{\text{CoN}_4(\text{OH})(\text{OH}_2)\}]^{2+}$  and  $[\text{H}_2\text{P}_2\text{O}_{10}]^{2-}$  for 3:1  $[\{\text{CoN}_4(\text{OH})(\text{OH}_2)\}]^{2+}$  to  $[\text{H}_2\text{P}_2\text{O}_7]^{2-}$  ratios.

Time (min)	DATA 1	DATA 2	DATA 3	MEAN
0.5	-317.8	-313.4	-316.8	316.0 ± 2.3
1	-328.2	-315.5	-317.2	320.3 ± 6.9
2	-327.4	-317.2	-318.4	321.0 ± 5.6
3	-325.5	-319.4	-319.0	321.3 ± 3.6
4	-324.0	-320.1	-319.9	321.3 ± 2.3
5	-322.4	-320.6	-320.8	321.2 ± 1.0
6	-321.5	-321.0	-322.4	321.6 ± 0.7
7	-320.4	-321.8	-322.4	321.5 ± 1.0
8	-319.0	-321.9	-322.1	321.0 ± 1.7
9	-318.7	-322.1	-321.8	320.8 ± 1.9
10	-318.4	-321.9	-321.4	320.5 ± 1.9

The addition of 2 mole ratio of  $[\{\text{CoN}_4(\text{OH})(\text{OH}_2)\}]^{2+}$  to one mole ratio of  $[\text{H}_2\text{P}_2\text{O}_7]^{2-}$  at pH 7.0 and 25° C can result in the formation of double six membered chelates in a manner analogous to that described above. The tendency of the potent nucleophile such as  $\text{OH}^-$  to attack the phosphorus centre will depend, among other factors, on the number and nature of the electron withdrawing substituents attached to the oxygens of the pyrophosphate moiety and on the nature of the ligands around the cobalt(III) ion. Milburn and Hubner  $^{31}\text{P}$  NMR studies<sup>222</sup> have successfully demonstrated that the initial reaction is the formation of the monodentate complex by the loss water from the  $[\text{CoN}_4(\text{OH})(\text{H}_2\text{O})]^{2+}$  species. As a result the coordinated hydroxide might become partially protonated.

Chelate formation can take place through the attack of the phosphorous centres by the coordinated hydroxide and/or through dissociative loss of the coordinated water with entry of pyrophosphate oxygen. Formation of a six membered chelate is expected to take place without hydrolysis due to the stability of this ring system, while the generation of four membered chelates can give rise to some free phosphate. The formation of a stable six membered chelate in this reaction is further confirmed with our phosphate selective electrode as the main reaction pathway. This is because no free phosphate was detected in the solution as it would have been if a four membered chelate was formed.

For reaction solutions which were 3:1 in  $[\text{CoN}_4(\text{OH})(\text{H}_2\text{O})]^{2+}$  to  $[\text{H}_2\text{P}_2\text{O}_7]^{2-}$  ratio. No appreciable hydrolysis was noted with the possible formation of different chelates as evidenced by previous  $^{31}\text{P}$  NMR studies.<sup>232,236,237</sup> The EMF readings for the respective

reaction did not show production of free phosphate in solution. Had there been appreciable hydrolysis, the production of phosphates could have resulted in an increase in the EMF value. It might also be assumed that phosphates produced in solution are predominantly attached to a metal ion to form a metal-phosphate complex undetected by the phosphate ion selective electrode.

#### **4.3.4 RESULTS FOR COBALT(III)BIS-TRIMETHYLENEDIAMINE HYDROLYSIS OF SODIUM TRIPOLYPHOSPHATE**

The hydrolysis of tripolyphosphate by 1:1, 2:1 and 3:1 molar ratio of bis trimethylenediaminecobalt(III)  $[\text{CoN}_4(\text{OH})(\text{H}_2\text{O})]^{2+}$  with tripolyphosphate  $([\text{H}_2\text{P}_3\text{O}_{10}]^{3-})$  was monitored by preparing the respective solutions and measuring the resulting EMF by the electrode. When coordinated to a metal, the tripolyphosphates are unsymmetrical and are prone to hydrolysis. The EMF values recorded for the hydrolysis reactions are summarized in the tables 4.12, 4.13 and 4.14 for 1:1, 2:1 and 3:1 metal to polyphosphate ratio respectively.



Table 4.12 EMF (mV) values recorded for the reaction between  $[\text{CoN}_4(\text{OH})(\text{OH}_2)]^{2+}$  and  $[\text{H}_2\text{P}_2\text{O}_{10}]^{2-}$  for 1:1  $[\text{CoN}_4(\text{OH})(\text{OH}_2)]^{2+}$  to  $[\text{H}_2\text{P}_3\text{O}_{10}]^{3-}$  ratios.

Time (min)	DATA 1	DATA 2	DATA 3	MEAN
0.5	-294.7	-295.2	-291.4	293.7 ± 2.0
1	-297.1	-296.9	-294.3	296.1 ± 1.6
2	-296.7	-297.0	-295.8	296.5 ± 0.6
3	-298.6	-299.0	-294.8	297.4 ± 2.3
4	-297.3	-298.1	-295.1	296.8 ± 1.6
5	-295.3	-297.4	-294.0	295.5 ± 1.7
6	-293.1	-296.8	-292.1	294.0 ± 2.5
7	-290.7	-295.0	-290.0	292.0 ± 3.0
8	-289.8	-294.1	-288.1	290.6 ± 3.1
9	-289.2	-292.1	-287.5	289.6 ± 2.3
10	-285.2	-291.8	-284.8	287.2 ± 3.9

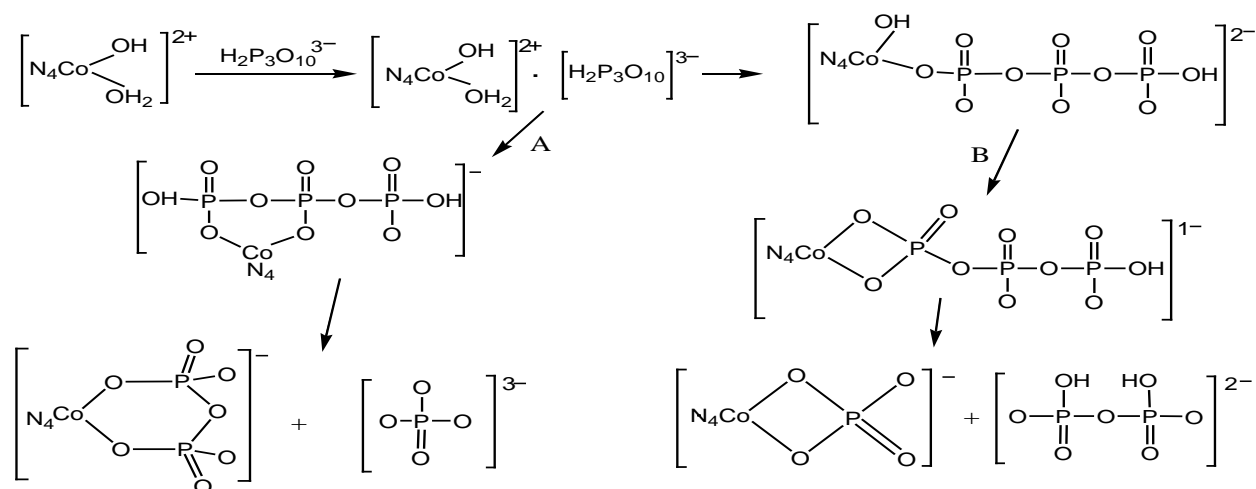
Table 4.13 EMF (mV) values recorded for the reaction between  $[\text{CoN}_4(\text{OH})(\text{OH}_2)]^{2+}$  and  $[\text{H}_2\text{P}_2\text{O}_{10}]^{2-}$  for 2:1  $[\text{CoN}_4(\text{OH})(\text{OH}_2)]^{2+}$  to  $[\text{H}_2\text{P}_3\text{O}_{10}]^{3-}$  ratios.

Time (min)	DATA 1	DATA 2	DATA 3	MEAN
0.5	-259.4	-260.1	-253.4	257.6 ± 3.7
1	-260.9	-260.5	-255.4	258.9 ± 3.1
2	-269.8	-270.1	-259.8	266.5 ± 5.9
3	-270.4	-271.3	-261.2	267.6 ± 5.6
4	-271.8	-272.4	-264.3	269.5 ± 4.5
5	-271.9	-272.5	-263.3	269.2 ± 5.1
6	-272.1	-272.1	-266.5	270.2 ± 3.2
7	-272.4	-271.9	-267.4	270.5 ± 2.8
8	-272.1	-271.4	-268.4	270.6 ± 2.0
9	-272.7	-271.0	-268.1	270.6 ± 2.3
10	-272.6	-270.9	-269.4	270.9 ± 1.6

Table 4.14 EMF (mV) values recorded for the reaction between  $[\text{CoN}_4(\text{OH})(\text{OH}_2)]^{2+}$  and  $[\text{H}_2\text{P}_3\text{O}_{10}]^{3-}$  for 3:1  $[\text{CoN}_4(\text{OH})(\text{OH}_2)]^{2+}$  to  $[\text{H}_2\text{P}_3\text{O}_{10}]^{3-}$  ratios.

Time (min)	DATA 1	DATA 2	DATA 3	MEAN
0.5	-242.8	-241.5	-244.3	$242.8 \pm 1.4$
1	-246.1	-243.4	-245.2	$244.9 \pm 1.4$
2	-252.7	-244.8	-245.7	$247.7 \pm 4.3$
3	-254.1	-247.1	-247.6	$249.6 \pm 3.9$
4	-254.0	-248.3	-248.1	$250.1 \pm 3.4$
5	-253.8	-249.8	-249.9	$251.1 \pm 2.3$
6	-251.6	-250.1	-250.4	$250.7 \pm 0.8$
7	-250.8	-250.4	-250.9	$250.7 \pm 0.3$
8	-250.4	-250.9	-251.5	$250.9 \pm 0.6$
9	-250.1	-250.5	-251.8	$250.8 \pm 0.9$
10	-250.3	-250.3	-252.1	$250.9 \pm 1.0$

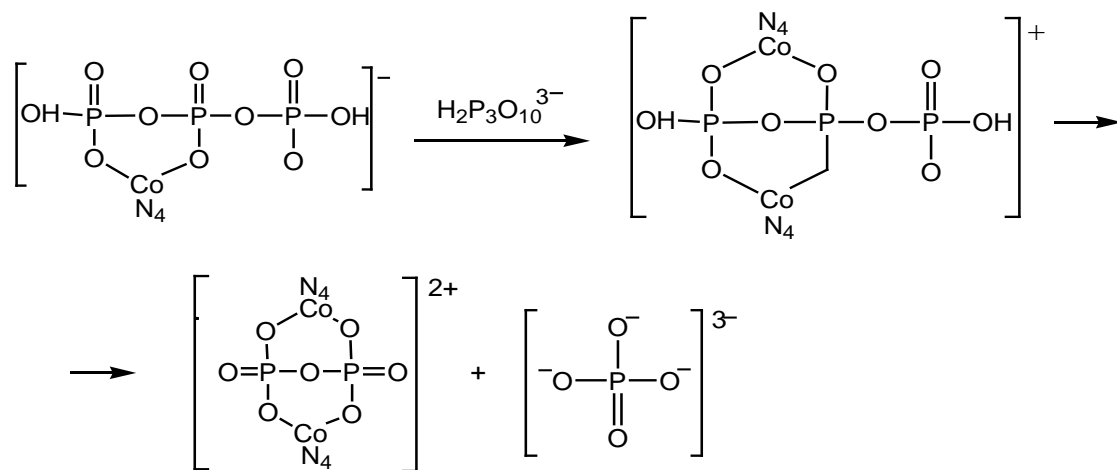
The 1:1 hydrolysis between  $[\text{CoN}_4(\text{OH})(\text{OH}_2)]^{2+}$  and  $[\text{H}_2\text{P}_3\text{O}_{10}]^{3-}$  has been documented<sup>237,244,245</sup> to predominantly produce metal phosphate chelates as shown below;

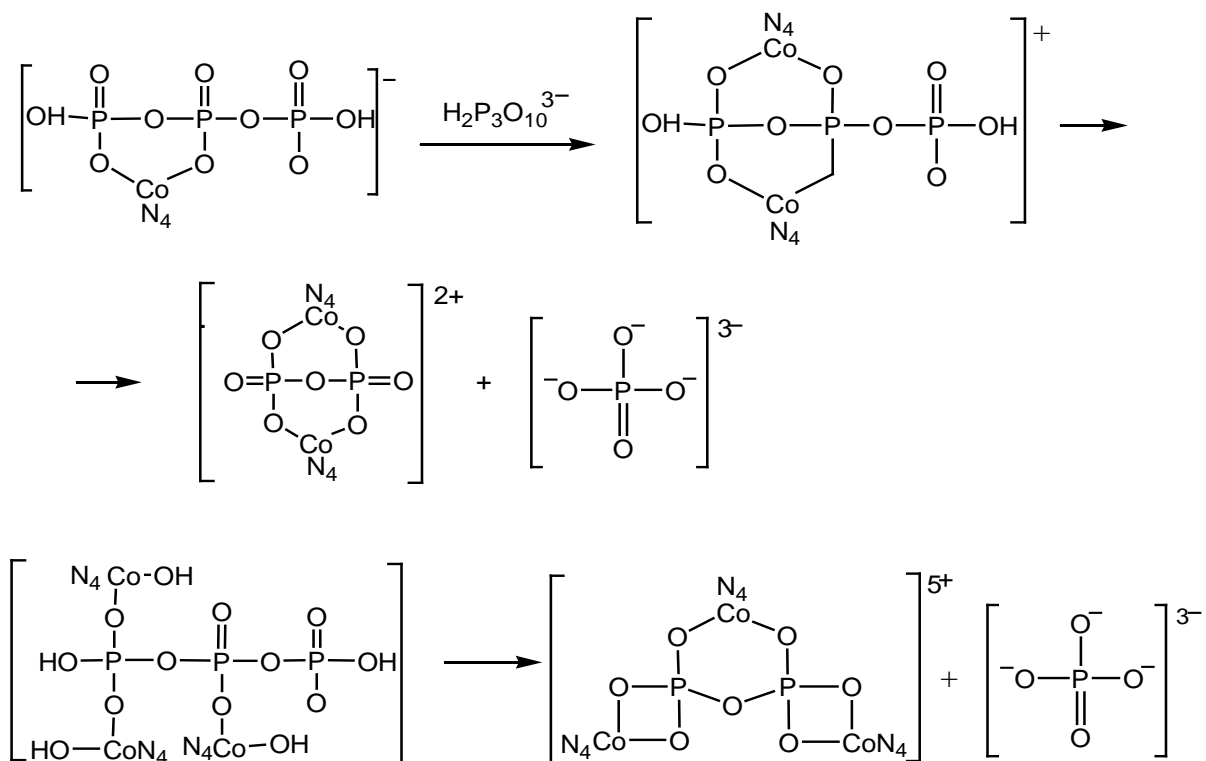


Scheme 4.1 Plausible scheme for the reaction of  $[\text{CoN}_4(\text{OH})(\text{H}_2\text{O})]^{2+}$  with triphosphate  $[\text{H}_2\text{P}_3\text{O}_{10}]^{2-}$  for 1:1  $[\text{CoN}_4(\text{OH})(\text{H}_2\text{O})]^{2+}$  to  $[\text{H}_2\text{P}_3\text{O}_{10}]^{2-}$  ratio.

The coordinated OH<sup>-</sup> on the cobalt centre may attack any of the phosphorus centers given rise to the above predominant chelated species. Both path A and B are plausible schemes that predominates in the solution. While path A may give rise to a Six membered ring phosphate chelate  $[\{\text{CoN}_4(\text{O})_2(\text{PO})_2\text{O}_3\}]^-$  and a phosphate moiety, Path B gives rise to a bicordinated phosphates  $[\{(\text{CoN}_4)_2\text{O}_3\text{PO}\}]^-$  and a pyrophosphate. The production of the phosphate species brought about a change in the EMF readings as shown in the results table.

Similarly, for 2:1 and 3:1 complexes the following species are expected to predominate in the reaction solution leading to the formation of free phosphate due to further hydrolysis.<sup>248</sup>





Scheme 4.2 Plausible scheme for the reaction of  $[\text{CoN}_4(\text{OH})(\text{H}_2\text{O})]^{2+}$  with triphosphate  $[\text{H}_2\text{P}_3\text{O}_{10}]^{2-}$  for 2:1 and 3:1  $[\text{CoN}_4(\text{OH})(\text{H}_2\text{O})]^{2+}$  to  $[\text{H}_2\text{P}_3\text{O}_{10}]^{2-}$  ratio.

Increase in the EMF reading as the metal substrate increases for the 2:1 and the 3:1 reactions indicates hydrolysis reaction giving rise to monodentate phosphates, bidentate phosphates and free phosphates as shown in the plausible schemes above. Hydrolysis has been reported in related experiments<sup>244,245</sup> and the above structures have been documented as the most plausible pathway. The formation of unsymmetrical phosphate complexes lead to hydrolysis thereby producing free phosphates in the reactions. The addition of metal complex to the phosphate substrates produces an ion pair complex. The ion pair rearranges to produce monodentately or bicoordinated species. The loss of coordinated water from the cobalt center and an attack by the hydroxides on the metal center is presumably the most dominant reaction during the

rearrangement. An attack of the most electrophilic phosphorous center by one of the coordinated metal hydroxide results in hydrolysis releasing one mole ratio of free phosphate in to the solution. Evidence of this reaction has been previously documented in the literature.<sup>237</sup>

# CHAPTER FIVE

## 5.0 GENERAL CONCLUSION

Measurements involving phosphates have been of tremendous interest in recent decades. More precise knowledge on the available phosphorous is mandatory to counter the ill-effects of excess phosphorous in the aquatic environment. Chemical analysis using  $^{31}\text{P}$  NMR or UV-Visible absorption spectroscopy to mention but a few is commonly carried out for the practical monitoring of phosphates. However, some of these systems are generally complicated, and in so many cases require trained professionals. Moreover, they also remain unsuitable for application in most locations that may require on-site analysis. Problems related to phosphate ion analysis with the above mentioned techniques can be circumvented by using suitable phosphate selective electrodes. Ideally a portable, phosphate selective electrode that can easily estimate the amount of phosphates in effluent is required for quick assessment of phosphate concentrations. The phosphate selective electrodes fabricated in this research have the ability to detect trace concentrations that ranges from  $1 \times 10^{-1}$  M to  $1 \times 10^{-6}$  M. The electrode's bodies are shock-proof, chemically resistant and can measure samples irrespective of colour changes and turbidity. These electrodes have the ability to monitor samples concentrations continuously. They can be placed in samples without sample pre-treatment or destruction of the sample. Above all, the electrodes are

inexpensive and they are great screening tools for identifying dissolved phosphates in the laboratory and water samples in the environment. The novel phosphate selective electrodes if commercialized will be the first of its kind among other sensors for other ions.

The fabricated phosphate selective electrodes give optimum response to free phosphates in solutions in record steady time of below 60 seconds. The detection limit for inorganic phosphate ion in solution is down to  $1 \times 10^{-7}$  M below which the response becomes unsteady. The ternary membrane electrodes showed more precision, sensitivity, selectivity, and stability in all analysis of phosphate ions than their binary counterparts. This is so due to the inherent properties of the constituting membrane materials which were carefully selected, owing to their chemical relationships with free phosphates in solution. The all solid state nature of the new phosphate selective electrodes ensures miniaturization and robustness of the assembly. Above all, the electrodes give steady responses in the absence of ionic strength control buffers (TISAB). This creates room for versatility as interferences inherent in many TISAB formulations are curbed.

The phosphate selective electrodes described here have membranes composed of mixtures of sparingly soluble crystalline components. The active ionophores in the membrane are aluminium phosphate and copper. Literature has cited chemisorption properties of copper in the presence of aluminium giving rise to coated wire electrodes.<sup>194</sup> Ternary surface complex formation of copper with anions such as free

phosphate ( $\text{PO}_4^{3-}$ ), chloride ( $\text{Cl}^-$ ) and sulphate ( $\text{SO}_4^{2-}$ ) has also been documented. This explains the electrodes sensitivity to chloride. It is envisaged that phosphate selective electrodes produced in this project will function similar to the solid state electrodes and the coated wire electrodes. The coated wire electrodes (CWEs) refer to a type of ion selective electrode in which an electroactive species is incorporated in a thin polymeric film coated directly on a metallic conductor. They generally involve electroactive species that are heterogeneously dispersed in the polymeric matrix.

The unique properties of the novel phosphate selective electrodes are their ability to detect free phosphates  $\text{PO}_4^{3-}$  in solution. Once a standard calibration curve is obtained within the concentration range, the solution's concentration can be determined by reading off from the standard. All electrodes fabricated in this research are sensitive to phosphates to certain degrees. More sensitivity was noted for the ternary membrane electrodes than the binary ones. This is so because of the inherent properties of the membrane components which make them specific target for free phosphates in solution. The phosphate selective electrodes described here are robust in terms of response time, unaffected by pH changes in the range of 4.5-8.9, and samples ionic strength.

Some conclusions which can be drawn from the different systems examined in the phosphorylation and dephosphorylation study are summarized below;

- (1) Reaction solutions which were 1:1, 2:1 and 3:1 in metal  $[\{\text{CoN}_4(\text{OH})(\text{OH}_2)\}]^{2+}$  to phosphate  $[\text{HPO}_4]^{2-}$  ratio, at pH 7.0 and  $25^\circ\text{C}$  result in rapid water substitution to form the monodentate complex which can then form a four membered chelate.



The EMF reading of the solution revealed the absence of any phosphate species in the solution. Hence it is concluded from the above observation that the reaction has proceeded to completion and no free phosphate exists in the solution after the reactants were mixed. The mean EMF reading for the phosphate species was -242.2 mV. It immediately dropped to the mean value of -349.8 mV after the addition of the metal  $[\{\text{CoN}_4(\text{OH})(\text{OH}_2)\}]^{2+}$  complex. This showed that the reaction is diffusion controlled and goes to 100% completion.

(2) In reaction solutions which were 1:1 in metal  $[\{\text{CoN}_4(\text{OH})(\text{OH}_2)\}]^{2+}$  to pyrophosphate  $[\text{H}_2\text{P}_2\text{O}_7]^{2-}$  ratio, at pH 7.0 and 25° C, the formation of six membered chelate,  $[\{\text{CoN}_4\text{P}_2\text{O}_7\}]^-$  is predominant. No hydrolysis is expected due to the stability of the symmetrical ring system. The EMF reading from those reaction solutions is consistent with the above observation. The addition of 2 mole ratio of  $[\{\text{CoN}_4(\text{OH})(\text{OH}_2)\}]^{2+}$  to one mole of  $[\text{H}_2\text{P}_2\text{O}_7]^{2-}$  result in the formation of double six membered chelates in a manner documented in the literatures<sup>222</sup>. The chelates are stable in solution and no appreciable hydrolysis was noted during the formation of the chelates. Also, for reaction solutions which were 3:1 in metal,  $[\{\text{CoN}_4(\text{OH})(\text{OH}_2)\}]^{2+}$  to pyrophosphate  $[\text{H}_2\text{P}_2\text{O}_7]^{2-}$  ratio, no hydrolysis was noted with our phosphate selective electrode and the reaction will be attributed to the possible formation of different chelates in solution.

(3) In reaction solutions which were 1:1, 2:1 and 3:1 in  $[\{\text{CoN}_4(\text{OH})(\text{OH}_2)\}]^{2+}$  to  $[\text{O}_2\text{NC}_6\text{H}_4\text{PO}_2(\text{O})(\text{OH})]^-$  (4-NPP) at the pH of 7.0 and 25° C, the formation of  $[\{\text{CoN}_4(\text{OH})4\text{-NPP}\}]^+$ ,  $[\{(\text{CoN}_4(\text{OH}))_24\text{-NPP}\}]^{2+}$  and  $[\{(\text{CoN}_4(\text{OH}))_34\text{-NPP}\}]^{2+}$  respectively are noted from the similarity in the EMF values of the reaction solutions with those of  $[\{\text{CoN}_4\text{O}_3\text{PO}\}]^-$ . It can be inferred that 4-NPP quantitatively hydrolyses to 4-nitrophenol (4-NP) and  $[\{\text{CoN}_4\text{O}_3\text{PO}\}]^-$  in the reacting solutions.

(4) For the hydrolysis reaction for 1:1, 2:1 and 3:1 molar ratio of  $[\{\text{CoN}_4(\text{OH})(\text{OH}_2)\}]^{2+}$  to  $[\text{H}_2\text{P}_3\text{O}_{10}]^{3-}$ , the EMF values obtained by the 1:1 solution is indicative of a monodentate or chelated species as the values are similar to those of  $[\text{H}_2\text{P}_3\text{O}_{10}]^{3-}$  in solution. There appears to be no hydrolysis. An increase in the EMF value for the 2:1 solution indicates hydrolysis reaction giving rise to chelated and unchelated pyrophosphate and monophosphate species which are unsymmetrical. A further increase of the EMF values for the 3:1 solution points to further hydrolysis leading to chelated and unchelated phosphates. The formation of unsymmetrical phosphate complexes leads to hydrolysis thereby producing monophosphate species in the solution. The direct addition of 3 mole ratio of the cobalt complex to one mole ratio of tripolyphosphate initially produces an ion pair complex. The ion pair then rearranges to produce monodentately coordinates PPPi species. The loss of coordinated water from the cobalt center and an attack by the phosphate oxygens on the metal center is presumably the most dominant reaction during the rearrangement. An attack of

the most electrophilic phosphorous center by one of the coordinated metal hydroxide results in hydrolysis releasing one mole ratio of free phosphate in to the solution.

In all, monitoring dephosphorylation reactions of all the species investigated could not be fully achieved. This is because the phosphate selective electrode detects only the free phosphate,  $[\text{HPO}_4]^{2-}$  in solution as a result of dephosphorylation. All other combined forms of phosphate in solution could not be detected and therefore unaccounted for. Phosphorylation in solution can only be accounted for when one of the initial reactants in solution is a free phosphate.

## **5.1 FUTURE WORK**

Interference studies conducted with the phosphate selective electrodes suggests that the fabricated electrode is also selective to chloride ions to some extent. Future work in this dimension entails efforts to curb chloride interferences and possibly utilize the phosphate selective electrode in the determination of chloride concentrations in solutions void of phosphates. Application of experimental designs to fabricate an optimized electrode will be undertaken in future investigations. Identification of ionophores sensitive to pyrophosphates or tripolyphosphates will be undertaken with a view to produce electrodes selective to those species in solution. The electrode systems are anticipated to be used for in-vivo real enzymatic system studies eventually. Hence the reaction of the biological molecules on the surface of the electrode (redox

characteristics) will be investigated before the in-vivo studies are conducted. Since interaction of copper with sulphur containing proteins is established in the literature, the presence of about 25% copper in the formulation of the electrode materials need to be investigated if it makes it suitable for in-vivo studies. The results of the model studies are a success as it does not have biological species that might interfere with the workings of the electrode. This will be revealed in future studies.

# REFERENCES

- (1) McKelvie, I. D. *Organic phosphates in the environment* (Editors; Turner, B. L.; Frossard, E.; Baldwin, D. S.), CABI Publishing, UK, 2005.
- (2) Johnes, P. J.; Heathwhite, A. L. *Water Res.* **1992**, 26, 1281-1287.
- (3) Turner, B. L.; Paphazy, M. J.; Haygarth, P. M.; Mckelvie, I. D. *Phil. Trans. R. Soc. Lond.* **2002**, B 357, 449-469.
- (4) Beeton, A. M. *Eutrophication of the St. Lawrence great lakes. In man's impact on environment;* (Editor; Detwyler, T. R.), McGraw-Hill Book Co, N Y, 1971.
- (5) Nevins, M. J.; Johnson, W. W. B. *Environ. Contam. Tox.* **1978**, 19(2), 250-256.
- (6) <http://ohsonline.com/articles/2011/11/23/eu-members-agree-to-ban-phosphates-from-household-detergents.aspx>, 24-02-2012.
- (7) [http://www.cognis.com/NR/rdonlyres/58F10426-3B9D-4741-8B2B-9FOD51254CED/0/1109\\_Happi\\_PhosphatefreeAutomatic.pdf](http://www.cognis.com/NR/rdonlyres/58F10426-3B9D-4741-8B2B-9FOD51254CED/0/1109_Happi_PhosphatefreeAutomatic.pdf), 24-02-2012.
- (8) Cisse, L.; Mrabet, T. *Phosphorus Research Bulletin.* **2004**, 15, 21-25.
- (9) Malek, R. S.; R S Kuntzman, R. S.; Barret, D. M. *J. Urol.* **2005**, 174, 4(1), 1344-1348.
- (10) Yarema, S. M.; Milam, D. *IEEE J. Quantum Electron.* **1982**, QE-18(11), 1941-1946.
- (11) Jiang, S.; Myers, J. D.; Rhonehouse, D. L.; Myers, M.; Belford, R. E.; Hamlin, S. J.; Belford, R. E. *SPIE*, **1994**, Vol. 2138, 1-5.
- (12) Brindley, D. N.; Pilquill, C. J. *Lipid Res.* **2009**, S225-S230.

- (13) Nagel, A.; Barker, C. J.; Berggren, P. O.; Illies, C. *Methods Mol. Biol.* **2010**, 645, 123-131.
- (14) Mason, P. W.; Carbone, D. P.; Cushman, R. A.; Waggoner, A. S. *J. Biol. Chem.* **1981**, 256(4), 1861-1866.
- (15) Roth, E. F. Jr.; Ruprecht, R. M.; Schulman, S.; Vanderberg, J.; Olsen, J. A. *J. Clin. Invest.* **1986**, 77(4), 1129-1135.
- (16) Braasch, D. A.; Corey, R. *Chem. Biol.* **2001**, 8(1), 1-7.
- (17) Ambuhl, P. M.; Meier, D.; Wolf, B.; Dydak, U.; Boesiger, P.; Binswanger, U. *Am. J. Kidney Dis.* **1999**, 34(5), 875-883.
- (18) Lemann, J. Jr, Bushinsky, D. A.; Lee-Hamm, L. *Am. J. Physiol. Renal Physiol.* **2003**, 285, F811-F832.
- (19) <http://www.lenntech.com/periodic/elements/P.htm#ixzz1dC2OOMRO>, 24-02-2012.
- (20) Ohnishi, M.; Razzaque, M. S. *FASEB J.* **2010**, 24(9), 3562-3571.
- (21) <http://emedicine.medscape.com/article/242280-overview>.
- (22) Brien, O.; Thomas, M.; Coberly, L. A. *Adv. Stud. Med.* **2003**, 3(6), 345-348.
- (23) Takeda, E.; Taketani, Y.; Sadawa, N.; Sato, T.; Yamamoto, H. *Biofactors*, **2004**, 21(1-4), 345-355.
- (24) Takeda, E.; Yamamoto, H.; Nashiki, K.; Arai, H.; Taketani, Y. *J. Cell. Mol. Med.* **2004**, 8(2), 191-200.
- (25) Sullivan, J. B.; Blose, J.; *Organophosphate and carbamate insecticides: Hazardous material toxicology*; Williams and Wilkins: Baltimore, **1992**.

- (26) Bondy, H. F.; Hughes, J. P. W.; Leahy, J. L.; Worden A. N. *Toxicology*, **1972**, 1(2), 143-150.
- (27) Slotkin, T. A.; Seidler, F. J. *Brain Res. Bull.* **2007**, 72, 232-274.
- (28) Slotkin, T. A. *Environ. Health Persp.* **1999**, 107(1), 71-80.
- (29) Kotak, B. G.; Kenefick, S. L.; Fritz, D. L.; Rousseaux, C. G.; Prepas, E. E.; Hrudley, S. E. *Water Res.* **1993**, 27(3), 495-506.
- (30) Hermes-Lime, M. J. *Mol. Evol.* **1990**, 31, 353-358.
- (31) Han, M. S.; Kim, D. H. *Angew. Chem. Int. Ed.* **2002**, 41(20), 3809-3811.
- (32) Harwood, J. E.; Van Steenderen, R. A.; Kuhn, A. L. *Water Res.* **1969**, 3, 417-423.
- (33) Glazier, S. A.; Arnold, M. A. *Anal. Chem.* **1991**, 63, 754-759.
- (34) Black, J. A. *Water pollution technology*; Reston Publishing Co: Reston VA, **1977**.
- (35) Hach Company. *Hach water analysis handbook, 2<sup>nd</sup> Ed.*, Loveland CO. **1992**.
- (36) Burton, J. D. *Water Res.* **1973**, 7, 291-307.
- (37) Bakker, E.; Pretsch, E. *Trends Anal. Chem.* **2001**, 20(1), 11-19.
- (38) Tafesse, T.; Enemchukwu, M. *Talanta*, **2011**, 83, 1491-1495.
- (39) Somer, G.; Kalayci, S.; Basak, I. *Talanta*, **2010**, 80, 1129-1132.
- (40) Ekemekci, G.; Kalayci, S.; Somer, G. *Sensor Actuator*, **2004**, B 101, 260-264.
- (41) Guilbaut, G. G.; Brignac, J. P. Jr. *J. Anal. Chem.* **1969**, 41, 1136-1138.
- (42) Ihn, G. S.; Nash, C. F.; Buck, R. P. *Anal. Chim. Acta.* **1980**, 121, 101-109.
- (43) Meruva, R. K.; Meyerhoff, M. E. *Anal. Chem.* **1996**, 68, 2022-2026.
- (44) Xiao, D.; Yuan, H. Y.; Li, J.; Yu, R. Q. *Anal. Chem.* **1995**, 67, 288-291.

- (45) Petrucelli, G. C.; Kawachi, E. Y.; Kubota, L. T.; Betran, C. A. *Anal. Commun.* **1996**, 33(7), 227-229.
- (46) Shimizu, Y.; Furuta, Y. *Solid state Ionics*, **1998**, 113-115, 241-245.
- (47) Shimizu, Y.; Yamashita, T.; Takase, S. *Jpn. J. Appl. Phys.* **2000**, 39(2), L384-L386.
- (48) Belluzo, M. S.; Ribone, M. E.; Lagier, C. L. *Sensors*, **2008**, 8, 1366-1399.
- (49) Prodromidis, M. I.; Karayanmis, M. I. *Electroanalysis*, **2002**, 14(4), 241-261.
- (50) Ganjali, M. R.; Norouzi, P.; Ghomi, M.; Salavati-Niasari, M. *Anal. Chim. Acta.* **2006**, 567, 196-201.
- (51) Jain, A. K.; Gupta, V. K.; Raison, J. R. *Talanta*, **2006**, 69, 1007-1012.
- (52) Ganjali, M. R.; Mizani, F.; Salavati-Niasari, M. *Anal. Chim. Acta.* **2003**, 481, 85-90.
- (53) Goff, T. L.; Braven, J.; Ebdon, L.; Scholefield, D. *Anal. Chim. Acta.* **2004**, 510, 175-182.
- (54) Kivlehan, F.; Mace, W. J.; Moynihan, H. A.; Arrigan, D. W. M. *Anal. Chim. Acta.* **2007**, 585, 154-160.
- (55) Liu, D.; Chen, W. C.; Yang, R. H.; Shen, G. L.; Yu, R. Q. *Anal. Chim. Acta.* **1997**, 338, 209-214.
- (56) Bulhmann, P.; Pretsch, E.; Bakker, E. *Chem. Rev.* **1998**, 98(4), 1593-1687.
- (57) Engblom, S. O. *Biosens Bioelectron.* **1998**, 13, 981-994.
- (58) Pinna, M. C.; Salis, A.; Monduzzi, M.; Ninham, B. W. *J. Phys. Chem.* **2005**, B 109, 5406-5408.
- (59) Broering, J. M.; Bommarius, A. S. *J. Phys. Chem.* **2005**, B109, 20612-20619.
- (60) Perez-Jimenez, R.; Godoy-Ruiz, R.; Ibarra-Moleru, B.; Sanchez-Ruiz, J. M. *Biophys. Chem.* **2005**, 115(2-3), 105-107.



- (61) Lyklema, J. *Chem. Phys. Lett.* **2009**, 467, 217-222.
- (62) Zhang, Y.; Cremer, P. S. *Curr. Opin. Chem. Biol.* **2006**, 10, 658-663.
- (63) Tsagatakis, J. K.; Chaniotakis, N. A.; Jurkschat, K. *Helv. Chim. Acta.* **1994**, 77(8), 2191-2196.
- (64) Chai, Y. Q.; Yuan, R.; Xu, L.; Xu, W. J.; Dai, J. Y.; Jiang, F. *Anal. Bioanal. Chem.* **2004**, 380, 333-338.
- (65) Wang, F. C.; Chai, Y. Q.; Yuan, R. *Russ. J. Electrochem.* **2008**, 44(3), 293-299.
- (66) Seo, H. R.; Lee, H. K.; Jeon, S. *Bull. Korean Chem. Soc.* **2004**, 25(10), 1484-1488.
- (67) Cadogan, A.; Gao, Z.; Lewenstam, A.; Ivaska, A. *Anal. Chem.* **1992**, 64, 2496-2501.
- (68) Bobacka, J.; Lindfors, T.; McCarrick, M.; Ivaska, A.; Lewenstam, A. *Anal. Chem.* **1995**, 67, 3819-3823.
- (69) Moss, B. A.; *Chem. Ind-London.*, **1996**, 11, 407-411.
- (70) Leinweber, P.; Turner, B. L.; Meissner, R. *Phosphate in agriculture, hydrology and water quality*, (Editors; Haygarth, P. M.; Jarvis, S. C.) CABI publishers: Wallingford, UK, 2002.
- (71) Haygarth, P. M.; Jarvis, S. C. *Adv. Agron.* **1999**, 66, 195-245.
- (72) Robards, K.; Mckelvie, I. D.; Benson, R. L.; Worsfold, P. J.; Brundell, N. J.; Casey, H. *Anal. Chim. Acta.* **1994**, 287, 147-190.
- (73) Hanrahan, G.; Gledhill, M.; House, W. A. Worsfold, P. J. *Water Res.*, **2003**, 37(15), 3579-3589.

- (74) Worsfold, P. J.; Gimbert, L. J.; Mankasingh, U.; Omaka, O.N.; Hanrahan, G.; Gardolinski P. C. F. C.; Haygarth, P. M.; Turner, B. L.; Keith-Roach, M. J.; McKelvie, I. D. *Talanta*, **2005**, *66*, 273-293.
- (75) Turner, B. L.; Rossard, E.; Baldwin, O. S. *Organic phosphorus in the environment*; CABI publishers: USA. 2003.
- (76) Alberts, B.; Bray, D.; Johnson, A.; Lewis, J.; Raff, M.; Roberts, K.; Walter, P. *Essential cell biology; 2<sup>nd</sup> edition*, Garland Science, Taylor-Francis group, 2004.
- (77) Skoog, D. A.; West, D. M.; Holler, F. J.; Crouch, S. R. *Fundamentals of analytical chemistry; 8<sup>th</sup> Ed*, Australia: Thomson Brooks/Cole, 2004.
- (78) Strickland, J. D. H. Parsons, T. R.; *A practical handbook of seawater analysis, 2<sup>nd</sup> Ed.*, Fisheries Research Board of Canada. 1972.
- (79) Halmann, M. *Analytical chemistry of phosphorus compounds*; John Wiley and sons: N Y. 1972.
- (80) Snoeyink, V. L.; Jenkins, D. *Water Chemistry*, John Wiley and Sons: N Y. 1982.
- (81) Van Wazar, J. R. *Phosphorus and its Compounds, Bd. 1: Chemistry*, Interscience Publishers: N Y. 1958.
- (82) Barrows, J. N.; Jameson, G. B.; Pope, M. T. *J. Am. Chem. Soc.* **1985**, *107*, 1771-1773.
- (83) Kozik, M.; Casan-Pastor, N.; Hammer, C. F.; Baker, L. C. W. *J. Am. Chem. Soc.* **1988**, *110*, 7697-7701.
- (84) Benson, R. L.; Truong, Y. B.; McKelvie, I. D.; Hart, B. T. *Water Res.* **1996**, *30*(9), 1959-1964.
- (85) Towns, T. G. *Anal. Chem.* **1986**, *58*, 223-229.

- (86) Armstrong, D. E. *Analysis of phosphorus compounds in natural waters*. (Editor, Halmann, M.), Wiley Interscience: N Y, 1972.
- (87) Going, J. E.; Eisenreich, S. J. *Anal. Chim. Acta*. **1974**, 70, 95-106.
- (88) Murphy, J.; Riley, J. P. *Anal. Chim. Acta*. **1962**, 27, 31-36.
- (89) Campbell, A. D.; Graham, P. B. *New Zeal. J. Sci.* **1983**, 26(4), 433-435.
- (90) Broberg, O.; Persson, G. *Hydrobiologia*, **1988**, 170, 61-90.
- (91) Broberg, O.; Petterson, K. *Hydrobiologia*, **1988**, 170, 45-59.
- (92) Motomizu, S.; Wakimoto, T.; Toei, K. *Talanta*, **1984**, 31(4), 235-240.
- (93) Motomizu, S.; Wakimoto, T.; Toei, K. *Analyst*, **1983**, 108, 361-367.
- (94) Motomizu, S.; Oshima, M.; Hirashima, A. *Anal. Chim. Acta*. **1988**, 211, 119-127.
- (95) Rao, C. N. R. *Ultraviolet and Visible spectroscopy, 2<sup>nd</sup> edition*, Butterworths: London, 1967.
- (96) Owen, T. *Fundamentals of modern UV-Visible spectroscopy*, Primer-Agilent Technologies Bulletin: Germany. 2000.
- (97) <http://www2.chemistry.msu.edu/faculty/reush/VirtTxtJml/Spectrpy/UV-Vis/spectrum.htm>, 11-12-2011.
- (98) Per-Kampus, H. H.; Grinter, H. C.; Threfall, T. L. *UV-Vis Spectroscopy and its applications*. Springer, 1994.
- (99) Clark, B. J.; Frost, T.; Russel, M. A. *UV spectroscopy-techniques instrumentation and data handling*. Chapman and Hall, 1993.

- (100) Burgess, C.; Knowles, A. *Techniques available in visible and ultraviolet spectrometry*, Chapman and Hall, 1984.
- (101) <http://teaching.shu.ac.uk/hwb/chemistry/tutorials/molspec/uvvisab1.htm>, 11-12-2011.
- (102) Jones, C.; Mulloy, B.; Thomas, A. H. *Microscopy, optical spectroscopy and macroscopic techniques*, Humana Press: N J, 1994.
- (103) Sekiguchi, Y.; Matsunaga, A.; Yamamoto, A.; Inoue, Y. *J. Chromatogr.* **2000**, *A881*, 639-644.
- (104) Gee, A.; Deitz, V. R. *Anal. Chem.* **1953**, *25(9)*, 1320-1324.
- (105) Dusek, M.; Kvoasnicka, F.; Lukaskova, L.; Kratka, J. *Meat Sci.* **2003**, *65*, 765-769.
- (106) Jastrzebska, A.; Brudka, B.; Szymanski, T.; Szlyk, E. *Food Chem.* **2003**, *83*, 463-467.
- (107) Cozzolino, D.; Kwiatkowski, M. J.; Damberg, R. G.; Cynkar, W. U.; Janik, L. J.; Skouroumounis, G.; Gishen, M. *Talanta*, **2008**, *74*, 711-716.
- (108) Bertram, H. C.; Stodkilde-Jorgensen, H.; Karlsson, A. H.; Andersen, H. J. *Meat Sci.* **2002**, *62*, 113-119.
- (109) Paytan, A.; McLaughling, K. *Handbook of Environmental Isotope Geochemistry, Advances in isotope Geochemistry* (Editor; Baskaran, M.). Springer-Verlag Berlin Hiedelberg, 2011.
- (110) Gorenstein, D. G. *Phosphorus-31 NMR principles and applications*, Academic Press, NY, 1984.
- (111) Gorenstein, D. G. *Method Enzymol.* **1989**, *177*, 295-316.
- (112) Gorenstein, D. G. *Method Enzymol.* **1992**, *211*, 254-286.

- (113) Gard, J. K.; Gard, D. R.; Callis, C. F. *ACS Sym Ser.* **1992**, 486, 41-55.
- (114) Akitt, J. W. *NMR and Chemistry*. Chapman and Hall Ltd, London, 1973.
- (115) Mason, J. *Multinuclear NMR*, Plenum Press, N Y, 1987.
- (116) Laane, J. *Frontiers of molecular spectroscopy, 1<sup>st</sup> Ed.*, Amsterdam Elsevier, 2009.
- (117) Quin, L. D. *A guide to organophosphorus chemistry*, John Wiley Publishers, N Y, 2000.
- (118) Basu, M.; Sarkar, S.; Pande, S.; Jana, S.; Sinha, A. K.; Sarkar, S.; Pradhan, M.; Pal, A.; Pal, T. *Chem. Commun.* **2009**, 7191-7193.
- (119) Moody, G. J.; Oke, R. B.; Thomas, J. D. R. *Analyst*, **1970**, 95, 910-918.
- (120) Liu, D.; Chen, W. C.; Yang R. H.; Shen, G. L.; Yu, R. Q. *Anal. Chim. Acta*, **1997**, 338, 209-214.
- (121) Borjigin, S.; Ashimura, Y.; Yoshioka, T.; Mizoguchi, T. *Anal. Sci.* **2009**, 25, 1437-1443.
- (122) Ekemekci, G.; Kalayci, S.; Somer, G. *Sensor Actuator*, **2004**, B 101, 260-264.
- (123) Meyernoff, M. E.; Opdycke, W. N. *Adv. Clin. Chem.* **1986**, 25, 1-47.
- (124) Covington, A. K. *Ion selective electrode methodology*, CRC Press, Boca Raton, 1980.
- (125) Frant, M. S. *Analyst*, **1994**, 199, 2293-2301.
- (126) [http://www.icpress.co.uk/etextbook/p726/p726\\_chap01](http://www.icpress.co.uk/etextbook/p726/p726_chap01), 02-04-2012.
- (127) Compton, R. G.; Banks, C. *Understanding Voltammetry, 2<sup>nd</sup> Ed.*, Imperial College Press, London, 2010.
- (128) Compton, R. G.; Sanders, G. H. W. *Electrode Potentials*, Oxford University Press, 1996.
- (129) Bard, A. J.; Parson, R.; Jordan, J. *Standard potentials in aqueous solutions*, Marcel Dekker, NY, 1985.

- (130) Bard, A. J.; Faulkner, L. R. *Electrochemical methods: Fundamentals and applications*, 2<sup>nd</sup> Ed., John Wiley Publishers, NY, 2001.
- (131) <http://www.chem1.com/acad/webtext/elchem/ec4.html>, 17-04-2012.
- (132) Pungor, E.; Toth, K.; *Anal. Sci.*, **1987**, 3, 387-393.
- (133) Settle, F. *Handbook of instrumental techniques for analytical chemistry*, Prentice- Hall PTR, N Y, 1997.
- (134) Wang, J. *Analytical electrochemistry*, 3<sup>rd</sup> Ed., John Wiley Publishers, N J, 2006.
- (135) <http://docstoc.com/docs/33681458/CHEM-540-Potentiometry-061ppt> —, 17-04-2012.
- (136) Bralic, M.; Radic, N.; Brinic, S.; Generalic, E. *Talanta*, **2001**, 55, 581-586.
- (137) Sun, Z.; West, S. J.; Wen, X.; O'Heilly, J. Y. *United States Patents*, US2007/0199816 A1, 2007.
- (138) Dervaes, N. E.; Dunkle, J. R. *United States Patent*, US005393402A, 1995.
- (139) Buck, R. P.; Lindner, E. *Pure Appl. Chem.* **1994**, 66(12), 2527-2536.
- (140) Generalic, E. KTF-split. <http://glossary.periodni.com>. 23-05-2012.
- (141) Santoso, F. <http://isjd.pdii.go.id/admin/jurnal/22087684.pdf>. 23-05-2012
- (142) Hirst, A. D.; Stevens, J. F. *Ann. Clin. Biochem.* **1985**, 5, 460-488.
- (143) Meyernoff, M. E.; Opdycke, W. N.; (Editors; Sobotka, H.; Stewart, C. P.), *Adv. Clin. Chem.* **1986**, 25, 1-41.
- (144) Ruffini, G.; Dunne, S.; Farres, E.; Marco-Pallares, J.; Ray, C.; Mendoza, E.; Silva, R.; Grau, C.; <http://arXiv.org/abs/physics/0510145>. 17-04-2012.
- (145) Poels, I.; Nagels, L. J. *Anal. Chim. Acta.* **2001**, 440(2), 89-98.

- (146) Sharma, B. K. *Instrumental methods of chemical analysis*, 25<sup>th</sup> Ed., GOEL publishing, Meerut, 2005.
- (147) Lunn, J. N. *Br. J. Anaesth.* **1963**, 35(11), 666-678.
- (148) Quan, D. P.; Duan, L. T.; Quang, C. X.; Viet, P. H. *Anal. Sci.* **2001**, 17, i749-i752.
- (149) Cadogan, A.; Gao, Z.; Lewenstam, A.; Ivaska, A. *Anal. Chem.* **1992**, 64, 2496-2501.
- (150) Freiser, H. *Pure Appl. Chem.* **1987**, 59(4), 539-544.
- (151) Rius Ferrus, F. X.; Aparicio, S. M.; G A C Paravano, G. A. C; Russel, J. R. *United States Patent US2010/0193376A1*, 2010.
- (152) Li, F.; Ye, J.; Zhou, M.; Gan, S.; Zhang, Q.; Han, D.; Niu, L. *Analyst*, **2012**, 137, 618-623.
- (153) Kobayashi, T.; Iwamoto, Y. *United States Patent, US6540894B2*, 2003.
- (154) Macca, C. *Electroanal.* **2003**, 15(12), 997-1010.
- (155) Umezawa, Y.; Buhlmann, P.; Umezawa, K.; Tohda, K.; Amemiya, S. *Pure Appl. Chem.* **2000**, 72(10), 1851-1856.
- (156) Umezawa, Y.; Umezawa, K.; Sato, H. *Pure Appl. Chem.* **1995**, 67(3), 507-518.
- (157) Light, T. S.; Cappuccino, C, C. *J. Chem. Educ.* **1975**, 52(4), 247-250.
- (158) Ochiai, E. I. *J. Chem. Educ.* **1990**, 67(6), 489.
- (159) Neff, G. W. *Anal. Chem.* **1970**, 42(13), 1579-1582.
- (160) Kielland, J. J. *Am. Chem. Soc.* **1937**, 59(9), 1675-1678.
- (161) Bokris, J. O. M.; Reddy, A. K. N. *Modern Electrochemistry, Vol.1*, Plenum Press, NY, 1973.
- (162) Netz, R. R. *Phys. Rev. E.* **1999**, 60(3), 3174-3182.

- (163) Macca, C. *Anal. Chim. Acta*, **1996**, 321, 1-10.
- (164) Srinivasan, K.; Rechnitz, G. A. *Anal. Chem.* **1969**, 41(10), 1203-1208.
- (165) Bakker, E.; Pretsch, E.; Bul, P. *Anal. Chem.* **2000**, 72, 1127-1133.
- (166) Nagele, M.; Bakker, E.; Pretsch, E. *Anal. Chem.* **1999**, 71, 1041-1048.
- (167) Wang, H. X.; Pu, M. *Chinese Chem. Lett.* **2002**, 13(4), 355-358.
- (168) Knowles, A.; Shabala, S. J. *Membr. Biol.* **2004**, 2002(1), 51-59.
- (169) Muxel, A. A.; De Jesus, D. A.; Alfaya, R. V. S.; Alfaya, A. A. S.; *J Braz. Chem. Soc.* **2007**, 18(3), 572-576.
- (170) Hiirio, K.; Wakida, S. I.; Yamane, M. *Anal. Sci.*, **1988**, 4, 149-151.
- (171) Rundle, C. C.; Chapter 7. [http://www.nico2000.net/Book/Guide 8.html](http://www.nico2000.net/Book/Guide%208.html), 12-05-2010.
- (172) Solomom, T. J. *Chem. Educ.* **2001**, 78(12), 1691-1692.
- (173) IUPAC, *The gold book, Compendium of Chemical Terminology-Ionic Strength*. 2<sup>nd</sup> Ed. Online corrected version, 2001.
- (174) Buck, R. P.; Cosofret, V. V. *Pure Appl. Chem.* **1993**, 65(5), 1849-1858.
- (175) Frant, M. S.; Ross, J. W. Jr. *Anal. Chem.* **1968**, 40(7), 1169-1171.
- (176) Liberti, A.; Mascini, M. *Anal. Chem.* **1969**, 41(4), 676-679.
- (177) Peters, M. A.; Ladd, D. M. *Talanta*, **1971**, 18, 655-664.
- (178) Borjigin, S.; Ashimura, Y.; Yoshioka, T.; Mizoguchi, T. *Anal. Sci.* **2009**, 25, 1437-1443.
- (179) Corbilon, M. S.; Carril, M. P.; Madariaga, J. M.; Uriarte, I. *Analyst.* **1995**, 120(8), 2227-2231.



- (180) Neelamegam, P.; Muruganathan, K.; Raghunathan, R.; Jamaludeen, A. *Instrum. Sci. Technol.* **2010**, *38*(1), 63-71.
- (181) Tanase, I. G.; Popa, D. E.; Buleandra, M.; *Analele Universitatii Bucuresti*, **2007**, *16*(2), 25-32.
- (182) <http://www.nico2000.net/datasheets/staddl.html>. 12-05-2010.
- (183) Chapman, B. R.; Goldsmith, I. R. *Analyst*. **1982**, *107*(1278), 1014-1018.
- (184) Quan, D. P.; Duan, L. T.; Quang, C. X.; Viet, P. H.; *Anal. Sci.* **2001**, *17*, i749-i752.
- (185) Cadogan, A.; Gao, Z.; Lewenstam, A.; Ivaska, A.; *Anal. Chem.* **1992**, *64*, 2496-2501.
- (186) Gomori, G. *Handbook of Biochemistry and Molecular Biology*, 4<sup>th</sup> Ed., (Editors; Lundbald, R. L.; Macdonald, F. M.). CRC Press, 2010.
- (187) Stenesh, J. *Biochemistry Volume 1*, Plenum Press, N Y, 1998.
- (188) Midley, D. *Talanta*, **1979**, *26*(4), 261-266.
- (189) Kim, H. J.; Hummel, J. W.; Sudduth, K. A.; Birrel, S. J. *T ASABE*, **2007**, *50*(2), 415-425.
- (190) Kobayashi, T.; Iwamoto, Y. *United States Patent. US 6,540,892 B2*, 2003.
- (191) <http://www.ktf-split.hr/periodni/enabc/kpt.html>. 23-05-2012.
- (192) Rudin, M.; Motschi, H. J. *Colloid Interf. Sci.* **1984**, *98*(2), 385-393.
- (193) Westall, J. C.; Hohl, H. *Adv. Colloid Interface Sci.* **1980**, *12*, 265-294.
- (194) Mohl, W.; Schweiger, A. Motschi, H.; *Inorg. Chem.* **1990**, *29*, 1536-1543.
- (195) Mohl, W.; Motschi, H.; *Langmuir*. **1988**, *4*, 580-583.
- (196) Zahran, E. M.; Gavalas, V.; Valiente, M.; Bachas, L. G. *Anal. Chem.* **2010**, *82*, 3622-3628.

- (197) Lindner, E.; Toth, K.; Pungor, E. *Dynamic characteristics of ion selective electrodes*, CRC Press, Boca Raton, Fl., 1988.
- (198) Marshall, C. J.; Leeves, S. J. *Method Enzymol.* **1995**, 255, 273-279.
- (199) Pines, J. *Biochem. Soc. T.* **1993**, 21(4), 921-925.
- (200) Frimpong, K.; Darnay, B. G.; Rodwell, V. W. *Protein Expr. Purif.* **1993**, 4(4), 337-344.
- (201) Knight, W. B.; Dunaway-Mariano, D.; Ransom, S. C; Villafranca, J. J. *J. Biol. Chem.* **1984**, 259(5), 2886-2895.
- (202) Tafesse, F.; Milburn, R. M. *Inorg. Chim. Acta.* **1987**, 135, 119-122.
- (203) Chin, J. *Acc. Chem. Res.* **1991**, 24, 145-152.
- (204) Lai, K.; Dave, K. I.; Wild, J. R. *J. Biol. Chem.* **1994**, 269(24), 16579-16584.
- (205) Tafesse, F. *Transit. Metal. Chem.* **1991**, 16, 114-118.
- (206) Tafesse, F. *Int. J. Mol. Sci.* **2003**, 4, 362-370.
- (207) Tafesse, F. *Synth. React. Inorgan. Met.* **2005**, 35(8), 645-650.
- (208) Knight, W. B.; Dunaway-Mariano, D.; Ransom, S. C; Villafranca, J. J. *J. Biol. Chem.* **1994**, 269(24), 16579-16584.
- (209) Mildvan, A. S. *Adv. Enzymol. RAMB.* **1979**, 49, 103-126.
- (210) Mildvan, A. S.; Grisham, C. M. *Struct. Bond.* **1974**, 20, 1-20.
- (211) Benkovic, S. J.; Shray, K. J. *In the enzymes*, (Editor; Boyer, P. D.), Academic Press, NY, 1973.
- (212) Kirby, A. J. *Adv. Phys. Org. Chem.* **1980**, 17, 183-278.
- (213) Page, M. I. *Angew. Chem. Int. Ed. Engl.* **1977**, 16, 449-459.
- (214) Jencks, W. P. *Adv. Enzymol. RAMB.* **1975**, 43, 219-410.

- (215) Hutter, M. C.; Helms, V. *Int. J. Quantum Chem.* **2003**, 95, 479-486.
- (216) Mildvan, A. S. *Proteins.* **1997**, 29, 401-416.
- (217) Smilkjo, A. *Chemical kinetics and inorganic reaction mechanisms, 2<sup>nd</sup> Ed.*, Springer, 2003.
- (218) Tafesse, F.; Enemchukwu, M. *Water Air Soil Poll.* **2010**, 207(1-4), 203-212.
- (219) Chin, J. *Acc. Chem. Res.* **1991**, 24, 145-152.
- (220) Tafesse, F.; Mndubu Y. *Water Air Soil Poll.* **2007**, 183(1-4), 107-113.
- (221) Tafesse, F.; Deppa, N. C. *Ecotoxicol. Environ. Saf.* **2004**, 58(2), 260-266.
- (222) Hubner, P. W. A.; Milburn, R. M. *Inorg. Chem.* **1980**, 19, 1267-1272.
- (223) Van Waser, J. R. *Phosphorus and its compounds, Vol I and II*, Wiley Interscience, NY, 1958.
- (224) Sigel, H; Hofstetter, F. *Eur. J. Biochem. FEBS.* **1983**, 132(3), 569-577.
- (225) Tafesse, F.; Enemchukwu, M. *Nitric Oxide*, **2008**, 18(4), 274-278.
- (226) Abbott, G. A. *J. Am. Chem. Soc.* **1909**, 31, 763-770.
- (227) Geue, R. J.; Sargeson, A. M.; Wijesekera, R. *Aust. J. Chem.* **1993**, 46(7), 1021-1040.
- (228) Bose, R. N.; Cornelius, R. D.; Viola, R. E. *Inorg. Chem.* **1985**, 24, 3989-3996.
- (229) Baldwin, D. S.; Beattie, J. K.; Coleman, L. M.; Jones, D. R. *Environ. Sci. Technol.* **1995**, 29(6), 1706-1809.
- (230) Anderson, B.; Milburn, R. M.; Harrowfield, J. M.; Robertson, G. B.; Sargeson, A. M. *J. Am. Chem. Soc.* **1977**, 99(8), 2652-2661.
- (231) Bauer, H. F.; Drinkard, W. C. *J. Am. Chem. Soc.* **1960**, 82, 5031-5032.
- (232) Lincoln, S. F.; Stranks, D. R. *Aust. J. Chem.* **1968**, 21, 37-56.

- (233) Zinder, B.; Hertz, J.; Oswald, H. R. *Water Res.* **1989**, *18*(5), 509-512.
- (234) Massoud, S. S.; Milburn, R. M. *Inorg. Chim. Acta.* **1989**, *163*, 87-91
- (235) Milburn, R. M.; Anderson, B.; Harrowfield, J. M.; Robertson, G. B. *J. Am. Chem. Soc.* **1977**, *99*(8), 2652-2661.
- (236) Jones, D. R.; Lindoy, L. F.; Sargeson, A. M. *J. Am. Chem. Soc.* **1983**, *105*, 7327-7336.
- (237) Tafesse, F.; Massoud, S. S.; Milburn, R. M. *Inorg. Chem.* **1993**, *32*, 1864-1865.
- (238) Haight, G. P.; Hambley, T. W.; Sargeson, A. M.; Hendry, P. L. *J. Chem. Soc. Chem. Commun.* **1984**, *23*, 1568-1571.
- (239) Jansco, A.; Torok, I.; Hegetschweiler, K.; Gadja, T. *ARKIVOC*, **2009**, 217-224.
- (240) Tafesse, F.; Eguzozie, K. *Ecotoxicol. Environ. Saf.* **2009**, *72*(3), 954-959.
- (241) Frey, S. T.; Hutchins, B. M.; Anderson, B. J.; Schreiber, T. K.; Hagerman, M. E. *Langmuir*, **2003**, *19*(6), 2188-2192.
- (242) Massoud, S. S.; Milburn, R. M. *Inorg. Chim. Acta.* **1988**, *146*, 3-4
- (243) Baldwin, D. S.; Beattie, J. K.; Coleman, L. M.; Jones, D. R. *Environ. Sci. Technol.* **1995**, *29*, 1706-1709.
- (244) Tafesse, F.; Massoud, S. S.; Milburn, R. M. *Inorg. Chem.* **1985**, *24*, 2591-2593.
- (245) Hediger, M.; Milburn, R. M. *J. Inorg. Biochem.* **1982**, *16*(3), 165-182.
- (246) Young, R. J.; Lovell, P. A. *Introduction to polymers*, CRC Press, Boca Raton, FL, 2011.
- (247) Sheenan, D. *Physical Biochemistry, Principles and Applications*, 2<sup>nd</sup> Ed., John Wiley and Sons, UK, 2009.
- (248) Zinder, B.; Hertz, J.; Oswald, H. R. *Water Res.* **1989**, *18*(5), 509-512.